UNIVERSITY OF BIRMINGHAM

UNIVERSITY OF BIRMINGHAM

SCHOOL OF CHEMICAL ENGINEERING

PH.D THESIS

MATHEMATICAL MODELLING OF GASTRIC EMPTYING AND NUTRIENT ABSORPTION IN THE HUMAN DIGESTIVE SYSTEM

Thomas Moxon

Supervised by

Prof. Serafim Bakalis

Prof. Peter J. Fryer

October 13, 2017

Abstract

Mathematical modelling of the digestive system can be achieved by assuming the digestive system is described as a series of ideal reactors. A well formulated model could give an understanding of how food products behave within the body, and offer some predictive possibility allowing the design of functional foods to have tailored nutritional responses.

The models developed showed good estimates of the gastric emptying rates and glucose absorption rates for solutions with different viscosities and glucose concentrations, when a feedback mechanism is included. Implementing a population balance for solid breakdown in the stomach allowed for parameters to be linked to meal type. With parameter estimates from experimental gastric emptying of a solid meal being further validated against results for the same food type from different experimental results.

The main outcomes of this work are (i) the inclusion of meals viscosity into models, and its effects on the gastric secretion and emptying rate as well as the mass transfer of nutrients in the intestinal lumen, (ii) the inclusion of a feedback mechanism on the rate of gastric emptying, and (iii) the development of a population balance to model solid breakdown within the stomach.

Aşkım Sena'ya.

Acknowledgements

I would like to thank my supervisors on the project Prof. Serafim Bakalis and Prof. Peter J. Fryer for their help and support. Along with Lynn Draper for help with administrative side of the project.

I would also like to thank Clifford Latty, Dr. Ourania Gouseti, Dr. Estefania Quiargo-Lopez, and Dr. Georgina Zimbitas for there valuable input throughout the project. Vasilis Valdramidis and the ERASMUS+ QSafe project for providing the funding and opportunity to carry out some research at KU Leuven, and Prof. Jan Van Impe, Dr Dries Tellen, and Philippe Nimmegeers for hosting myself and providing valuable input and advise to the project.

I would also like to acknowledge BBSRC for funding this Ph.D project.

Finally, a special thanks to my fiancée Sena for her support during my Ph.D, and to my family.

Contents

List of Figures

List of Tables

Chapter 1

Introduction

1.1 Overview

The aim of this PhD thesis is to develop computational models to look into the effect of food properties upon the processes occurring postprandially (after food is swallowed). An understanding of these processes could provide great insight into the development of functional foods, which aim to address the growing problem of food related diseases.

Obesity (body mass index $\geq 30kg/m^2$ (Berghöfer et al., 2008)) is becoming a major issue globally, with 33.8% of the adult population in the USA classed as obese in 2008, and in the UK the figure was around 25% of the adult population in 2012 (McPherson et al., 2007). This growing trend of obesity results in increased cost both in health care and in wider society. The cost in the UK in 2012 was estimated at £5.1 billion (McPherson et al., 2007), and if the growth in obesity persists it has been estimated that by 2050 the cost on society in the UK alone will be £50 billion (McPherson et al., 2007).

The trend in obesity prevalence can be linked to changes in diet and physical activity over time. The change from hunter gatherer societies during the neolithic revolution, around 10,000 years ago, to a diet with a higher glycemic load (area under the curve of blood glucose after meal consumption as a fraction of a equi-carbohydrate reference food e.g., white bread, multiplied by the amount of carbohydrates in a meal; Equations 1.1 & 1.2), and different nutrient profiles (e.g., consumption of more wheat and grains etc.) (Kendall et al., 2010). Around 200 years ago the human diet was again changed dramatically by the industrial revolution and as a result consumption of processed food has increased and the fibre content in meals has decreased. Due to this rapid shift in

diet it is believed that humans are still adapted to more ancient environments, and this poor adaption to modern diets has resulted in the current prevalence of chronic food related diseases (Jew et al., 2009).

$$\text{Glycaemic Index (GI)} = \frac{\text{AUC}_{\text{meal}}}{\text{AUC}_{\text{ref}}} \times 100 \tag{1.1}$$

$$\text{AUC} = \text{Area under Blood glucose curve after meal consumption}$$

$$\text{Glycaemic Load (GL)} = \text{GI} \times m_{\text{meal}} \tag{1.2}$$

$$m_{\text{meal}} = \text{mass of carbohydrates in meal consumed}$$

Human diet and the effect upon obesity has been studied by numerous authors, and these have been collated by others to produce reviews of the current state of research (Berghöfer et al., 2008; Haslam and James, 2005; Kopelman, 2007; Mishra and Dubey, 2016; Popkin, 2006). These works highlight the increase in risk obese individuals encounter to a variety of health problems which can lower the life expectancy, including heart disease, diabetes, hypertension, strokes, and cancers. A major area of research is into the effect of hydrocolloids in food, and how these could have positive health implications either alleviating or preventing all together some of the prevalent problems (Gidley, 2013; Kendall et al., 2010; Li and Nie, 2015; Salmeron et al., 1997a; Viebke et al., 2014; Weickert and Pfeiffer, 2008).

A variety of explanations have been presented for the health effects of hydrocolloids. *In vitro* experiments have shown how hydrocolloids reduce the absorption of glucose through permeable membranes (Gouseti et al., 2014; Tharakan et al., 2010) which was attributed to a reduction of the mixing efficacy or diffusion rate (Tharakan

et al., 2010). Others have speculated that hydrocolloids will reduce nutrient absorption through other methods such as encapsulation of absorbable molecules or enzymes (Sasaki and Kohyama, 2012) or through the inhibition of enzymes (Slaughter et al., 2002).

To classify the effect of carbohydrate meals upon the body Jenkins et al. (1981) defined the term *Glycemic Index* (GI). This method classifies different foods in terms of blood glucose measurement taken postprandially. The work proposed that after the consumption of a food, containing 50g of carbohydrate, blood glucose measurements can then be taken, over a period of 2 hours, and the area under this curve compared to that of the curve after the consumption of a 50g glucose solution, and multiplied by 100 (Equation 1.1). A GI of 100 is that of a pure glucose solution (or other reference meal), foods with GIs above 70 would be considered to have a high GI, ones with values between 55 and 69 would be considered to have medium GI, and foods with values below 55 would be considered low GI (Brand-Miller et al., 2009).

To address some of the controversy surrounding clinical applications of glycemic index, Wolever et al. (1991) published a more complete methodology, with the aim of showing that the glycemic index was able to fulfil the following criterion:

1. Repeatability for the same food
2. Application to individual subjects
3. Application to mixed meals
4. Demonstration of improvement due to dietary changes

The following methodology was proposed: The test food chosen to test should contain 50g of available carbohydrate, along with a reference meal of white bread containing the equivalent carbohydrate (white bread chosen over glucose due to concerns of the osmotic pressure in the glucose meal having an effect upon the gastric emptying rate (Wolever et al., 1991)). The subjects should fast overnight and foods be tested in triplicates upon each subject, with blood been tested before each meal and at the following time intervals: 15, 30, 45, 60, 90, & 120 minutes after consumption (blood glucose plots for white breads with different GIs are shown in Figure 1.1). The glycemic index is then the area under the curve of the blood glucose of the meal as a percentage of the area under the curve of the reference meal. The procedure was then recommended by the FAO/WHO joint report on carbohydrates (FAO/WHO, 1998).

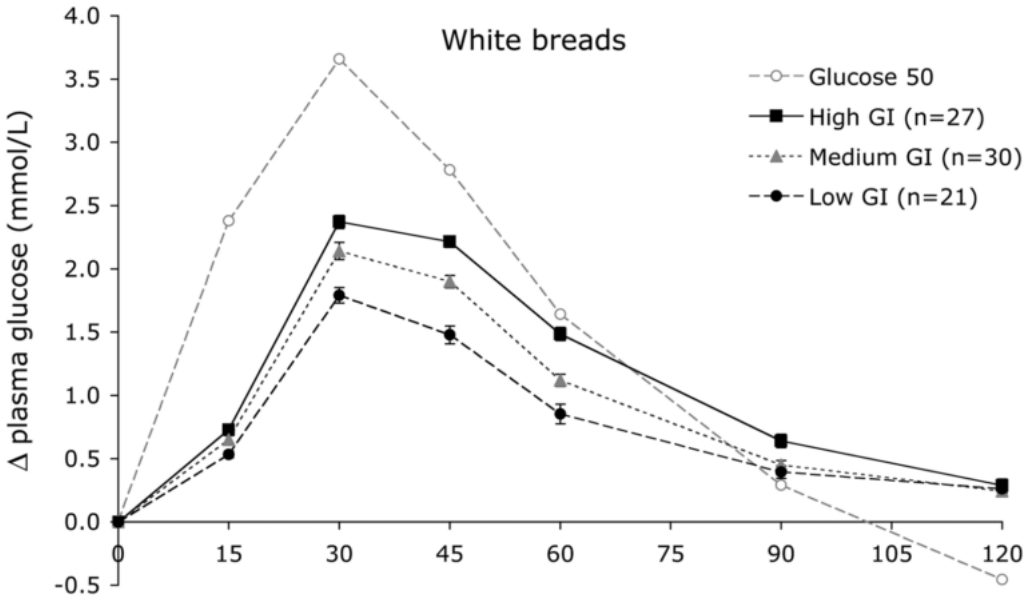

Figure 1.1: Change in plasma glucose concentration after the consumption of white breads with different glycemic indexes along with a reference meal of glucose. The plot is taken from work by Brand-Miller et al. (2009)

Building upon the definition of glycemic index, one can define the glycemic load (GL) (Equation 1.2), this is calculated by multiplying the glycemic index by the total amount of carbohydrate consumed. The glycemic load was linked in some long term studies of diet and risk of developing type 2 diabetes both in men (Salmeron et al., 1997a) and in women (Salmeron et al., 1997b), these show that people who consumed a diet with a high glycemic load and low dietary fibre content had a higher chance of developing diabetes. The same results were found for women who consumed a diet with low cereal fibre content and a high glycemic index (Schulze et al., 2004).

From these studies it is clear that the addition of dietary fibre to diets along with reduction in the glycemic index/load will reduce the chances of diabetes (Salmeron et al., 1997a,b; Schulze et al., 2004), by improving the insulin sensitivity (Kim and White, 2013; Wolever et al., 1991). Thus an understanding of how food properties affect the digestive processes will play a role in developing foods which will be both as palatable and readily available as some of the foods identified as predictors of type 2 diabetes e.g., Chips, crisps, white bread, carbonated drinks, white rice, pasta (Willett et al., 2002), but reduce the negative effects.

This work will focus mainly on the digestion of carbohydrates, with starch been the largest source of this in the human diet (Singh et al., 2010). We can then breakdown the starch into 3 categories by its digestibility, through *in vitro* digestion (Singh et al., 2010):

- Rapidly digestible starch - where the glucose will be released within 20 mins
- Slowly digestible starch- where the glucose will be released within 20-120 mins
- Resistant starch - the starch remaining after 120 mins

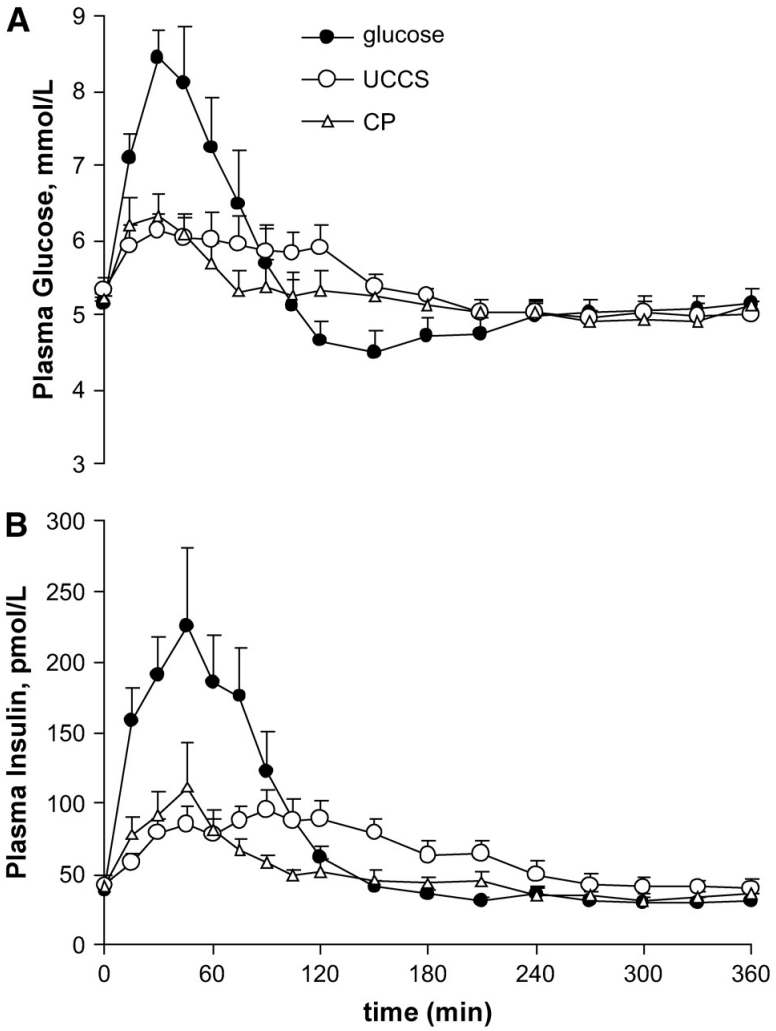

Figure 1.2: Plasma glucose (A) and insulin (B) response after the consumption of 3 meals: Glucose solution, Uncooked corn starch (UCCS), and corn pasta (CP). Taken from Wachters-Hagedoorn et al. (2006)

This digestibility is due to the requirement of the starch to be hydrolysed to smaller chain, this is done by α-amylase present in saliva and pancreatic secretions. Starch consists of two types of molecules: Amylose, which is a linear polymer, and Amylopectin, a branched polymer. The α-amylase enzymes act on the α-(1,4) glycosidic bonds of the Amylose and Amylopectin molecules (Singh et al., 2010).

One would expect a lower peak in blood glucose and overall slower glycaemic response when the digestibility of starch is increased. This is highlighted in work by Wachters-Hagedoorn et al. (2006), which shows the effect of consumption of rapidly available sugars (glucose), and starches with lower digestibility (Uncooked corn starch (UCCS) and corn pasta (CP)) on the blood glucose levels and insulin levels, Figure 1.2. The main difference seen is the much higher peak in plasma glucose in the rapidly absorbable meal (glucose), but we also observe a drop below basal glucose levels (after 120 min) before returning, whereas the meals with lower starch digestibility do not instigate such a large rise, neither in plasma glucose nor insulin, and the levels stay closer within to the basal levels, these will translate into lower glycaemic index's.

Whilst this approach of GI or equivalent approaches in pharmacokinetics such as the area under the curve (AUC) or the maximum plasma concentration/time (Peng and Cheung, 2009) provide information about the system- they do not offer any predictive opportunity nor any understanding of the mechanisms involved. To this end mathematical modellers of the stomach and small intestine aim to elucidate upon the dominate mechanism controlling the rate of digestion and/or absorption of nutrients or drug molecules after oral consumption, and when used in conjunction with *in vivo* or *in vitro* data may provide salient information during drug development or the design of functional foods.

1.2 Overview of Thesis Structure

Chapter 2 will provide an introduction to the physiology of the human gut which will give an overview sufficient for the subsequent modelling of the system, the chapter will then go on to provide a literature review of the gastric processes: focusing on gastric emptying, secretions, and solid breakdown. The chapter will then look at the current state of modelling in the small intestine with a literature review of models for drug/nutrient absorption.

Chapter 3 will contain a paper published in the *Journal of Food Engineering* as Moxon et al. (2016), which will cover a simple model comparing the effect of gastric emptying rate and gut lumen nutrient mass transfer rate upon the absorption rate, followed by the introduction of a multi component model, and the effect of enzymatic hydrolysis upon the absorption of nutrients.

Chapter 4 will build upon this model by looking in more detail at the gastric emptying rate, this work was published in *Chemical Engineering Science* as Moxon et al. (2017). The gastric emptying rate will be linked to the intestinal bioaccessibility of nutrients via a feedback mechanism, and also some of the properties of the liquid meal, such as the viscosity of the chyme in the stomach. A gastric secretion model will also be implemented.

Chapter 5 will look at validating the assumptions made in Chapters 3 & 4, this will be done against a simple oral glucose tolerance test and literature data for the appearance of glucose in plasma.

Chapter 6 will aim to develop a model for a 2-phase system. This will introduce the consumption of solid foods and provide a framework for modelling the breakdown

in the gastric and intestinal compartments and subsequent absorption of the nutrients therein.

Finally, Chapter 7 will conclude the main points of the thesis and present recommendations for continuation of the work.

Chapter 2

Literature Review

2.1 The Human gut

This thesis will look into presenting mathematical models to describe some of the processes which occur during food digestion in the human gut, and as such an understanding of the physiology of the human digestive system is required. The models developed will attempt to describe what happens postprandially in the stomach and small intestine but will not consider the mastication processes or processes occurring after the ileum in the large intestine.

2.1.1 Overview

Figure 2.1 shows the parts of the digestive system and there positioning in the human body. In simplistic terms when one consumes a meal it is broken down mechanically in the mouth through the process of mastication. During this process the food is mixed with saliva which will provide α-amylase to initiate the enzymatic break down of carbohydrates. The food will be formed into bolus, with the saliva also acting to lubricate, allowing it to be easily swallowed (Jalabert-Malbos et al., 2007) and pass down the oesophagus to the stomach. Once in the stomach the food bolus is mixed with gastric juices which facilitates further chemical breakdown of macronutrients such as proteins which will be broken down by pepsin to peptides and amino acids, and lipids which will be broken down by sgastric lipase to fatty acids and glycerides, respectively. Along with the chemical breakdown peristaltic activity of the gastric walls will provide mechanical breakdown of the meal. This mixture of food and gastric juices will be referred to as gastric *chyme*. The amount of time a meal spends in the stomach will vary (generally expressed as half time), some emptying rates for liquid meals are shown in Table 2.3, with

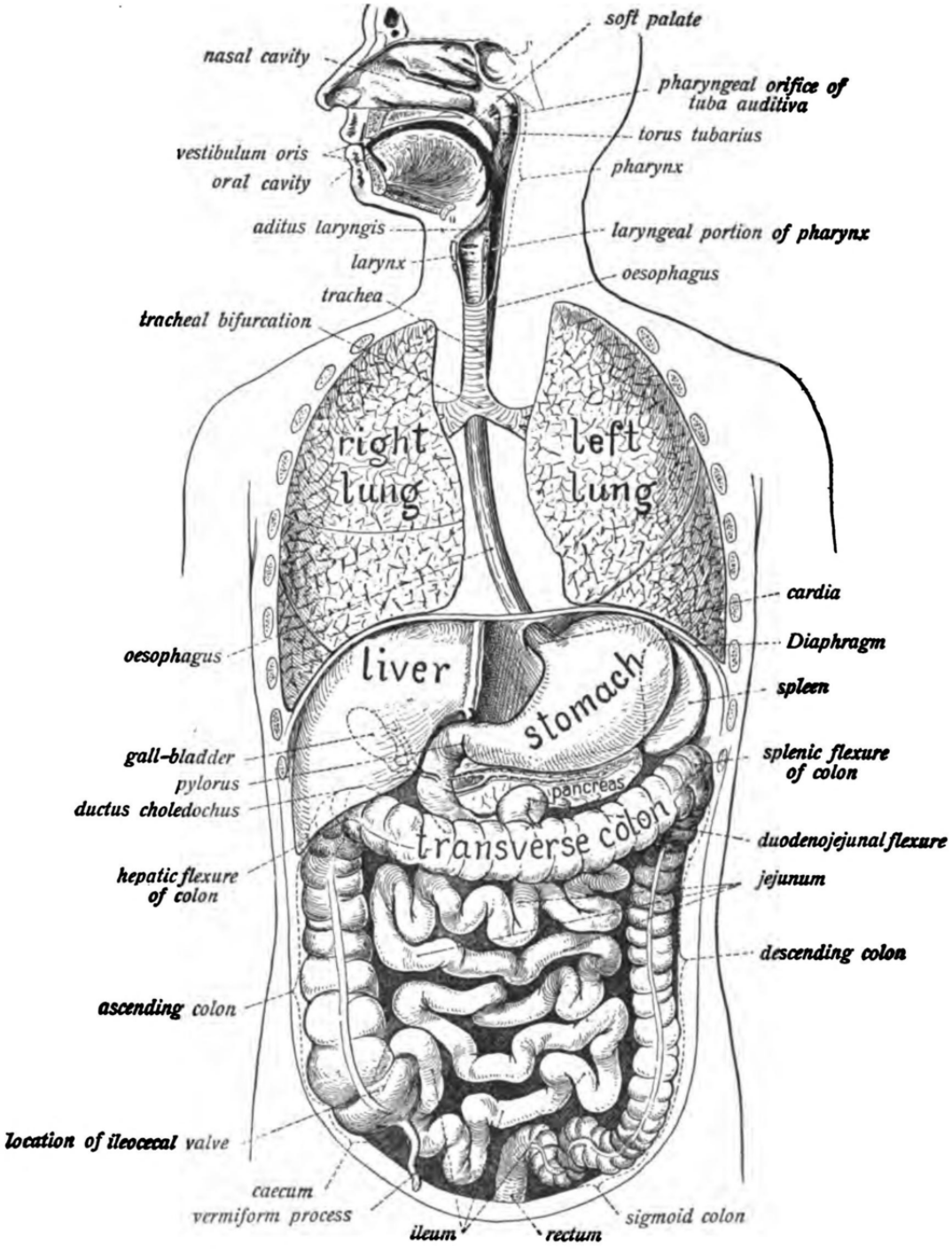

Figure 2.1: Overview of the human digestion system and position in the body. taken from Sobotta (1906).

a *'normal'* meal (535kcal) having a mean half time of 1.2 hours (Read et al., 1986). The gastric chyme passes through the pyloric sphincter into the duodenum, the first section of the small intestine, here the chyme is mixed with pancreatic juices and bile, these neutralise the acid and provide enzymes for the hydrolysis of macronutrients. The small intestine will act as the main site of absorption of nutrients into the blood stream, through the intestinal epithelium. The chyme moves along the length of the small intestine via peristaltic contractions of the gut wall. The mean transit time for a meal is around 4.0 hours (standard deviation ± 1.4 hours) from entering the duodenum via the pyloric sphincter to reaching the colon (Read et al., 1986). Once in the large intestine most of the water, from the meal and various digestive tract secretions, will be reabsorbed. The large intestine also plays host to a large number of gut microflora. Gastric and pancreatic secretions limit the amount of colonisation in the stomach and proximal small intestine, but the number of bacteria rise towards the distal end of the small intestine, and reaching around $10^{11} - 10^{12}$ bacteria per gram of colonic content in the large intestine (O'Hara and Shanahan, 2006). These will facilitate the fermentation of some of the fibre etc. which cannot be hydrolysed by salivary or pancreatic α-amylase, before the stool passes to the rectum and is excreted from the body via the anus.

2.1.2 Stomach

The stomach has a variety of functions to aid the optimal absorption of nutrients for consumed foods, these can be listed briefly as follows:

- Mechanically breakdown solid foods through gastric wall contractions
- Chemically breakdown food through enzymatic hydrolysis

- Act as a reservoir to store food
- Control the release of food into the proximal small intestine

The stomach can be broken up into 3 areas: The *Fundus*, the *Body* or *Corpus*, and the *Antrum*. These areas of the stomach are highlighted in Figure 2.2.

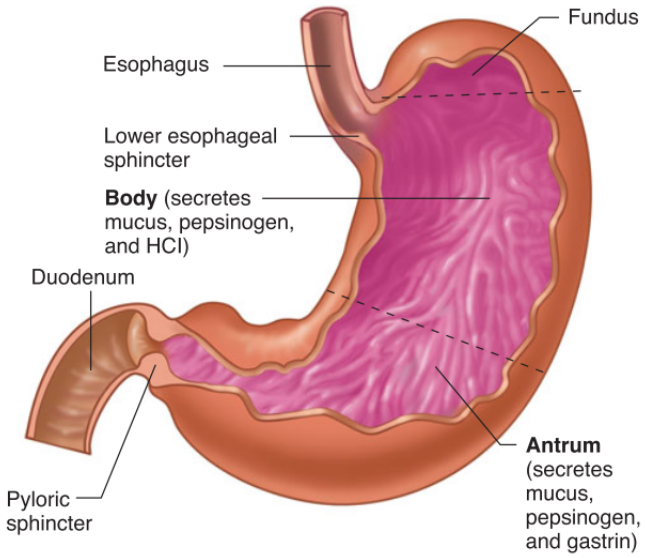

Figure 2.2: Figure showing the anatomy of the gastric compartment from Barrett et al. (2005), with the sections of the stomach labelled.

Gastric Secretions

To provide chemical breakdown of foods the stomach must secrete enzymes which will facilitate the process. Pepsin and gastric lipase are the major enzymes secreted to facilitate the breakdown of proteins and lipids, respectively, in the stomach. Table 2.1 summarises the secretions from the stomach and there main function.

Table 2.1: List of secretions into stomach (Barrett et al., 2005)

Pepsin	Breakdown proteins
Gastric Lipase	Breakdown lipids
Mucin	Protects gastric mucosa from damage (from acidic environment, damage from pepsin & abrasive damage from solid particles)
Gastric Intrinsic Factor	Facilitate the absorption of vitamin B_{12}
Gastric Acid	Provide an acidic pH to optimise protein hydrolysis, and kill microorganisms

Secretion can be said to occur in three phases: *Cephalic*, *Gastric*, and *Intestinal* (Di Mario and Goni, 2014). This is summarised in Figure 2.3, and the gastric hormones with there main function is shown in Table 2.2. The first phase, *Cephaic*, is stimulated prior to the meal entering the stomach, e.g., due to the taste of food. This is facilitated by vagal nerve pathways where Acetylcholine (ACh) and Gastrin releasing peptide (GRP) are released from enteric nerve endings (Barrett et al., 2005). The GRP stimulates G cells in the antrum to secrete Gastrin into the blood stream which passes to the fundus and stimulates the Parietal cells and Chief cells, these cells are also stimulated by the release of ACh. Once stimulated the Parietal cells secrete gastric acid and gastric intrinsic factor (Levine et al., 1981), the Chief cells secrete lipase (Wøjdemann et al., 1998) and pepsinogen, which is converted to pepsin in the presence of HCl (Gritti et al., 2000).

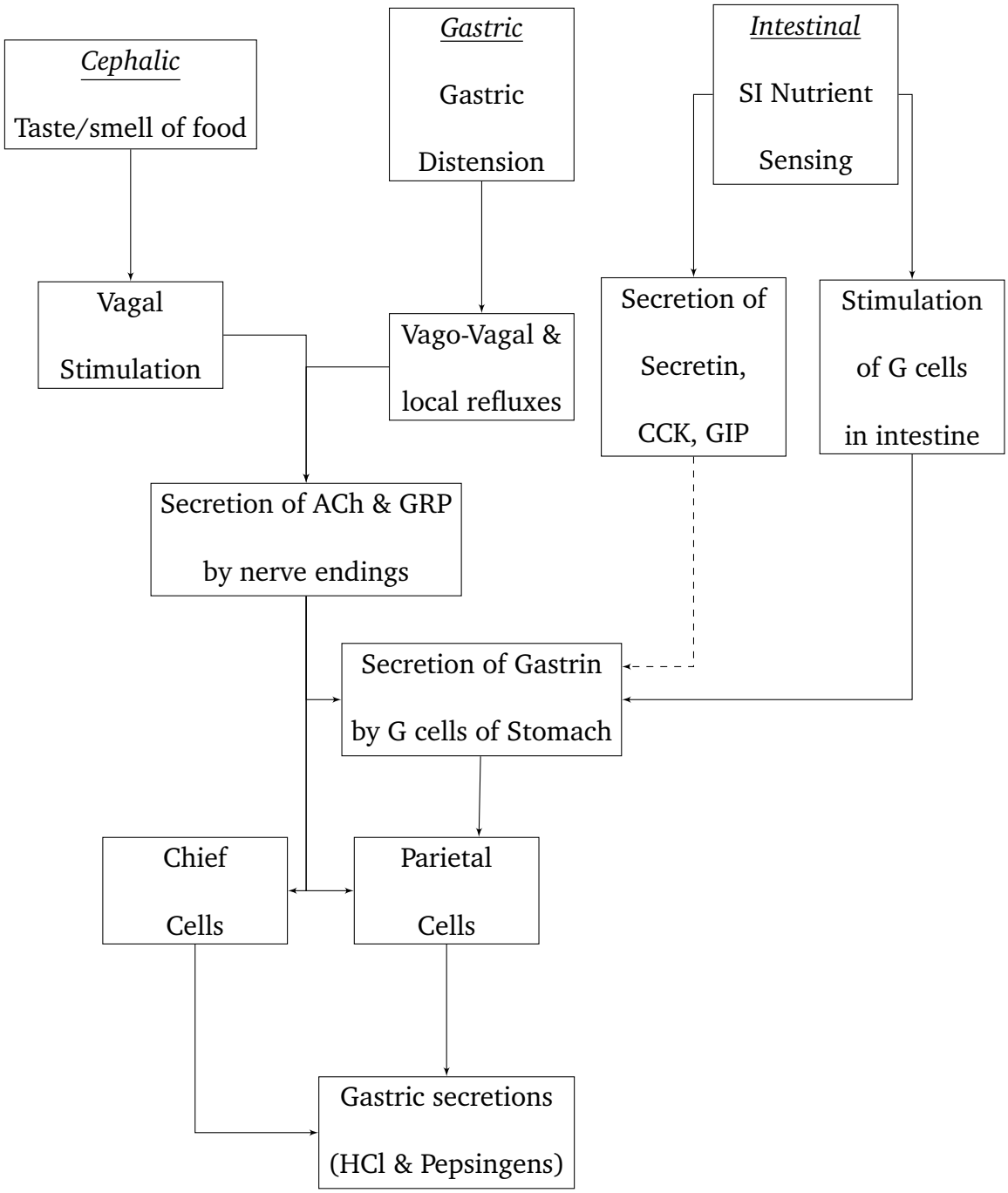

Figure 2.3: Flow chart of different phases and pathways for initiation of gastric secretions, modified from Pocock and Richards (2006), dotted line shows inhibition.

Once the food has been consumed and enters the stomach the second phase of secretions initiates- the *Gastric* phase. The nutrients in the meal stimulate the secretion of gastrin (Barrett et al., 2005), and the distension of the gastric walls due to the

meal entering activates mechanoreceptors, these initiate vago-vagal reflexes (Pocock and Richards, 2006) which further stimulate secretion through the release of ACh and GRP from the enteric nerve endings.

The third phase of gastric secretion is stimulated by the presence of the products of protein digestion within the duodenum. The Amino acids stimulate the G cells within the intestine which secrete gastrin into the blood, this stimulates Parietal and Chief cells in the gastric fundus (Pocock and Richards, 2006). The presence of nutrients within the duodenum and jejunum also stimulate the secretion of Secretin (from S-cells in the intestinal mucosa) and Cholecystokinin (CCK) (from I-cells in intestinal mucosa) which have the effect of inhibiting gastrin secretion from antral G cells (Pocock and Richards, 2006), and stimulating the release of somatostatin, from D cells in the stomach and duodenum which inhibits pathways of parietal cell secretion of acid (Komasaka et al., 2002).

Table 2.2: List of Gastric hormones and role (Barrett et al., 2005)

Hormone	Origin	Role
Gastrin	Antral G-cells	• Stimulates release of Histamine via ECL-cells • Stimulates Parietal acid secretion
Histamine	Fundic ECL-cells	• Stimulates Parietal acid secretion
Secretin	Intestinal S-cells	• Stimulate secretion from bile & pancretic duct • Triggers release of insulin • Reduces Parietal acid secretion
Cholecystokinin	Intestinal I-cells	• Stimulated by fatty acids & amino acids in Duodenum • Inhibits gastric emptying & acid secretion
Somatostatin	Antral & duodenal D-cells	• Reduces acid secretion from Parietal cells • Inhibits production of Gastrin, Secretin, Histamine

Gastric Motility & Solid Processing

As the food passes down the oesophagus and enters the stomach the fundus dilates to allow an increase in volume to accommodate the meal without an increase in pressure, this process is called *receptive relaxation*. A second mechanism called *adaptive relaxation* allows the fundus to dilate due to small changes in the gastric pressure from food entering the stomach (Arakawa et al., 1997; Schwizer et al., 2002).

Once the meal is in the stomach peristaltic contraction will occur in the body and distal regions of the stomach, which will act to mix, grind and facilitate emptying through the pyloric sphincter. The pyloric sphincter is the area connecting the stomach and intestine, the muscles of the pylorus allow the diameter of the area to be controlled and prevent the movement of gastric chyme to the small intestine until it has been sufficiently processed (Dillard et al., 2007). When the stomach is at rest (no food within it) the pylorus is open with a maximum diameter of around 1.9mm (Keet, 1962). It has been measured, by fitting transducers in different gastric regions of dogs, that the muscles of the pyloric sphincter begins to contract when the peristaltic wave travels over the terminal part of the antrum (Pröve and Ehrlein, 1982). These contractions of the pylorus as the peristaltic waves arrives results in a retropulsion of the chyme back into the stomach, this retropulsion result in high levels of mixing and grinding of solid particles (Kong and Singh, 2008; Pröve and Ehrlein, 1982; Rayner et al., 2012; Schulze, 2006). As the pylorus partially opens there is a *sieving effect*, where by liquids and particles less than 1-2mm in diameter can empty into the duodenum (Kong and Singh, 2008). The pyloric contractions have been shown to be linked to the rate of gastric emptying (Treacy et al., 1990), who measured the gastric emptying rate, in pigs, of radio labelled dextrose via sampling from a duodenal cannula whilst also measuring the antral, pyloric and duodenal pressures with manometers. The pyloric contractions (both number of isolated pyloric pressure waves (IPPW) and the pyloric pressure) increase with intraduodenal infusion of nutrients, along with decreases of antral pressure waves (Heddle et al., 1988a,b; Rayner et al., 2000). These works highlight the presence of nutrient initiated feedback mechanism controlling the gastric emptying rate (the rate

at which gastric content leaves the stomach) observed by others (Brener et al., 1983; Hunt and Stubbs, 1975), but also elucidating that this mechanism is expressed through changes in the antral and pyloric contractions.

To determine the amount of force which the stomach can impart upon solid particles Marciani et al. (2001a) used agar beads. Subjects ingested 7 agar beads, of diameter 1.27 cm of the same fracture strength (6 different agar gel concentrations were used giving fracture strengths between 0.15-0.9 N) without chewing along with a 500ml drink of either high or low viscosity. With the low viscosity meal it was determined that beads with a strength greater than 0.65N emptied slower than beads of a lower strength, with weaker beads fragmenting in the stomach. With the higher viscosity meals they found that the beads emptied faster than the equivalent strength beads in lower viscosity meals, speculating that the viscous liquid prevents the solids from sedimenting, thus enhancing the efficacy of the induced grinding (Marciani et al., 2001a).

Gastric Emptying

The rate of gastric emptying of liquid meals has been linked to a number of factors: Nutrient content (type & amount), meal volume, meal osmolality, meal viscosity. A selection of gastric emptying rates for liquid meals with different viscosity and calorific contents is shown in Table 2.3 (Moxon et al., 2016).

Table 2.3: Summary of gastric emptying data from literature, showing emptying rate for different liquid meals and the method of measurement, as well as comments to highlight the salient points of the studies.

Nutrient & Thickener	Half-Time [min]	Empty rate [Kcal/ min]	Measurement methods	Comments	References
500 mL 0.25 g/100 g LBG (μ_0: 0.01 Pa s)	17 ± 6	-	Echo-planar magnetic resonance imaging	• No significant variation of emptying time with changes in viscosity • Large changes in viscosity occurred in the stomach, pointing to the importance of gastric secretions • Over 40min, the viscosity of the 0.01 Pa s solution was reduced to 0.005 Pa s and that of the 11 Pa s solution was reduced to 0.3 Pa s.	(Marciani et al., 2000)
500 mL 0.5 g/100 g LBG (μ_0: 0.1 Pa s)	18 ± 4	-			
500 mL 1.0 g/100 g LBG (μ_0: 2 Pa s)	18 ± 7	-			
500 mL 1.5 g/100 g LBG (μ_0: 11 Pa s)	19 ± 9	-			
500 mL 64 kcal, LV	32 ± 7	1	Echo-planar magnetic resonance imaging	• Slowing of gastric emptying observed with addition of nutrient for both HV & LV • HV low calorie solution emptied slower than LV, the effect was diminished for high calorie solutions but still significant • Antral volumes were higher with HV meals compared to LV meals	(Marciani et al., 2001b)
500 mL 64 kcal, HV	46 ± 9	0.7			
500mL 323 kcal (63% lipid, 27% carbohydrate) LV	67 ± 9	2.4			
500mL 323 kcal (63% lipid, 27% carbohydrate) HV	79 ± 6	2.0			

600mL, 96 kcal Glucose, LV 600mL, 96kcal Glucose, HV 600mL, 451 kcal Glucose, LV 600mL, 451 kcal Glucose, HV	17 ± 1 14 ± 1 130 ± 18 64 ± 8	2.8 3.4 1.7 3.5	Double sampling gastric aspiration technique	• Increase in emptying time (4-8 fold) with increased solutin energy content (4 fold) • Show longer emptying for lower viscosity equicarbohydrate solutions, contrary to other authors	(Vist and Maughan, 1995)
600mL, 60 kcal Glucose 600mL, 132 kcal PPH 600mL, 138 kcal WPH 600mL, 396 kcal MP	9.4 ± 1.2 16.3 ± 5.4 17.2 ± 6.1 26.4 ± 10	3.2 4.05 4.01 7.5	Double sampling gastric aspiration technique	• Linear relationship between calorific density and calorific empty rate was observed • Main factor in the emptying rate is the calorific density	(Calbet and MacLean, 1997)
300mL, 400kcal Glucose 450mL, 200kcal Glucose	107 66	1.9 1.5	Scintigraphy	• Solutions with high calories have longer emptying times • Solutions used varied in both volume and calorific content, hence most important factor cannot be identified	(Phillips et al., 1991)
500mL, 500kcal (mixed) LV 500mL, 500kcal (mixed) HV	72.1 ± 19.5 85.5 ± 16.5	3.5 2.9	Ultra-sonography	• With higher viscosity solutions having slightly longer emptying times • Results here show large variability (-20 - +25%) • Calories are from mixed source not just glucose	(Yu et al., 2014)

5400mL, 400kcal (mixed), LV 400mL, 400kcal (mixed), HV 400mL, Water	257.9 ± 31.8 195.1 ± 16.3 99.4 ± 2.8	0.8 1.0 -	^{13}C breath sampling with continuous IR specrometry	• Overall emptying faster for HV • Initial empty rate faster for LV • Author linked this to inhibition due to nutrient sensing in the duodenum	(Shimoyama et al., 2007)
240kcal Solid/Liquid meal 240kcal Soup	77 ± 6 92 ± 7	1.56 1.3	Echo-planar magnetic resonance imaging	• Looked at effect of blended (soup) vs. Solid meal with water drink • Longer emptying for soup, linked by author to sieving mechanism whereby low nutrient liquid phase empties separately from high nutrient solid phase • The soup has homogenous nutrient composition and the emptying will stimulate the nutrient feedback mechanism, slowing the emptying rate.	(Marciani et al., 2012)

LBG-Locust bean gum, PPH-Pea peptide hydrolysate solution, WPH-Whey peptide hydrolysate solution, MP-Milk protein solution, LV-Low viscosity, HV-High viscosity, 1g glucose = 4kcal.

The volume of a meal has been shown to have an effect upon the gastric emptying rate (Hunt and Stubbs, 1975) such that a liquid meal will empty in a characteristic exponential fashion (Hellström et al., 2006; Hunt and Stubbs, 1975) as highlighted in Figure 2.4. Viscosity is also thought to play a role in the emptying of a meal from the stomach (Marciani et al., 2001b; Shimoyama et al., 2007), with high viscosity meals resulting in greater antral distension, and stimulating a greater volume of secretions (Marciani et al., 2001b) than lower viscosity meals. The literature data shows contradictory results, with some showing longer emptying times for more viscous meals (Marciani et al., 2001b; Yu et al., 2014), some showing longer emptying times for lower viscosity meals (Shimoyama et al., 2007; Vist and Maughan, 1995), with Shimoyama et al. (2007) showing lower viscosity meals have a faster initial emptying rate but are slower overall, speculating that the overall slower emptying rate is due to the inhibition of emptying due to the sensing of nutrients in the small intestine, where lower viscosity solutions will have a greater mass transfer rate within the intestinal lumen than higher viscosity solutions, this can be seen from work by Ellis et al. (1995) on pigs and Kim (2005) on rats which both showed an inverse relationship between digesta viscosity in the small intestine and the rate of glucose absorption. A further study of non nutrient meals showed that there is no significant difference in the half emptying time for solutions of different viscosities (0.01-11Pa.s) (Marciani et al., 2000). Along with this the authors showed how there can be large changes in viscosity over a 40 minute period (11 to 0.3 Pa.s) due to the increased rates of gastric secretions of high viscosity meals.

The nutrient content is a major factor in the gastric emptying of a meal, Hunt and Stubbs (1975) showed a clear trend between the half emptying time over the original

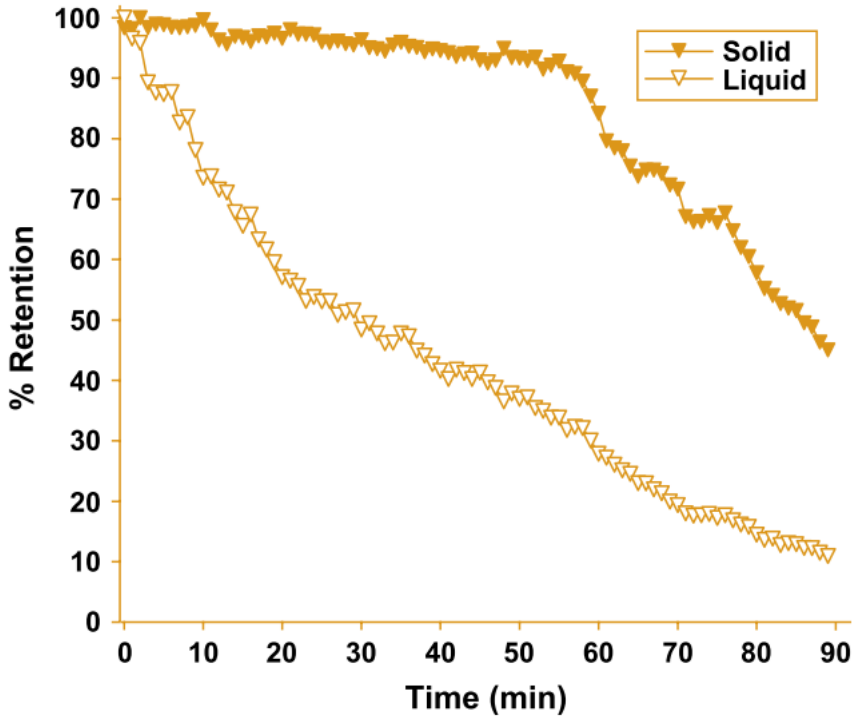

Figure 2.4: Figure showing the characteristic curve of meal volume remaining in the stomach after consumption for a liquid (soft drink) and solid meal (omelette). Taken from (Hellström et al., 2006).

meal volume against the kcal/ml. This has been shown to be due to a feedback mechanism by sensing of nutrients in the duodenum and reproduced by others in primates (McHugh, 1983; McHugh and Moran, 1979; Moran et al., 1999), in dogs (Shahidullah et al., 1975), and in humans (Brener et al., 1983; Calbet and MacLean, 1997). Shahidullah et al. (1975) showed that the sensors controlling the inhibition of gastric emptying are within the first 50cm of the small intestine for dogs, and after this they do not occur in any numbers to significantly affect the emptying.

In human subjects Brener et al. (1983) showed that glucose solutions initially empty at a rapid rate prior to the feedback initiating, this can also be seen in work by Hellström

et al. (2006) shown in Figure 2.4 where almost 50% of the meal is emptied in the first 20 minutes, but only around 10% of the initial meal is emptied between 20 and 40 minutes after the meal. Once the feedback mechanism is initiated then the average flow rate of glucose solutions out of the stomach is reduced to around 2.13 kcal/min (Brener et al., 1983). Calbet and MacLean (1997) studied the emptying rate of different types of calories (glucose, pea peptide hydrolysate, whey peptide hydrolysate, and milk protein) and found that the type of calories also has an effect upon the calorific emptying rate (e.g., milk protein empties faster per calorie than glucose).

Osmolality (a measure of a solutions osmotic pressure) has been shown to have the effect of slowing the gastric emptying rate (Vist and Maughan, 1995), but Vist and Maughan (1995) points out that the effect of nutrients upon the gastric emptying is far greater than that of osmolality. Others however concluded that the osmolality does not influence the gastric emptying (Brouns et al., 1994). Meeroff et al. (1975) suggests that the effect of osmolality upon the gastric emptying rate is due to osmoreceptors within the duodenum, suggesting that these receptors are not present beyond the *ligament of Trietz* (the junction between the duodenum and jejunum) nor within the stomach, hence if there is an effect of chyme osmolality upon the gastric emptying rate is will be due to a feedback mechanism.

Gastric receptors

Gastric distension is seen as a key contributor, along with intestinal nutrient sensing, in satiety after consumption of a meal (Cummings and Overduin, 2007). This idea has been studied over many years, theorising that stretch receptors similar to those in

the skeletal muscles and lungs, initiate signals along the vagal afferent fibres (Paintal, 1954), with most of these receptors been found towards the pyloric region of the stomach. This is supported by more recent work which shows the signals for satiety are carried by vagal afferents (Powley and Phillips, 2004; Williams et al., 2016), more specifically the stretching of the stomach and intestine is detected by GLP1R neurons (Williams et al., 2016). Distension of the gastric walls have also been shown to be a potent stimulant of gastric secretions (Grötzinger et al., 1977), when induced via inflation of a ballon in the fundus.

A study by Carmagnola et al. (2005) attempted to verify the type of receptor used to perceive gastric distension, splitting mechanoreceptors in to two classes: tension receptors, which are sensitive to elongation and contractions, and stretch receptors which are sensitive to elongation only. This work found that the main contributor to fullness was the stretch receptors and not tension receptors.

The effect of viscous meals increasing satiety may also be explained via these gastric stretch receptors, it has been found that viscous meals will occupy the antral region of the stomach more so than lower viscosity meals, increasing the antral distension (Marciani et al., 2001b; Pröve and Ehrlein, 1982), which is in agreement with the findings of Paintal (1954), who identified a greater amount of stretch receptors towards the pyloric end of the stomach.

We can therefore say that gastric distension in increases the stimulation of gastric stretch receptors, will have the effect of increasing satiety, but will also influence the secretion of gastric juices. The secretion increase is mediated through increased Gastrin

secretion due to the distension (Higham et al., 1997; Schubert and Makhlouf, 1993), which will increase the gastric acid secretion (Chaudhri et al., 2006).

2.1.3 Small Intestine

The small intestine forms the main site of absorption of nutrients into the body. It is split up into 3 sections: Duodenum, Jejunum, and Ileum. The Small intestine begins at the pyloric sphincter which controls the passage of chyme from the stomach into the Dudenum and ends with the Ileocecal sphincter which separates the ileum from the large intestine- with a rough length of around 3m (Barrett et al., 2005). The position of the small intestine is shown in Figure 2.5.

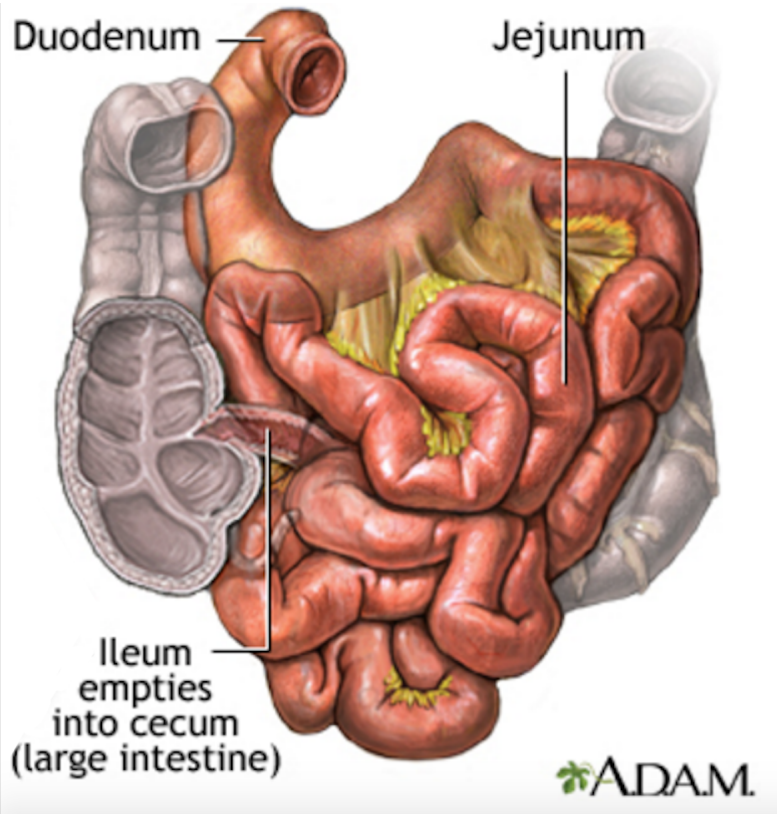

Figure 2.5: Diagram of small intestine taken from US National Library of Medicine (2012)

The Morphology of the small intestine is highlighted in Figure 2.6. There are four layers of tissue which make up the small intestine. The outermost layer is called the *Serosa* or *Adventia* depending upon whether it is next to the *peritoneal cavity* or attaching to the surrounding tissue, respectively (Reed and Wickham, 2009). Moving closer to the lumen the next layer is the *Muscularis propia* which contains a layer of longitudinal muscle and a layer of circular muscles separated by the *Myenteric plexus* (Barrett et al., 2005), these contain nerves which will coordinate the contractions of the two muscle layers (Reed and Wickham, 2009) allowing for the production of different contractile patters (*Peristalsis, Segmentation*, and *Pendular activity*) at different frequencies. The next layer is the *Submucosa*, this contains the blood vessels and lymphatic vessels as well as nerve endings to optimise the functionality of the intestine (Barrett et al., 2005). The final layer and closest to the intestinal lumen is the *Mucosa*, this consists of the *Muscularis mucosa, Lamina propria*, and the *Epithelium* (Barrett et al., 2005). The *Laminar propria* contains the blood and lymphatic vessels which will transport nutrients absorbed through the *epithelium* and digestion hormones (Reed and Wickham, 2009). The Epithelium cells which line the intestinal lumen are specialised to optimise the absorption of nutrients with the surface of each cell having small projections known as *microvilli*.

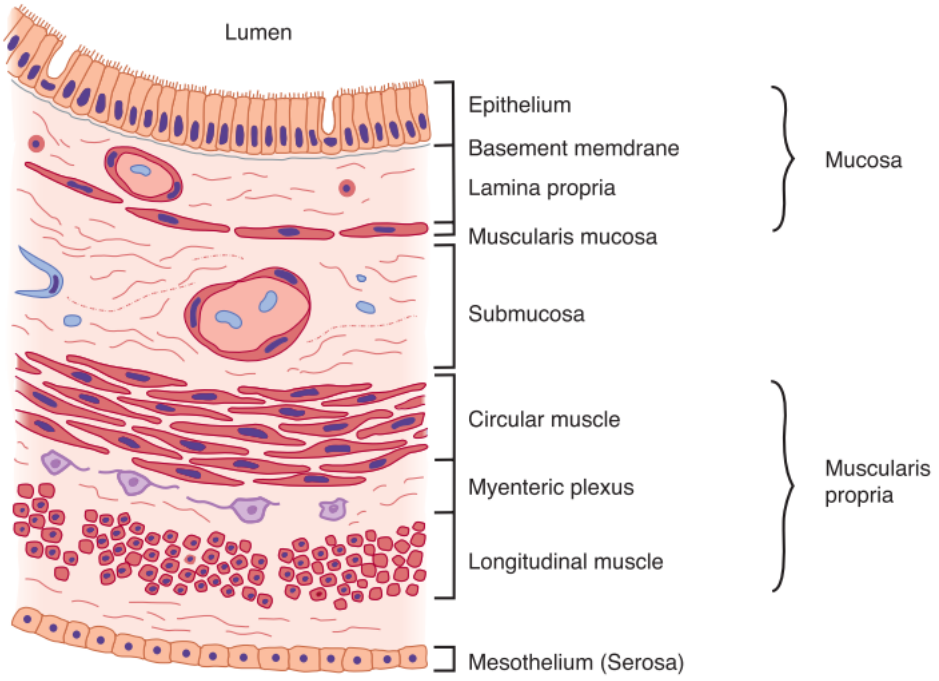

Figure 2.6: Small intestine morphology (figure adapted by (Barrett et al., 2005) from (Barrett, 2005))

Intestinal Mucosa

Figure 2.7 shows the different features of the small intestine mucosa at 4 different length scales, highlighting how the *Plicea circulares*, *villi*, and *microvilli* play a role in increasing the overall surface area of the small intestine. A major feature of the small intestine Mucosa is the *villi*; these are small protrusions from the surface of the intestine, with a height of around 690μm in the duodenum close to the stomach increasing to around 720μm further along the duodenum (Hasan and Ferguson, 1981), the height of these protrusion is greatest in the jejunum (Lentle and Janssen, 2011). The *microvilli* create a *brush border* along the length of the intestine wall, where enzymes such as glucoamylase can act (Reed and Wickham, 2009). These folds could also aid the formation of a *unstirred water layer* (a layer covering the intestinal membrane which

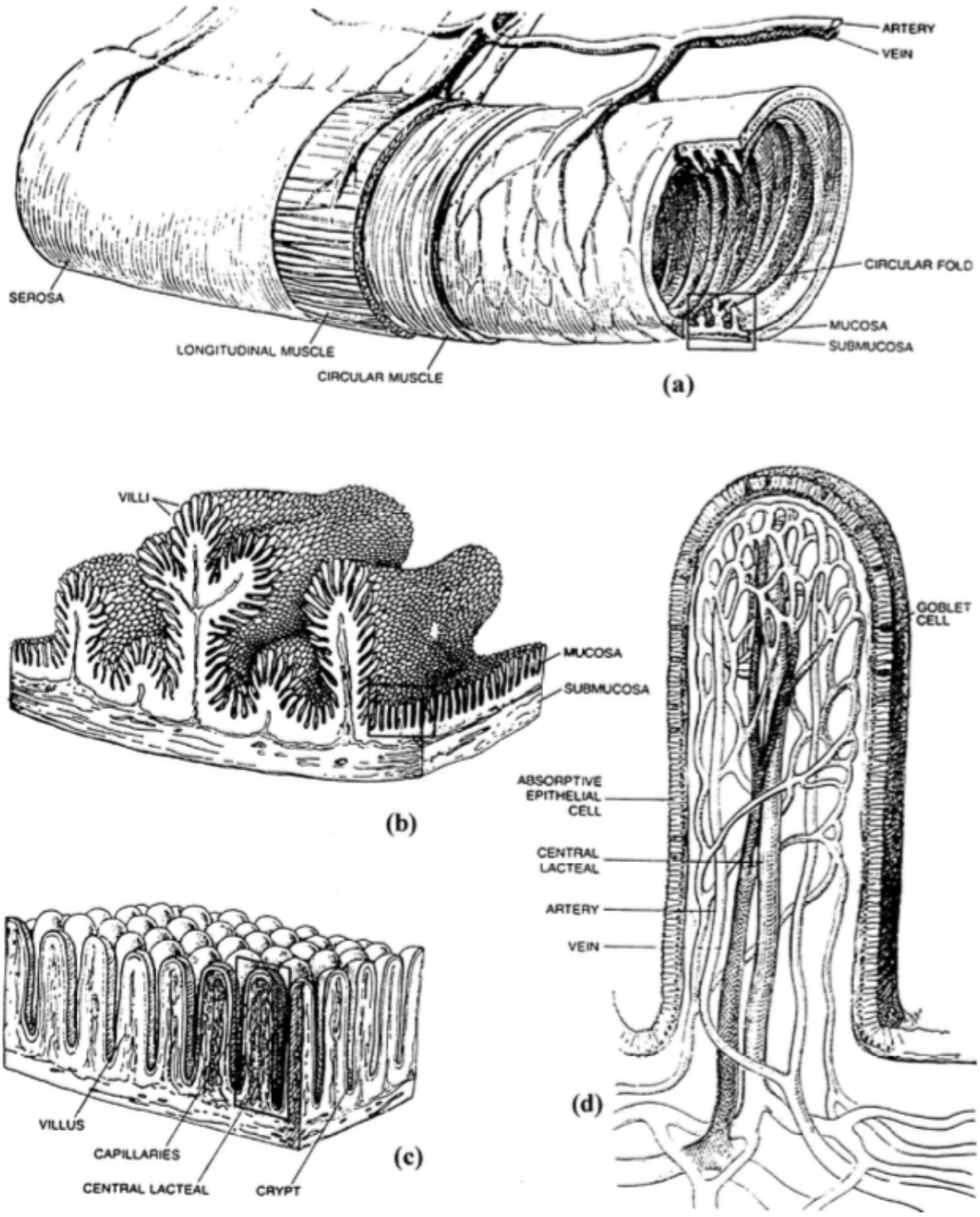

Figure 2.7: Features of the small intestine mucosa at different length scales: (a) mesoscale, (b) submesoscale, (c) microscale, and (d) submicroscale (figure adapted by (Stoll et al., 2000) from Moog (1981))

nutrients must diffuse through before they can be absorbed), which has been estimated to be around 20-45μm thick Levitt (2013), and has been viewed as the limiting factor in nutrient/drug absorption (Levitt, 2013; Sallee et al., 1972). The increase in surface area due to the presence of the villus is thought by some to have the function of maximising the nutrient absorption- this idea is stated in textbooks, e.g., (Barrett et al., 2005), whilst others consider this 'dogma' (Strocchi and Levitt, 1993), showing, with the assumption of 40μm spacing between villi, that rapidly absorbing nutrients such as glucose will not diffuse down the length of the villi but that the majority of the absorption will take place at the tips, estimating only 2% of the surface area will be utilised for the absorption process (Strocchi and Levitt, 1993). Another group produced a 2D lattice Boltzmann model of the intestinal villi to analyse the effect of villi motility upon the absorption of nutrients (Wang et al., 2010). The model shows that a micro mixing layer is produced from the villi motility which when coupled with the macro-scale mixing, due to the intestinal wall contractions, enhances the absorption of nutrients. The model also highlights with and without the villi motility the majority of absorption occurs at the tips of the villi which shows agreement with the work by Strocchi and Levitt (1993). Similar results were also found using a 3D lattice Boltzmann model of the intestinal villi (Lim et al., 2015) also agree that the villi motility significantly enhance mixing and absorption of nutrients, as well as showing the absorption of nutrients such as glucose occur at the tips of the villi.

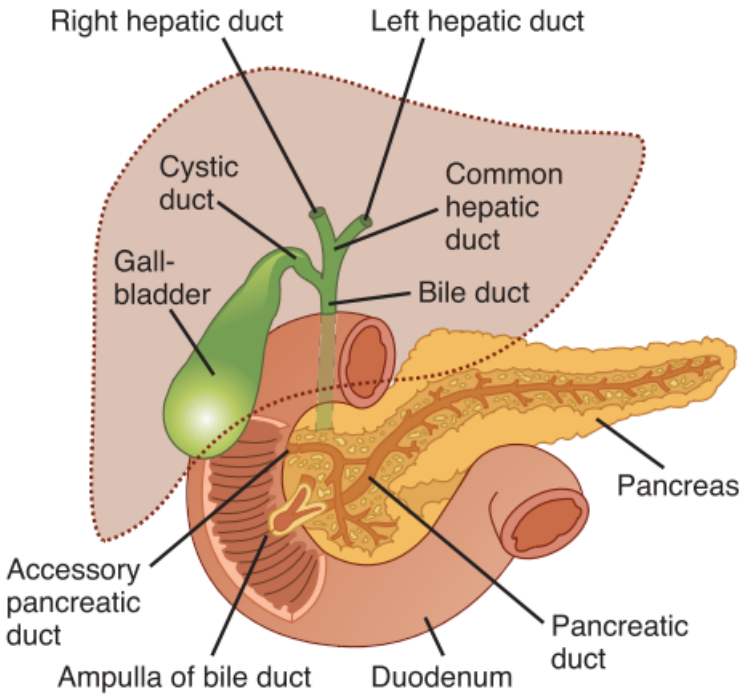

Figure 2.8: Diagram showing the Duodenum with the ducts connecting to the liver (dotted outline), Gallbladder, and Pancreas. Figure taken from Barrett et al. (2005)

Secretions

The chyme entering the duodenum from the gastric compartment will contain the gastric secretions and therefore will have a low pH (around pH 2 for optimal activity of Pepsin (Piper and Fenton, 1965)). The optimal pH for the enzymes in the small intestine is higher, for pancreatic α-amylase the optimal pH will be closer to pH 7 (Sky-Peck and Thuvasethakul, 1977). To neutralise the acidic conditions, from stomach, and to introduce digestive enzymes to the small intestine secretions are introduced from the gall bladder (Cystic duct), liver (Common hepatic duct), and the pancreas (Pancreatic duct), these are shown in Figure 2.8. These join the duodenum at the *Ampulla of Vater*, with the flow into the duodenum controlled by the *Sphincter of Oddi* (Barrett et al.,

2005). The *Sphincter of Oddi* (or *Ampulla of bile duct*) will act as either a pump or resistor dependent upon the pressure difference between the ducts and duodenum, as well as preventing a reflux of intestinal content into the ducts (Woods et al., 2005).

Flow in the Intestine

Movement of the chyme in the small intestine is controlled by contractions of the intestinal wall, contraction of the circular and longitudinal muscles produces peristaltic movements, to propel the content aborally, and segmentation and pendular contractions which aid the mixing of the content. During the consumption of an average meal the chyme entering the small intestine from the stomach will be a mixture of solid particles, liquid and gases, additional liquid will be added in the form of pancreatic and intestinal secretions in the duodenal section of the intestine. As the chyme moves along the the intestine, the liquid will be absorbed, and the chyme will behave more liquid a particulate aggregate (Lentle and Janssen, 2008). The flow and absorption will be primarily controlled by the liquid the particles are suspended in, affected by the concentration, shape, size and buoyancy, this will change to a chyme whose property are controlled by the strength, plasticity, elasticity, cohesion and permeability of the solids (Lentle and Janssen, 2008).

It is evident that the flow in the intestine will be influenced by the rheological properties of the liquid phase, and the effective viscosity when a multiphase chyme. The viscosity of the centrifuged liquid phase in the small intestine was around 1.3 mPa s for pigs (Takahashi and Sakata, 2004), and 6.5-9.5 mPa s for dogs (Dikeman et al., 2007), when natural diets were maintained, the liquids were also newtonian in nature.

The addition of thickeners will likely produce chyme which is shear-thinning (Lentle and Janssen, 2008), with the addition of CMC (carboxymethylcellulose) added to a rice meal fed to pig significantly increasing the viscosity of the liquid phase, and moving it from a newtonian to a shear thinning fluid (McDonald et al., 2001). This has implication on the mixing of meals in the intestine, as greater shear will be induced near the intestinal wall than towards the centre of the lumen, hence the effective viscosity will be greater towards the centre of the lumen, and mixing accordingly reduced (Lim et al., 2015). The addition of guar gum to a meal was found to significantly increase the zero-shear viscosity in the jejunum of pigs, increasing to around a maximum of 6.75 Pa s, after 50 min for a meal with 40 g/kg of guar gum, compared to a maximum measured zero-shear viscosity of 0.05 Pa s from a control meal (Ellis et al., 1995), this addition of guar gum also reduced the maximum plasma glucose concentration and AUC (area under the curve), though it should be noted that gastric emptying was not shown, and thus this may have also influenced the rate of glucose appearance in the plasma.

Effect of digesta properties on flow have been studied using CFD techniques (de Loubens et al., 2013; Love et al., 2013; Tripathi, 2011a; Tripathi et al., 2011). The results highlight that intestinal digesta with higher effective viscosity and increased shear thinning (e.g., a meal with high fibre or insoluble residue) will promote creep flow and reduce vortices (Love et al., 2013), which the author points out will impair absorption efficiency if the transit time is not increased. This explains the results by Ellis et al. (1995) which show decreased peak and lower AUC for blood glucose when guar gum is added to the meal.

Rheology of model solutions

This work will try to simplify complex food structures to simple model meals, in order to simulate the digestive processes. Most of the work will focus upon glucose/starch liquid solutions with the addition of thickeners in order to modulate the viscosity and study the effect of mass transfer in the intestinal lumen. The thesis of Fonseca (2011) looked at engineering digestion, and provided viscosity profiles for different thickeners in 55mM glucose solutions (Figure 2.9). The works highlight the shear thinning nature of the different solutions with low shear rate resulting in higher viscosities, and increasing thickener concentrations resulting in high viscosities. Though it should be noted that the maximum shear likely in the small intestine is $0.5\,s^{-1}$, which is likely to occur near the boundary (de Loubens et al., 2013; Lim et al., 2015; Love et al., 2013). This means that without the effect of secretions reducing the viscosity of the digesta (Marciani et al., 2000), it is unlikely an order of magnitude reduction in the effective viscosity is going to be achieved due to the shear thinning nature of these solutions.

Carbohydrate Digestion & Absorption

Carbohydrates are the main source of energy in the human diet, of which starch is the most common type (Singh et al., 2010). Starch can be made up of two different molecules amylose and amylopectin. Amylose consists of a linear chain of α-D-glucose units joined by α-1,4 glycosidic linkages, amylopectin will have a more branched structure wit the α-D-glucose units joined by α-1,4 and α-1,6 glycosidic linkages (Singh et al., 2010). These molecules cannot be absorbed directly into the body and require breaking down to smaller molecules prior to absorption, this is achieved through hydrolysis

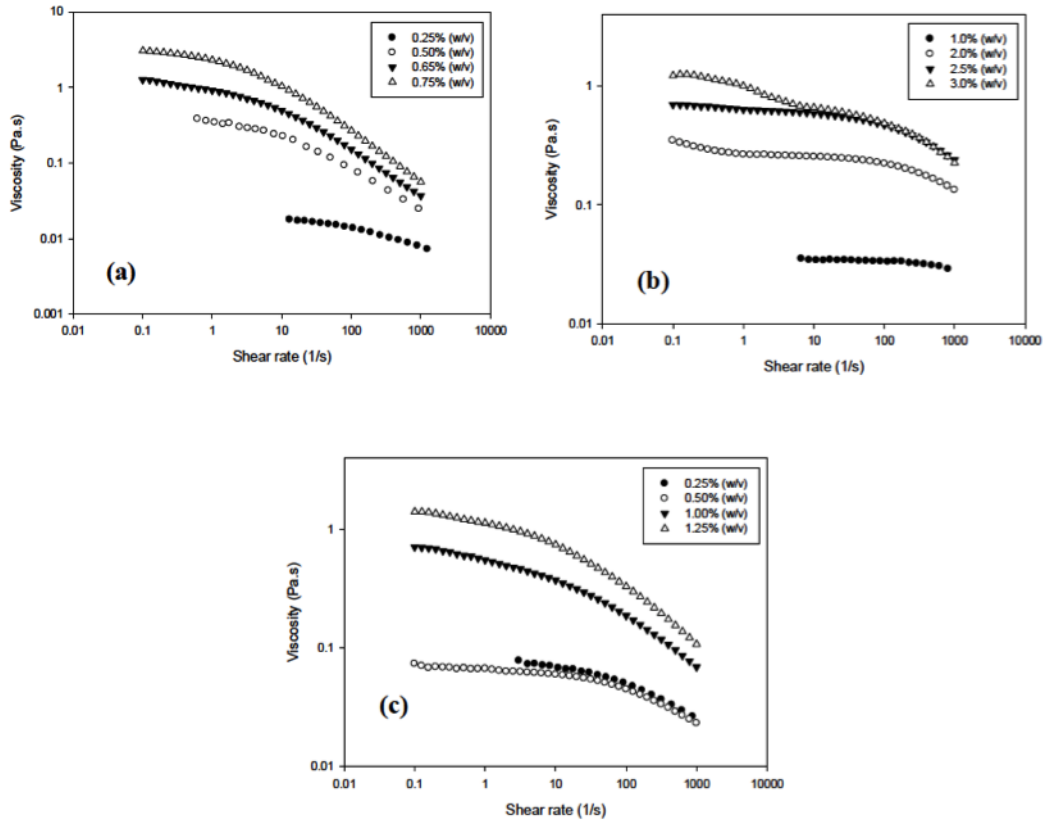

Figure 2.9: Viscosity for solutions of 55 mM glucose with different thickeners (a) guar gum, (b) high methoxyl pectin, and (c) CMC at different concentrations, taken from the work by Fonseca (2011).

through the action of α-amylase enzymes. This process of hydrolysis will begin in the mouth. As the food is masticated it will be mixed with saliva, this saliva will contain salivary α-amylase which will begin the process of hydrolysis of the starch by breaking hydrolysing the α-1,4 glycosidic linkages. Once the food bolus is swallowed it will enter the stomach which has an acidic environment, this will be lower than the optimal pH range of the α-amylase (Sky-Peck and Thuvasethakul, 1977) and the activity will be reduced. But it should be noted that the gastric secretions maybe slow and penetrating boli in the gastric compartment, this is shown in work by Marciani et al. (2001b) who

measured dilution by MRI in high viscosity meal (≈30 Pa.s), showing only the outer layers were significantly diluted within the first hour. This implies that salivary α-amylase may still be able to hydrolyse starch within bolus (solid/viscous liquids) in the stomach.

Once in the small intestine the pH will be increased due to the pancreatic secretions, and pancreatic α-amylase introduced in to the chyme. This will continue the process of hydrolysing the starch molecule started by the salivary α-amylase, this results in 2 main products malto-oligosaccharides, which contain two or more glucose molecules joined by α-1,4 glycosidic linkages, and limit dextrins which contain glucose molecules joined α-1,6 glycosidic linkages, which the α-amylase cannot hydrolyse, along with some α-1,4 glycosidic linkages (Williamson, 2013). The final steps of breakdown are carried out by brush-boarder enzymes, there are two types: maltase-glucoamylase and sucrase-isomaltase (Sim et al., 2008). These brush boarder enzymes are joined to the membrane of enterocytes on the intestinal wall and can hydrolyse both the α-1,4 and α-1,6 glycosidic bond, this leads to a final product of predominantly glucose molecules.

The movement of glucose across cell membranes is controlled mainly by two classes of transporters GLUTs (GLUcose Transporters) and SGLTs (Sodium-dependent GLucose co-Transporters). Glucose in the small intestine will be transported by the SGLT-1 transporter, these molecules are permanently present on the brush boarder membrane. The SGLT1 transporters work by the process of active transport with two sodium molecules (Na^+) transported for each glucose molecule (Williamson, 2013). When high concentrations of glucose are sensed in the small intestine GLUT2 transporters are moved to the luminal side of the intestinal membrane to mediate the facilitated transport of glucose (Williamson, 2013). GLUT2 transporters are also found on the basolateral membrane to

transport the glucose out of the enterocytes into the blood (Cheeseman, 2002). Fructose molecule will be transported across the membranes by GLUT5 transporters (Ebert and Witt, 2016). The presence of GLUT2 transporters on the luminal side of the membrane can also be stimulated by some artificial sweeteners, and it has been found that the transporters are permanently fixed to the luminal side in diabetes (Williamson, 2013).

This movement over the membrane can be described as *transcellular transport* and is the method utilised to transport ions and small molecules, two other pathways can be described: the first, *transcytosis transport*, is a method of transporting *macromolecules* across the membrane, this is done within membrane bounded carrier; the second, *paracellular transport*, is the movement of small molecules between cells (Tuma and Hubbard, 2003).

The work in this thesis will focus on the absorption of glucose and this will occur via the transcellular pathways, hence the others will not be considered, though other groups when modelling small intestine have included all absorption pathways when considering drug absorption (Stoll et al., 2000).

2.2 Modelling Gastric Processes

As previously stated the stomach has 4 main functions:

- Physical breakdown (Solid bolus/particles) & mix food
- Chemical breakdown (macronutrients)
- Act as a reservoir for food
- Control release to Duodenum

These processes have been analysed from a variety of perspectives: *In Vivo*, *In Vitro*, and *In Silico*.

This section contains works adapted from two published book chapters (Moxon and Bakalis, 2016; Moxon et al., 2015) and will cover some of the *in silico* gastric emptying and nutrient/drug absorption models developed from literature.

2.2.1 Gastric Emptying

The gastric emptying of liquids from the stomach has been shown to be exponential with time for low/non nutrient meals (Hellström et al., 2006), but as the amount of nutrient increases the emptying occurs in two phases (Brener et al., 1983; Calbet and MacLean, 1997), an initial rapid emptying phase followed by a linear emptying phase once the nutrient based feedback mechanism is initiated, similar to the results shown by Hellström et al. (2006) in Figure 2.4. With the case of more solid meals a lag phase is generally seen, whereby bolus must be broken down in size before they can empty from stomach. Characteristic curves for liquid and solid meals are shown in Figure 2.4.

A variety of different models proposed to describe the gastric emptying rate, these generally stem from the work byHunt and Stubbs (1975) who applied exponential equations to describe the gastric emptying rate, and linked this to the nutrient density. Equation 2.1 shows a common exponential emptying equation used (Hellström et al., 2006; McHugh and Moran, 1979):

$$m(t) = m_0 e^{-\gamma m} \tag{2.1}$$

here m is the mass of meal remaining in the stomach, t is the time after consumption of a meal of mass m_0, and γ is the rate of gastric emptying. A term for the gastric half-time (time for half the content to empty) can also be defined as:

$$t_{1/2} = \frac{\ln(2)}{\gamma} \tag{2.2}$$

This equation has been modified by others to take into account the lag phase commonly observed during the emptying of solid meals. One of these modifications included adding an additional parameter, β which is a shape factor (Siegel et al., 1988) (a term which has no physiological interpretation) and was also used to describe the emptying of solids and liquid (Kong and Singh, 2008):

$$m(t) = 1 - \left(1 - e^{\gamma t}\right)^{\beta} \tag{2.3}$$

A delayed sigmoidal model has also been proposed to describe the emptying of solids (Kong and Singh, 2009), where β represents the lag phase:

$$m(t) = (1 + \beta\gamma t)e^{-\gamma t} \tag{2.4}$$

Elashoff et al. (1982) also proposed a taking the following form:

$$y(t) = \exp((-\gamma t)^{\beta}) \tag{2.5}$$

The generic curves for these three black box approaches (Equations 2.1, 2.3, & 2.4) are shown in Figure 2.10, where Equations 2.3 & 2.4 can be seen to have curves more similar to what would be expected from the emptying of solids, i.e., an amount of time is required to break the solids down before it can empty.

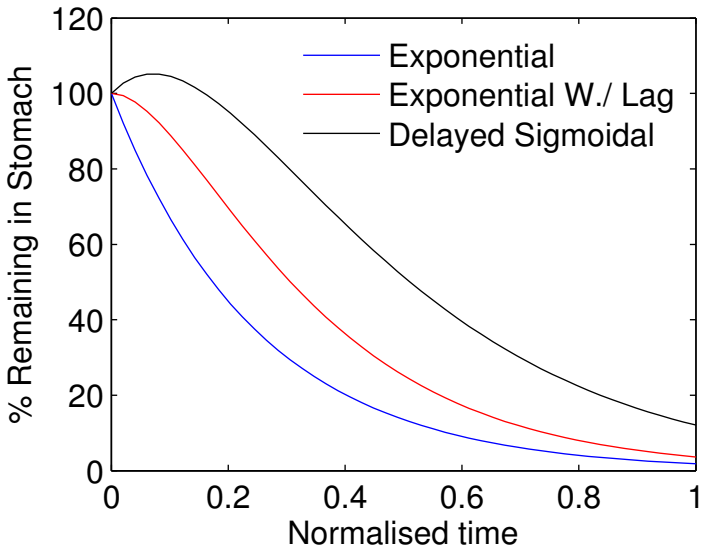

Figure 2.10: Emptying of a meal from the stomach following Equations 2.1, 2.3, & 2.4

A different approach was taken by Dalla Man et al. (2006). Validating against glucose absorption rates the group modelled the stomach as two compartments; the first with a Dirac delta input to signify the meal consumption of mass, m_0, and a term for the grinding of a solid meal, at rate k_{12}, the second has an input from the first compartment and empties at rate, k_{empt}, into the small intestine:

$$\frac{dm_{sto1}}{dt} = -k_{12}m_{sto1}(t) + m_0\delta(t) \tag{2.6}$$

$$\frac{dm_{sto2}}{dt} = -k_{empt}m_{sto2}(t) + k_{12}m_{sto1}(t) \tag{2.7}$$

A key area of the model presented in the paper is the description of k_{empt}. The rate of emptying is presented as a function of the initial input level, m_0, and the total mass of glucose remaining in the stomach m_{sto}, this agrees with other work that the gastric emptying rate will be a function of the nutrient density (Hunt and Stubbs, 1975), and takes the following form:

$$k_{empt}(m_{sto}) = k_{min} + \frac{k_{max} - k_{min}}{2} [\tanh(\alpha(m_{sto} - bm_0)) - \tanh(\beta(m_{sto} - cm_0)) + 2] \tag{2.8}$$

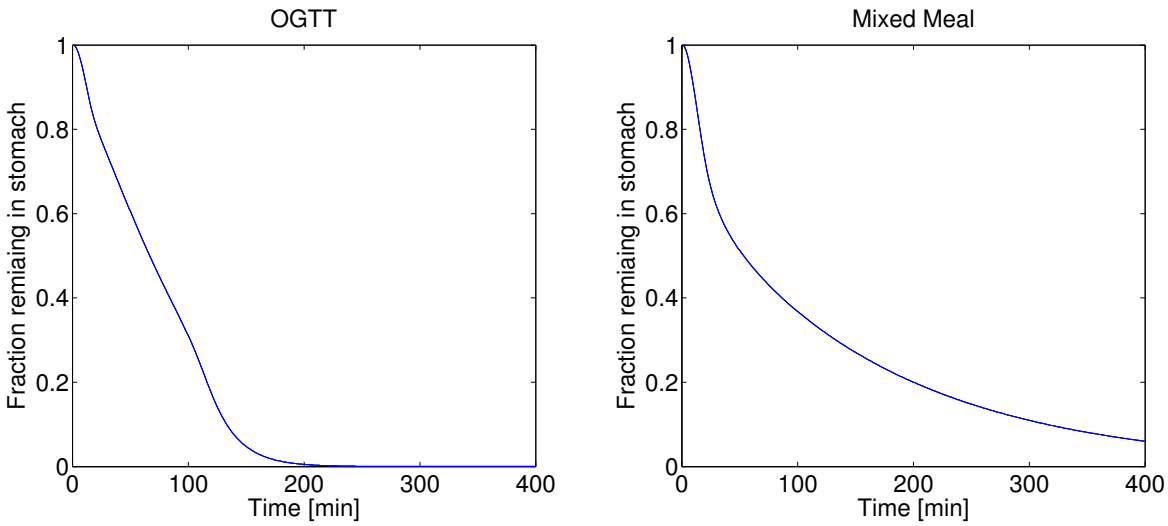

Figure 2.11: The graphs show the simulated emptying curves using Equations 2.6:2.8 and data from the paper by Dalla Man et al. (2006), the first plot is for a OGTT and the second for a mixed meal.

This introduces the following parameter values which require estimation, a minimum and maximum emptying rate (k_{min} and k_{max}). The parameters b and c are fractions of the meal remaining in the stomach, b is the fraction for which the rate decreases at $(k_{max} - k_{min})/2$ and c the fraction for which the rate increase at rate $(k_{max} - k_{min})/2$.

The parameters α and β represent the rate at which the emptying rate decreases to a minimum or increases to maximum rate, respectively, with the parameter expressed as follows:

$$\alpha = \frac{5}{2m_0(1-b)} \tag{2.9}$$

$$\beta = \frac{5}{2m_0 c} \tag{2.10}$$

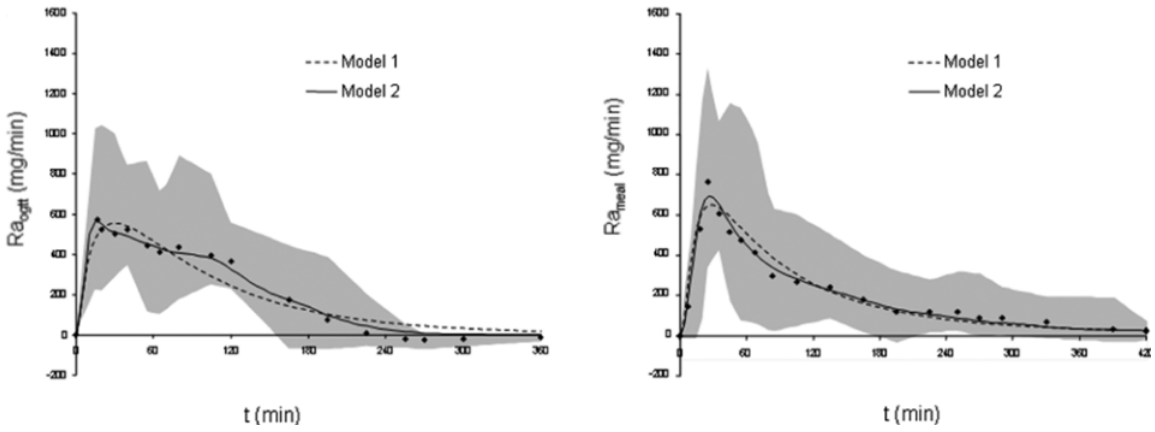

Figure 2.12: Results from model output and experimental data from Dalla Man et al. (2006) showing the rate of glucose appearance for an oral glucose tolerance test meal and a mixed meal. Model 1 is the prediction when k_{empt} is assumed constant and Model 2 when k_{empt} is described by Equation 2.8

The emptying simulated emptying curves are shown in Figure 2.11, with the OGTT (Oral Glucose Tolerance Test) curve showing rapid initial emptying followed by a linear period. The mixed meal shows a rapid initial emptying followed by a more exponential curve, but no experimental data for the gastric emptying rate was given to verify the curve. The model instead was fit to experimental results for the absorption rate of a mixed meal and a standardised oral glucose tolerance test meal (Figure 2.12), with 5

parameter requiring estimation for each meal. The work compared this approach to the approach by Elashoff et al. (1982) and Lehmann and Deutsch (1992) along with a linear model (Equation 2.8 set to constant). The work quotes the sum of squared residual (RSS) to compare the models and states the best fit is when the non-linear empty model is used (model using Equation 2.8), giving the lowest RSS for both a OGTT meal and a mixed meal, but each model contains a different number of fitted parameters (Elashtoff: 4, Lehmann: 3, Dalla Man linear:2, Dalla Man non-linear: 5), so it is improper to compare the RSS directly. Applying the AIC (Akakie Information Criterion) to the work (explained in Section 2.5, Equation 2.94) to penalise for increasing number of parameters, we find similar results as to when comparing directly the RSS, with the non-linear model giving the best fit, and being the most appropriate model.

Physiologically the model is limited: whilst implementing an emptying rate which is dependent upon the nutrient content offers good agreement with the experimental data, with regards to glucose absorption, *in vivo* this is likely controlled via a feedback mechanism (Brener et al., 1983; Calbet and MacLean, 1997). Hence, a more comprehensive description of the intestinal processes is likely required to implement a physiological description of the emptying rate post prandially.

Bürmen et al. (2014) approached the problem by applying a double Weibull model (Equation 2.11) for the gastric emptying of solid pellets to each individual in a trial, rather than the average of all the individuals as is commonly carried out. The experimental data for the paper was gathered from literature, this described the gastric emptying of pellets when consumed with a meal, the authors assumed that the meal and pellets emptied at the same rate. Three mathematical models were used to fit the

data, two of the models from literature from Siegel et al. (1988) (Equation 2.3) along with the model developed by Elashoff et al. (1982) (Equation 2.5)

The third model proposed by Bürmen et al. (2014) was a weighted double Weibull model taking the following form:

$$m(t) = (100 - H)\exp(-(t/\eta_1)^{\beta_1}) + H\exp(-(t/\eta_2)^{\beta_2}) \tag{2.11}$$

This gives 5 parameters: a weight (H), two parameters for the *scatter* (η_1, η_2) and two parameters for the shape of the curve (β_1, β_2).None of the three models had a physiological interpretation of the parameters. The effectiveness of the different models to describe the experimental data were compared using the Akaike Information Criterion (AIC), which allows a comparison of the sum of squared errors for models with different numbers of fitted parameters and different numbers of experimental data points.

Figure 2.13 shows the results for 8 individual Bürmen et al. (2014) simulated using results by Wilding et al. (1991). The experimental results highlight the variability in emptying profiles for individuals given the same meal. the profiles show the simulated results with the Elashoff (dashed line) and Siegel (dotted line) models giving similar curves. These give good fits when the emptying profile is simple, e.g., profile w2 in Figure 2.13 which follows an almost exponential curve. Some of the emptying patterns show more complex curves e.g., profile w1 which takes around 10 hours for the content to empty around half of the contents profile, w5 which seems to show rapid emptying around 250 minutes of around 25% of the total volume, which is preceded and followed by a more steady emptying rate. These more complex patterns of emptying appear to be described well by the double Weibull model, but the model parameters offer no

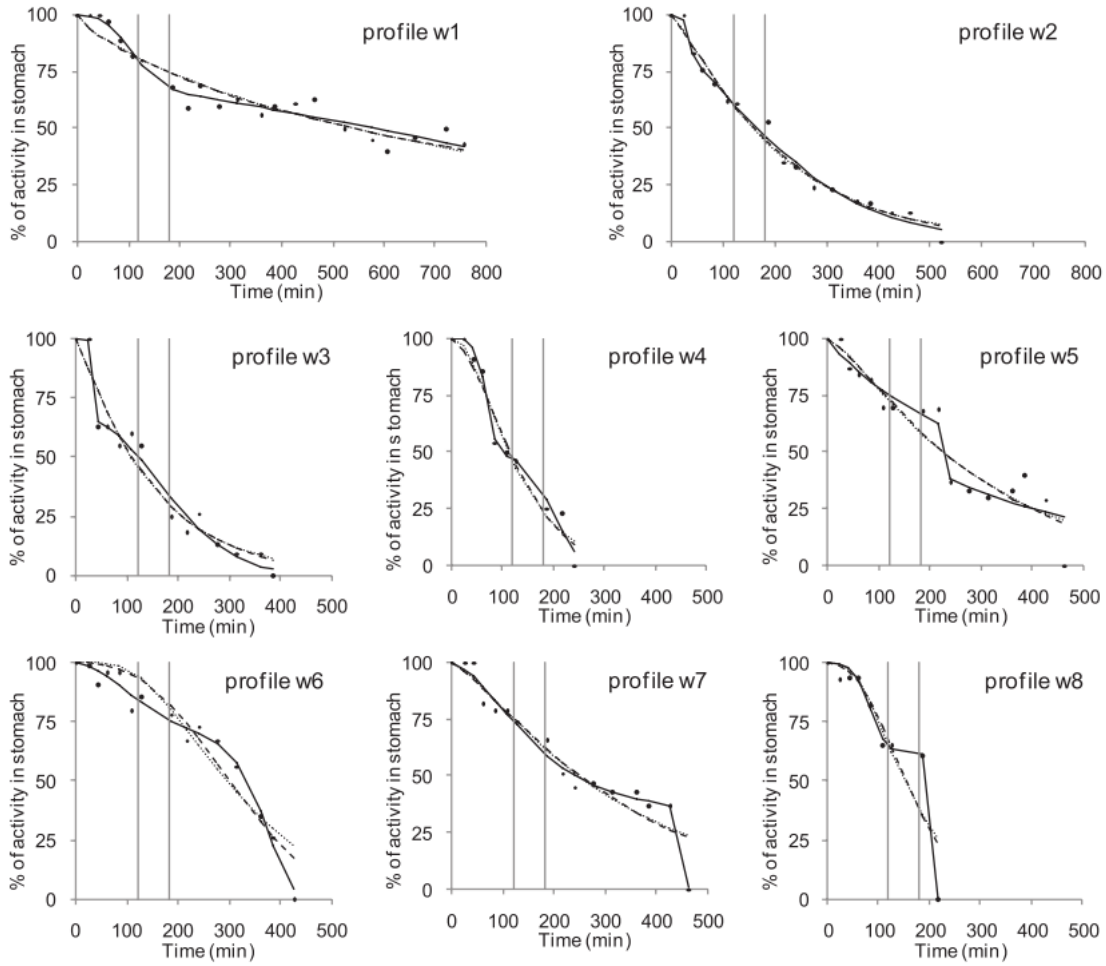

Figure 2.13: The figure showd gastric profiles for 8 different individual taken from Bürmen et al. (2014). Bürmen et al. (2014) used experimental data from Wilding et al. (1991) (points on graphs), with lines showing: Elashoff model output (dashed line), Siegel model output (dotted line), and Double Weibull model output (solid line). The first vertical line represent when a drink was given, second vertical line when a second meal was given.

physiological interpretation and hence the model give no insight into why these patterns occur or why there is such variability between individual. When comparing the results for the different models and taking into account the number of parameters i.e., using AIC, the double Weibull model gives the lowest value, hence being the most appropriate

model, despite requiring a greater number of parameters to fit, except when comparing to results by Wilding et al. (1991), which Bürmen et al. (2014) points out could be due to the low number of experimental data points compared to other data sets.

Hunt and Stubbs (1975) described the gastric emptying rate as a function of nutrient density and linked this to duodenal receptors, one set for osmotic pressure of monosaccharide products of carbohydrates and one set for fatty acids. A linear relationship was found when plotting the kcal emptied after 15 min or 45 min and the nutrient density of the meal (kcal/ml), for a variety of different nutrient sources and initial meal volumes. A relationship was also plotted for the for the ratio of half emptying time ($t_{1/2}$) to initial meal volume (V_0) against the exponential of the minus of the meal calorific density (ρ_n). A logistic relation was proposed to describe the relationship:

$$\frac{V_0}{t_{1/2}} = \frac{a_1}{1 - a_2 e^{-a_3 \rho_n}} \tag{2.12}$$

This equation includes 3 unknown constants. The values were predicted using regression analysis, a_3 was found to be equal 1. $a_1 = 5.56$, and $a_2 = 0.93$, thus Equation 2.12 becomes:

$$\frac{V_0}{t_{1/2}} = \frac{5.56}{1 - 0.93 e^{-\rho_n}} \tag{2.13}$$

This approach is a first attempt at including a feedback mechanism, although without modelling the hydrolysis and mass transfer of nutrients within the small intestine the approach is limited to simple meals. The authors speculate that the feedback from duodenum to gastric emptying rate for carbohydrates is due to the sensing of osmotic pressure of monosaccharides, this implies for starch meals unless hydrolysis is rapid the

nutrient density will not be sufficient to predict rate of emptying without a delay term to take into account the hydrolysis. It should also be noted that more recent research links the sensing of sugars in the intestine to taste receptors, e.g., T1R2/T1R3 (Depoortere, 2014; Hass et al., 2010; Young, 2011; Zhang et al., 2015), and not sensing of osmotic pressure, as suggested by Hunt and Stubbs (1975), though this does not change the fundamental idea of the feedback mechanism.

2.2.2 Gastric Secretions

Modelling of gastric secretions has been approached from a number of perspectives; firstly modelling the total secretions of gastric juices (Marciani et al., 2001b; Sauter et al., 2012), whilst others look in more detail at the secretion of gastric acid and how the cell population of different gastric cell types differentiate from stem cells and die to look at secretion over larger time scales (Joseph et al., 2003; Marino et al., 2003).

One experiment outlining the volume extent of gastric secretions is that by Marciani et al. (2000), in this work 4 non-nutrient liquids of viscosity 0.01, 0.2, 2, and 11 Pa.s were consumed and the viscosity (measured by two methods: sampling via nasogastric tube and measuring η_0 on rheometer & echo-planar imaging) and gastric emptying rate (from echo-planar imaging) were measured. It was shown within 40 minutes of the solution been consumed the viscosity of the gastric chyme was reduced from 11Pa.s to 0.3Pa.s, and from 0.01Pa.s to 0.005 Pa.s. This highlights how the secretion rate is not linear, and that higher viscosity solutions will induce greater secretion rates possibly due to increased distension of the antral region of the stomach (Grötzinger et al., 1977; Marciani et al., 2001b; Pröve and Ehrlein, 1982).

The same group looked into the emptying of low and high viscosity meals with low and high nutrient content (Marciani et al., 2001b). From the experimental data they put together a model to look into the secretion rates, this took the form of two ordinary differential equations, one representing the meal volume (v_m), the other the secretion volume (v_s), showing how these vary over time (t):

$$\frac{dv_m}{dt} = -pv_m \tag{2.14}$$

$$\frac{dv_s}{dt} = kv_m + ds_0 - pv_s \tag{2.15}$$

here, p is the rate constant of gastric emptying, ds_0 is the basal secretion rate, and the secretion rate is also linked to the volume of meal in the stomach by rate constant k.

This approach showed similar results to those measurements taken, but did not take into account any meal properties on the emptying rate, such as viscosity or nutrient content which has been shown to affect the emptying rate, nor was the secretion linked to these factors only the meal volume.

Sauter et al. (2012) proposed two models for the gastric secretions, the first was through two non coupled ordinary differential equations:

$$\frac{dv_m}{dt} = -kv_m \tag{2.16}$$

$$\frac{dv_s}{dt} = -k_s(v_{s,max} - v_s) \tag{2.17}$$

The secretion rate here is not linked to the meal volume, but has a maximum secretion volume $v_{s,max}$ and secretion rate k_s.

Like Marciani et al. (2001b) this model does not take a mechanistic approach, neither linking the secretion rate nor emptying rate to chyme properties.

The authors attempted to apply a more mechanistic approach by linking the secretion rate to the meal volume, using two coupled ordinary differential equations:

$$\frac{dv_m}{dt} = -kv_m - k_{ms}v_m + k_{sm}v_s \tag{2.18}$$

$$\frac{dv_s}{dt} = -k_{sm}v_s + k_{ms}v_m \tag{2.19}$$

these introduce two new rate constants, which the authors try and give physiological justification to. The first, k_{ms}, is takes into account the ability of the emptied meal to stimulated gastric secretions (feedback). The second, k_{sm}, describes how the secretions inhibit the gastric emptying of a meal.

The parameter estimation for the second model (Equations 2.18-2.19), using *in vivo* measurement, showed that the secretion rate constant due to a meal was greater than that of secretions inhibiting emptying for a viscous chocolate drink, with the former being 2.3 times larger than the latter value. It was also calculated from the model that the secretion rate was between 48% and 74% of the original volume of the viscous chocolate drink. Marciani et al. (2001b) calculated a secretion volume of between 29% and 34% of the original meal volume for a high nutrient high viscosity meal, although the calorific content of Sauter et al. (2012) was higher (450kcal to 322kcal). The rheological properties of neither meal were given so cannot be compared. Neither of these model provide any predictive capability as the parameters require fitting against *in vivo* data from MRI studies.

A more complex approach to the secretion of gastric acid was taken by Marino et al. (2003). This took work originally produced by Joseph et al. (2003) which modelled both the differentiation of stem cells in the antrum and body (corpus) of the stomach and the death rate of cells, before modelling the rate of secretion from the cells. This lead to a number of ordinary differential equations modelling the following: Antral stem cells, corpus stem cells, G cells, corpus D cells, antral D cells, ECL cells, and Parietal cells. The following hormonal secretions were modelled: Antral gastric, corpus gastrin, antral somatostatin, corpus somatostatin, and histamine. Secretions into the stomach for the following components were also modelled: antral gastric acid, corpus gastric acid, antral bicarbonate, and corpus bicarbonate. Finally the neural stimuli of the central and enteric nervous system were modelled.

Marino et al. (2003) modified this approach by removing the equation for corpus gastrin and adding a delay function on the corpus gastric acid secretion, along with this histamine and ECL cells are also removed from the model.

A delay of 30 minutes for the secretion of corpus gastric acid upon stimulation by corpus gastrin was chosen, and simulations over 24 hours found that there was no significant difference between the results of the original and new model. Over shorter periods of time it was assumed that the cell population remains constant, and the series of equations was reduced to 8 with similar results to the original 18 equation model. This highlight how the addition of a delay term to the model allows reduction in the number of model equations whilst retaining the same accuracy of output.

2.3 Modelling the Small Intestine

From a mass balance based approach the small intestine has been modelled as a Continuous Stirred Tank Reactor (CSTR) (either one or multiple in series), or a Plug Flow Reactor (PFR). These approaches have been taken from both a pharmacokinetic (Di Muria et al., 2010; Stoll et al., 2000; Yu and Amidon, 1999; Yu et al., 1996), with reviews and overviews by numerous authors (Hoang, 1995; Peng and Cheung, 2009; Urso et al., 2002), and from a food research perspective (Bastianelli et al., 1996; Dalla Man et al., 2006; Penry and Jumars, 1986, 1987; Taghipoor et al., 2014, 2012).

To compare the different types of reactor systems used to represent the small intestine Yu et al. (1996) used small intestinal transit time data from numerous publications and compared that to simulated results: (i) for a single continuous stirred reactor, (ii) for multiple in series and, (iii) for a plug flow model. Analysing the data set they found that the mean transit time through the small intestine was 199 min, with a standard deviation of 78 min and 95% confidence interval of 7 min (Yu et al., 1996). To compare the models to this data, parameter were estimated and the sum of squared errors (SSE) found. The parameters estimated were (i) the velocity and dispersion rates for the plug flow reactor model, and (ii) rate constants for each compartment in the CSTR models. The models were then compared to see which offers the best approximation for the transit data. The single compartment model had a higher SSE than the multi compartment or PFR model. For the multi compartment model 3 different set ups were chosen containing 5, 7, or 9 stirred tanks in series which gave SSE values of 79, 8, and 52, respectively, showing that the 7 compartment set up gives the best description. For the PFR model an SSE value of 20 was found. In this case the author found that both

the multi compartmental approach and the PFR approach give a good description of the mean transit time along the small intestine, but that using only a single stirred tank is not adequate at describing this mean transit time (Yu et al., 1996).

Others have looked in more detail at the residence time distribution, by using pulses of dye in isolated segments of the ileum of brushtail possums (Janssen et al., 2007). For guar gum solutions which have viscosity similar to that of intestinal digesta the authors found that there will likely be laminar flow in the small intestine with large eddies. They point out that in this case mass transfer of nutrients to the intestinal wall will rely upon molecular diffusion, more so than lower viscosity solutions which resulted in a more turbulent flow regime with different length scales of eddies. The author points out that the segment of possum ileum used was straight, but *in vivo* the intestine is curved. Flow through curved pipes will induce dean roll cells which will increase radial mixing and likely induce chaotic advection (Janssen et al., 2007), further increasing the mass transfer of nutrients to the intestinal membrane.

2.3.1 Single CSTR Small Intestine

Looking at the absorption and elimination of drug molecules from the body, Di Muria et al. (2010) chose to use 1 compartment to represent the mass transfer of the molecules within the small intestine, this was one of 7 continuous stirred tank reactors for distribution of the drug through out the body, the other CSTRs represented each of the following: the stomach, large intestine, gastrointestinal circulatory system, liver, plasma, and tissue. The model was fitted to data from the consumption of zinc sulphate by rats, and compared to a more complex model by Jain et al. (1981). Di Muria et al. (2010)

aimed to produce an accurate model with fewer parameters than Jain et al. (1981) who proposed 99 parameters in the model where 37 required fitting. The number of parameters requiring estimation was reduced to 5 in the work of Di Muria et al. (2010). The model by Jain et al. (1981) gives a better fit but takes significatly greater computation.

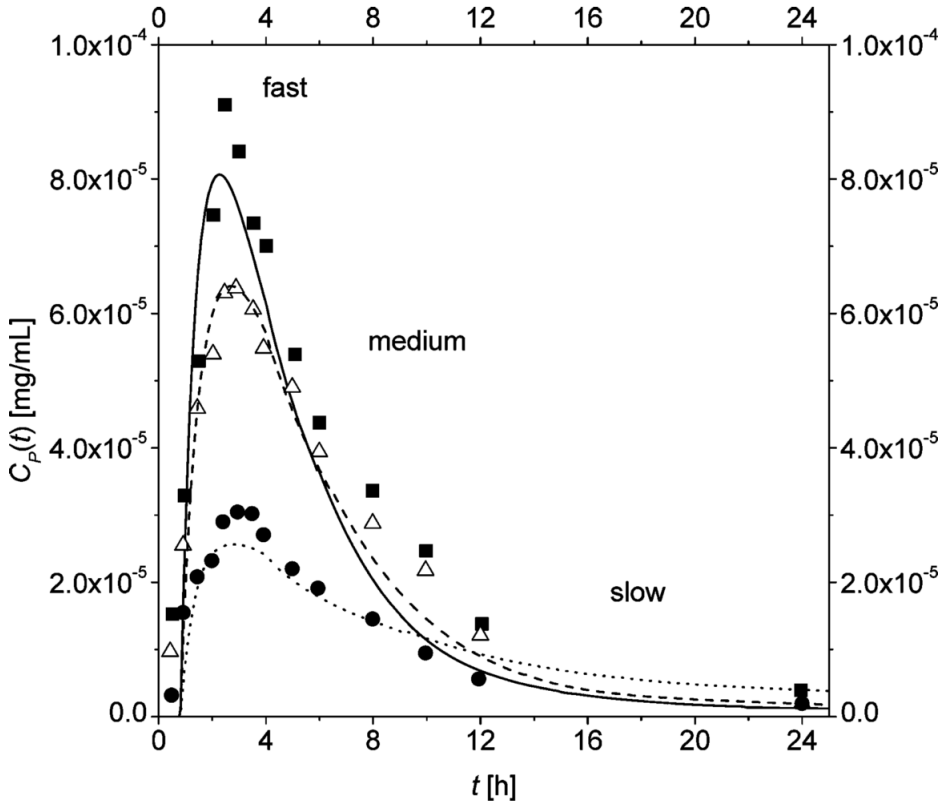

Figure 2.14: Figures taken from Di Muria et al. (2010) showing the concentration of the drug Dilitiazem in the blood plasma of human after consumption of formulations with slow, medium, and fast release kinetics

Di Muria et al. (2010) then went on to test the consumption of the drug Diltiazem after oral consumption by humans. Using the same model with parameter values appropriate to humans and the drug consumed, the model was used to give a fit for low, medium and high release rate formulations of the drug with the fitting of only two

parameters, one representing the constant of elimination of the drug from the blood plasma, and the other the distribution volume of the plasma. The simulations gave good fits showing similar peak concentrations and terminal phases for the drug concentration in the plasma for the medium release formulation, but under estimated the peak in the slow and fast release formulations and had a faster clearance of the drug from the plasma in the terminal phase for fast release formulation, these results are highlighted in Figure 2.14

Dalla Man et al. (2006) used a single stirred tank for the small intestine when looking at glucose absorption and plasma glucose dynamics post prandially. The model assumes that glucose within the small intestine (m_{gut}) is absorbed with rate k_{abs}, but that only a certain fraction, f, appears in the plasma. The rate of appearance of the glucose in the blood is defined as Ra. The small intestine is fed from the stomach which is modelled as two stirred tanks, the first takes into account the solid portion of a meal (m_{sto1}), where there is a grinding rate, k_{12}, with input into the second stirred tank which contains meal mass which can empty (m_{sto2}). This empties at a rate k_{empt}- the equations are as follows:

$$\frac{dm_{sto1}}{dt} = -k_{12}m_{sto1}(t) + m_0\delta(t) \tag{2.20}$$

$$\frac{dm_{sto2}}{dt} = -k_{empt}m_{sto2}(t) + k_{12}m_{sto1}(t) \tag{2.21}$$

$$\frac{dm_{gut}}{dt} = -k_{abs}m_{gut}(t) + k_{empt}m_{sto2}(t) \tag{2.22}$$

$$Ra(t) = fk_{abs}m_{gut}(t) \tag{2.23}$$

The results of this model are shown in Figure 2.12, which show good agreement with the experimental data for the rate of appearance of glucose in the blood plasma after consumption of both a OGTT and a mixed meal.

Taghipoor et al. (2012) researched the effect of insoluble components on the digestion and absorption of nutrients in the intestine of a pig. The work modelled only a single cylindrical bolus but applied a novel transport equation. The bolus acts as a single compartment containing a fixed amount of chyme from the stomach. This bolus moves according to a transport equation that takes into account both the pulsatile nature of peristaltic contraction and frictional drag of the fluid as a function of bolus viscosity.

The author develops 3 different models to look at the different components of the bolus and different reaction pathways: the first (the simplest) contains component A, which undergoes enzymatic hydrolysis to B which can subsequently be absorbed. The mass balances are as follows:

$$\frac{dm_A}{dt} = -Ck(x,e)m_A \tag{2.24}$$

$$\frac{dm_B}{dt} = Ck(x,e)m_A - k_{abs}m_B \tag{2.25}$$

where, C is the degradation rate, and $k(x,e)$ is the enzyme activity which is a function of the pH and amount of enzyme at each point along the small intestine, k_{abs} is the rate of absorption.

The transport equation will take the following form:

$$\frac{d^2x}{dt^2}(t) = \frac{c_0 + c_1V(t)}{a + bx(t)}\frac{d}{dt}\left[y(t - x(t))/c\right] - K(t)\frac{dx}{dt}(t) \tag{2.26}$$

$$\frac{dx}{dt}(0) = \nu_0, \qquad x(0) = 0 \tag{2.27}$$

The first term in the equation takes into account the pulsating nature of the flow, where:

$$\int_0^{10} \frac{d}{dt} y(t) dt = 1 \tag{2.28}$$

assumes one peristaltic wave every 10 seconds whose efficiency is a function of the size of the bolus and the axial distance from the pylorus. The second term ($-K(t)(\partial x/\partial t)$) represents the frictional effect introduced by the bolus viscosity. The Simulated velocity of the bolus over time is shown in Figure 2.15.

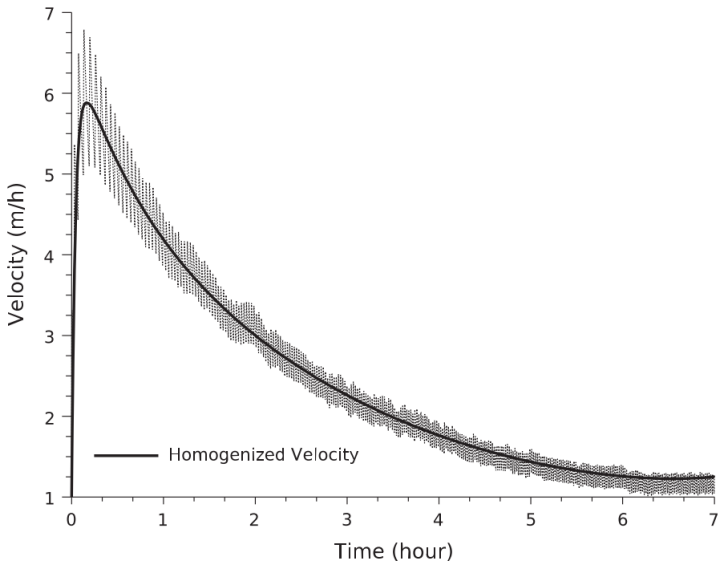

Figure 2.15: Simulated velocity of the bolus against time as it moves along the length of a pigs intestine. Taken from Taghipoor et al. (2012).

In the 2nd and 3rd models the author build up the complexity to look at the effect of insoluble components and the effect of additional water upon digestion (Taghipoor et al., 2012). This work was further developed in Taghipoor et al. (2014) which looked at the effect of dietary fibre on bolus breakdown, and showed that the introduction of fibre to the bolus had the effect of decreasing the residence time within the small

intestine, this is in line with experimental observations. The author did not however look into the effect of mass transfer of nutrients within the bolus, which will likely have an effect upon the absorption rate of nutrients.

One of Taghipoor et al. (2014) aims was to produce a generic model for digestion which can be applied to any food stock and the model did not try to include the effects of gastric emptying and viscosity etc., nor did the author attempt to build a description of multiply bolus in the small intestine. These limit the predictive scope of the model but model still provides an insight into the behaviour of individual bolus in the small intestine.

2.3.2 Multiple Compartment Small Intestine

A multi compartmental approach was taken by Bastianelli et al. (1996) to analyse the absorption of a multicomponent meal after consumption by pigs. The model contains 4 compartments in total: one representing the stomach, one the proximal small intestine (Duodenum and proximal Jejunum), one the distal small intestine (remaining jejunum and ileum), and a final compartment for the large intestine (colon). Therefore two compartments are used to describe the small intestine, a smaller number than the 7 specified by Yu et al. (1996) to give the best fit for the transit time along the small intestine. The input to the model was into the stomach with nutrients representing that of a common meal for pigs, containing: protein, carbohydrates (starch, sugars, and cell walls (digestible and undigestible)), lipids, and minerals. These undergo enzymatic hydrolysis, with the secretions into each compartments linearly dependent upon the

mass of meal within each compartment. The absorption of nutrients follows Michaelis-Menten kinetics from the respective compartment.

This model suffers from some limitations as outlined in Moxon and Bakalis (2016). One is the effect of meal structure and physical properties, e.g., viscosity, upon the absorption rate (Marciani et al., 2000, 2001b; Shimoyama et al., 2007). It is likely for small molecular weight molecules and rapidly absorbing molecules that the limiting factor in absorption will be the movement from the intestinal lumen to the intestinal epithelium (Stoll et al., 2000; Strocchi and Levitt, 1993; Wang et al., 2010). Another factor not considered is the interactions between different components, numerous authors have shown addition of thickeners can influence the rate of absorption (Gouseti et al., 2014; Sasaki and Kohyama, 2012; Singh et al., 2010; Slaughter et al., 2002; Tharakan et al., 2010), either by increased resistance to diffusion (Johnson and Gee, 1981) or- in the case of nutrients requiring enzymatic break down prior to absorption- through encapsulation or inhibition of the enzyme.

Another attempt at a multi compartmental model was made by Yu and Amidon (1999), building upon work from previous publications (Yu et al., 1996), 7 compartments were utilised in modelling the absorption of drugs from the small intestine along with one for the stomach and one for the colon.

The drug empties exponentially from the stomach, and moves from compartment to compartment with first order constants, along with this there is absorption from the small intestinal compartments- again via first order kinetics. The absorption rate is assumed to be a function of the intestinal epithelium permeability (Yu and Amidon,

1999), ignoring any mass transfer or diffusive processes occurring within the intestinal lumen.

The equations therefore take the following form (Yu and Amidon, 1999):

$$\frac{dm_s}{dt} = -k_s m_s \tag{2.29}$$

$$\frac{dm_n}{dt} = k_t m_{n-1} - k_t m_n - k_a m_n \qquad n = 1, 2, ..., 7 \tag{2.30}$$

$$\frac{dm_c}{dt} = k_t m_7 \tag{2.31}$$

with the following initial conditions:

$$m_s(0) = m_0 \tag{2.32}$$

$$m_n(0) = 0, \qquad \text{for } n = 1, 2, ..., 7 \tag{2.33}$$

$$m_c(0) = 0 \tag{2.34}$$

where m is the mass in different compartments, where the subscript, s is the stomach, c is the colon, and n is represents on of the small intestine compartments ($n = 1, 2, ..., 7$), and k_a represents the rate of absorption, k_s the gastric emptying rate, and k_t the rate of transfer between intestinal compartments. The effective permeability and the fraction of the dose absorbed for 10 different drug compounds was gathered from literature. Using the effective permeability values from literature within the model the simulated values of the fractional absorption were similar to those from the literature results (Yu and Amidon, 1999). The authors then implemented a model for drug concentration in plasma from a book by Wagner (1993), where it is assumed there are 3 plasma compartments. Whilst providing agreement with experimental data this model does not have a physiological interpretation:

$$\frac{dC_1}{dt} = \frac{1}{V_1}\frac{dm_a}{dt} - (k_{12} + k_{13} + k_{10})C_1 + k_{21}C_2 + k_{31}C_3 \tag{2.35}$$

$$\frac{dC_2}{dt} = k_{12}C_1 - k_{21}C_2 \tag{2.36}$$

$$\frac{dC_3}{dt} = k_{13}C_1 - k_{31}C_3 \tag{2.37}$$

These equations (2.35:2.37) are represented schematically in Figure 2.16.

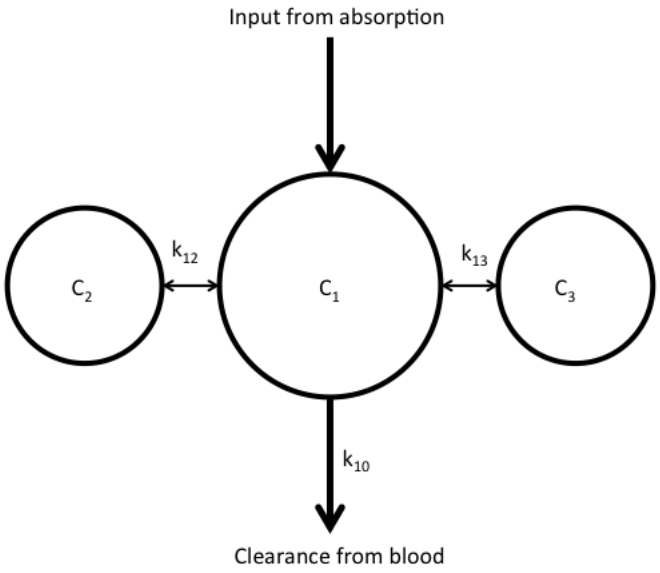

Figure 2.16: Schematic showing the compartments represented by Equations 2.35:2.37, Where C_1 is the central compartment and C_2 & C_3 are peripheral compartments.

V_1 is the volume of the central compartment, and k represents different microscopic rate constants (Yu and Amidon, 1999), the values of which Yu and Amidon (1999) took from work by Mason et al. (1979) for the kinetics and bioavailability of Atenolol for three oral solution containing 25, 50, and 100mg of the drug and a intravenous input of 50mg solution.

The simulated results were compared with the experimental values utilising both an exponential gastric emptying rate and a biphasic gastric emptying rate (Figure 2.17).

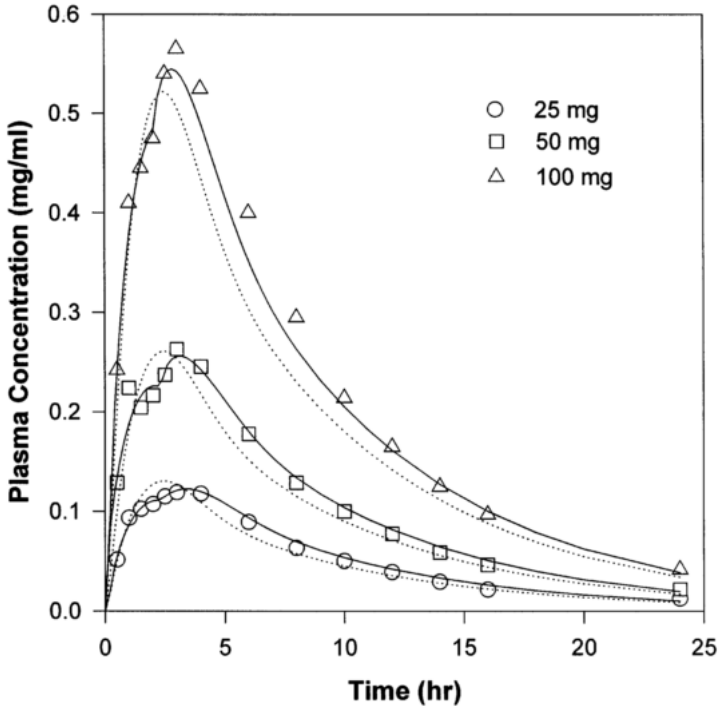

Figure 2.17: This shows the experimental results from Mason et al. (1979) for the plasma concentration of atenolol after doses of 25, 50, and 100 mg. The Simulated results by Yu and Amidon (1999) are shown for each dose, with the dotted line for exponential gastric emptying and the solid line for biphasic gastric emptying.

Both gastric model were able to give results similar to that seen *in vivo* but the biphasic emptying rate along with the small intestine modelled as 7 stirred tanks in series gave closer results. The biphasic emptying model resulted in a 2 hour break in the emptying (nothing emptied from the stomach for a 2 hour period) which, as pointed out by Yu and Amidon (1999), is unlikely to occur *in vivo*. Hence, whilst the results are in good agreement with experimental data, the model does not seem physiologically accurate. It should also be noted that the colon does not have a term to empty, this implies any mass exiting the small intestine remains in the colon. Whilst most models are over short periods of time relative to the transit time of the colon, the model by Yu and Amidon

(1999) models results over a period of 24 hr and hence a more complete model may consider the removal of waste from the colon. Though in this case no absorption form the colon is considered and as such the mass will not influence the drug concentration in the blood.

Jumars (2000) work with the assumption that a tubular gut could be described with a series of CSTR reactors. In each CSTR hydrolysis of components could occur along with absorption of nutrients. Three different types of kinetics were considered for the rates (r) or reaction and absorption: linear (Equation 2.38), hyperbolic (Equation 2.39), or sigmoidal (Equation 2.40):

$$-r = kC \tag{2.38}$$

$$-r = \frac{V_{max}C}{K_m + C} \tag{2.39}$$

$$-r = \frac{V_{max}C^2}{K_m^2 + C^2} \tag{2.40}$$

The work analysed at how increasing the number of CSTRs affects the optimal flow rate (rate of food ingestion), absorption efficiency, and maximum absorption rate. The absorption efficiency was defined as:

$$1 - \left[\frac{C_{Ff} + C_{Pf}}{C_{F0}}\right] \tag{2.41}$$

where C is the concentration and initial subscript represents the component (F- food, or P- product) and the second represents the position along the gut (0- entrance, f- leaving the gut).

With the assumption that the absorption can occur uniformly across all CSTRs it was found that varying the number of compartments has little effect upon the maximum absorption rate that can be achieved, but that it does effect the optimal flow rate (ingestion

rate) and the absorption efficiency, but there is little effect when increasing the number of reactors above 20. But it should be stated that as the number of CSTRs in series increases the results will tend to those expected from a plug flow reactor (PFR) model, this explains why there is little change in optimal flow rate or absorption efficiency as the number of CSTRs increase to this level (10-20+).

The author then included the assumption that the absorption sites were not distributed uniformly, but that the same amount were distributed towards the proximal end of the gut (the author experimented with altering the number of CSTRs which absorption can occur from), in this case there was an increase in the maximum absorption rate, but a decrease in the absorption efficiency due to less time in regions where absorption can occur.

The author then looked at the quality of the food, this was defined by the input concentration divided by the Michaelis constant for the conversion of the food to absorbable product (C_{F0}/K_m), where low quality had a value of 0.1, and high quality a value of 10. For the low quality food the absorption rate when hyperbolic kinetics are used has a much higher absorption efficiency than those seen with sigmoidal kinetics (linear kinetics not shown). No real difference is seen with either kinetics for uniform or nonuniform distributions of absorption sites.

High quality food results in high absorption efficiencies. In this case no real differences are found between different reaction/absorption kinetics nor with different absorption site distributions. The authors also showed increasing the number of CSTRs above around 20 had no effect upon the absorption efficiency.

Jumars (2000) highlights some points which may be important in developing digestive models which can offer close predictions to what is seen in reality, such as taking into account volume changes during digestion or adding a water component to the mass balance.

2.3.3 Plug Flow Small Intestine

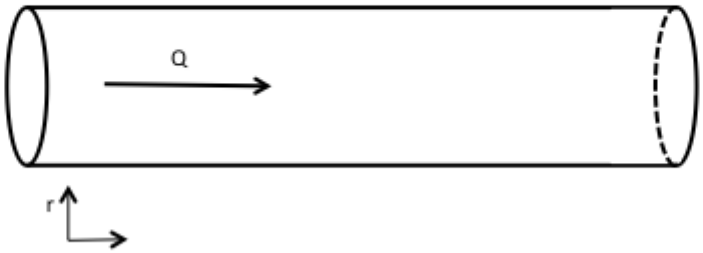

Figure 2.18: Simple schematic of a plug flow reactor

The work by Ni et al. (1980) aimed to present a rigorous mathematical model to describe the flow, turbulent diffusion, and absorption of a drug from the small intestine. To achieve this plug flow assumptions were assumed (simple schematic shown in Figure 2.18) and a 1D diffusive-convective-reactive equation was proposed, taking the following general form:

$$\frac{\partial C}{\partial t} = \alpha \frac{\partial^2 C}{\partial z^2} - \beta \frac{\partial C}{\partial z} - \gamma C \tag{2.42}$$

the parameters were then defined as follows:

$$\alpha = D_e \qquad [m^2 s^{-1}] \tag{2.43}$$

$$\beta = \frac{Q}{\pi r^2} \qquad [m s^{-1}] \tag{2.44}$$

$$\gamma = \frac{2P_e}{r} \qquad [s^{-1}] \tag{2.45}$$

where, D_e is the effective axial diffusion, Q is the flow rate of the bulk fluid, P_e is the apparent permeability of the drug through the intestinal membrane, r is the radius of the intestine, and z is the axial position.

The initial condition was set as follows:

$$C(z, 0) = 0 \tag{2.46}$$

and the boundary condition as z approaches infinity:

$$C(\infty, t) = 0 \tag{2.47}$$

The model tested a variety of different boundary conditions at the input to the intestine:

Constant input

$$C(0, t) = C_0 \tag{2.48}$$

zeroth order input

$$C(0, t) = C_0 - k_0 t \tag{2.49}$$

first order input

$$C(0, t) = C_0 e^{-k_1 t} \tag{2.50}$$

Pulse input

$$C(0, t) = C_0 e^{-kt} \tag{2.51}$$

here C_0 is the concentration entering the small intestine, and k represents the different rate constants for the different input types (Ni et al., 1980).

Whilst the constant input model is not likely to occur *in vivo*, the zeroth and first order input may give similar patterns to what is expected. The pulse input may be more physiologically relevant as the pylorus will allow gastric chyme to leave in squirts (due to the peristaltic contractions of the gastric walls), though the rate of these squirts is unlikely to be constant.

The equations were solved with the different boundary conditions using a Laplace transform with Ni et al. (1980) utilising the inverse transforms previously solved by Carlslaw and Jaeger (1959). This work by Ni et al. (1980) introduced the idea of using a ideal plug flow reactor to describe the absorption of drugs from the small intestine, but did not compare or validate against any data for drug absorption. The paper mainly looked at how varying the boundary conditions or varying the parameters (D_e, Q, or P_e) influenced the concentration along the length of the small intestine or with time. Hence this work cannot be assumed to give accurate or reliable results without first validating the models against real data for drug absorption or drug concentration in the small intestine. But the work does serve as a source of analytical solutions for the plug flow model for a variety of different boundary conditions.

Stoll et al. (2000) modelled the transit and absorption of a drug bolus within the small intestine as a plug flow reactor. The model also attempted to take into account the different length scales involved in the intestinal absorption of nutrients and drugs from the bulk transport along the length of the intestine to the microscale epithelium cells. The concentration of drug in the intestinal lumen was expressed as the average over the cross section of the lumen, $C(z,t)$, varying along the axial length, $z \in [0, L]$ and time, $t \in [0, t_f]$. The mass balance takes the form of an advective-diffusive-reactive

equation in 1D:

$$\frac{\partial C}{\partial t} = \bar{D}^* \frac{\partial C}{\partial z} - \bar{u}^* \frac{\partial^2 C}{\partial z^2} - k^* C \tag{2.52}$$

With initial conditions:

$$C(z,0) = \begin{cases} \bar{A}^* C_0 & \text{if } 0 \leq z \leq l_0 \\ 0 & \text{if } l_0 < z \leq L \end{cases} \tag{2.53}$$

and boundary conditions:

$$\left.\frac{\partial C}{\partial z}\right|_{z=0} = \left.\frac{\partial C}{\partial z}\right|_{z=L} = 0 \tag{2.54}$$

This equation introduces 4 parameters which were defined as: $\bar{u}^*$, the mean axial velocity, $\bar{D}^*$ the macroscale dispersion coefficient, k^* the mean absorption and degradation rate constant, and $\bar{A}^*$ which is the apparent initial conditions (Stoll et al., 2000).

The authors defined two dimensionless Damköhler numbers, one for the membrane and one for the intestinal lumen:

$$Da_m = \frac{\kappa R_0}{D} \tag{2.55}$$

$$Da_L = \frac{k_d R_0^2}{D} \tag{2.56}$$

Where R_0 is the mean intestinal radius, k_d is the rate constant of degradation of the drug in the small intestine lumen, and κ is the absorption rate constant, which takes the following form:

$$\kappa = \left(\frac{A^{pc}}{A^{ppc}}\right)\left(\frac{A^{\nu}}{A^{p\nu}}\right)\left(\frac{A^{m\nu}}{A^{pm\nu}}\right)\left(\frac{kD_L}{l} + k_t + k_p\right) \tag{2.57}$$

Equation 2.57 takes into account the increase in surface area due to the protrusions on the intestinal wall: A^{pc}/A^{ppc} is the increase in surface area due to *plicae circulares*,

$A^{\nu}/A^{p\nu}$, is the increase due to *villi*, and $A^{m\nu}/A^{pm\nu}$ is the increase due to *microvilli*. The final terms in Equation 2.57 takes into account the different transport pathways through the intestinal epithelium. kD_L/l represents the rate due to *transcellular passive diffusion*, k_t is the rate due to *transcytotic* transport (movement through the epithelium after been captured by a vesicle), and k_p is the rate due to *paracellular* transport (passing between spaces in between epithelium cells) (Stoll et al., 2000).

The parameter D is a combination of the molecular diffusion (D_M) and convectional diffusion, where the convection term in this case is due to the presence of roll cells due to the gut wall contractions (Stoll et al., 2000), where Γ is the strength of the cells, and d is the diameter of the cells:

$$D = D_M + \frac{(\Gamma d)^2}{8\pi^2 D_M} \tag{2.58}$$

In vivo data for the distribution of drugs generally is expressed as plasma concentration against time, or analysed from this curve, such as the area under the curve (AUC), as such Stoll et al. (2000) the absorbed mass in the systemic circulation as:

$$m_A(t) = (1 - E_H)e^{-k_c t}\bar{K}_A^* \int_0^t e^{k_c t} m(t)dt \tag{2.59}$$

with the concentration of the drug in the systemic circulation been the mass divided by the plasma volume:

$$C_s(t) = \frac{m_A(t)}{V_d} \tag{2.60}$$

where k_c is the rate of elimination of the drug from the body, E_H is the hepatic extraction rate (elimination due to liver function), and $m(t)$ is the mass present in the small intestine and is found from the following integral:

$$m(t) = \pi R_0^2 \int_0^L C(z,t)dz \tag{2.61}$$

Once developed Stoll et al. (2000) compared the results of the model to experimental data for four different molecules: Ibuprofen, Growth hormone releasing peptide (GHRP-1), Salmon calcitonin (sCT), and insulin, a plot of the model output and experimental data for GHRP-1 is shown in figure 2.19. The model was also developed to allow simulations for different animal system: Human, Primate, and Rat, as such the authors suggest that fitting with experimental data for the plasma concentrations of a known dose allows for predictions of responses to different doses within the same animal system as well as estimations for different animal systems, i.e., drug plasma concentration curves from rats can be used to estimate the plasma concentration to doses in humans.

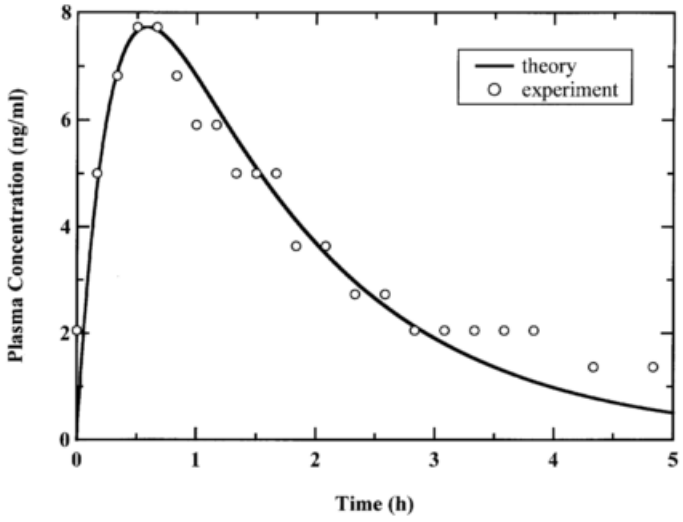

Figure 2.19: plot from Stoll et al. (2000) showing the output of model for the plasma concentration of GHRP-1 against experimental data

The authors used the Damköhler numbers (Equation 2.55) to look at the relative effect of the absorption across the membrane and diffusion rate to the membrane to see

which may be the limiting factor in the absorption. It was found that the Damköhler number for Ibuprofen and GHRP-1 were around one with these molecules been small relative to the others tested (Molecular weight: 206.2 & 915.7, respectively), whereas the heavier molecules, Calcitonin and Insulin (Molecular weight: 3500 & 6000, respectively) had much smaller Damköhler numbers ($Da_m << 1$). This implies that the larger molecular weight molecules are limited by the transport across the intestinal epithelium, whereas the smaller molecules are not limited by this barrier.

Logan et al. (2002) used a plug flow reactor model to look at how various factors could affect nutrient uptake by animal guts, these factors include: reactor rate, absorption rate, and morphological differences.

The model defines a gut of length L, where $x \in [0, L]$, which has a cross sectional area $A(x)$. The concentration of a nutrient in the gut ($C(x,t)$) is defined by the partial differential equation, when the surface area is assumed constant:

$$\frac{\partial C}{\partial t} = -\bar{u}\frac{\partial C}{\partial x} - r(x,t,n) \tag{2.62}$$

where $\bar{u}$ is the mean velocity of the nutrient along the length of the small intestine, and $r(x,t)$ is the reaction/absorption rate, which like Jumars (2000) were described by either of the following three kinetics:

First-order kinetics

$$r = kC \tag{2.63}$$

Michaelis-Menten kinetics

$$r = \frac{k_1 C}{C + k_2} \tag{2.64}$$

Sigmoid kinetics

$$r = \frac{k_1 C^2}{C^2 + k_2} \tag{2.65}$$

The following initial and boundary conditions were also defined:

$$C(x, 0) = C_0(x), \qquad 0 < x < L \tag{2.66}$$

$$C(0, t) = C_b(t), \qquad t > 0 \tag{2.67}$$

To include the variations in cross sectional area, Logan et al. (2002) assumed that the flow rate (Q) along the intestine is constant, and allowed for variation in the velocity, hence:

$$\bar{u}(x) = \frac{Q}{A(x)} \tag{2.68}$$

finally Logan et al. (2002) goes on to assume a multicomponent input, in which case C_i is the concentration of component i, where $i = 1, 2, ..., N$. For a system with two components, where one breaks down by first order kinetics to a product which can be absorbed we get the following equations:

$$\frac{\partial C_i}{\partial t} = -\bar{u}\frac{\partial C_i}{\partial x} - r_i(x, t), \qquad i = 1, 2 \tag{2.69}$$

$$-r_1 = -kc_1, \quad -r_2 = kr_1 - ar_2 \tag{2.70}$$

where k is the reaction rate and a is the absorption rate.

From these equations the authors were able show how variations in digestion speed and other factors, such as the ratio of rate constants affect the absorption rate of nutrients. Though the models developed were not compared against any experimental data, to either discriminate against the different choices of reaction/absorption kinetics nor to validate the absorption rates calculated by the model.

2.4 Conclusion

Most models for the gastric emptying of nutrients take the approach of fitting one or two parameters to experimental data, where by the fitted parameters do not have a physiological interpretation. This approach, whilst it can provide a good fit, does not give any information as to why certain meals will empty at different rate, or follow different dynamics. The work by Dalla Man et al. (2006) presents a model to take into account how the amount of nutrient affects the emptying rate, and also presents a multiple compartment approach to the stomach to attempt to take into account the breakdown of solids. This approach gave good results when coupled with a small intestine model and fitted to experimental data for glucose rate of appearance in the blood plasma, but the content remaining in the stomach was not validated against experimental data therefore cannot be said whether it gives an adequate fit. Assuming the gastric emptying rate is a function of gastric nutrient content is not entirely physiologically accurate as the rate of emptying is linked to the nutrients sensed in the proximal small intestine (Brener et al., 1983; Calbet and MacLean, 1997), therefore the model will not take into account how the bioavailability of the nutrients will affect the emptying rate, nor does it take into account other physical properties of the meals and how these affect the emptying rate, e.g., the viscosity (see Table 2.3).

Yu et al. (1996) highlighted how the use of a single CSTR to describe the small intestine transit is inadequate, although some author still utilise this approach (Dalla Man et al., 2006). They proposed that the small intestine should be described as 7 CSTRs in series (chosen over a PFR as it is a simpler approach), and showed good results against experimental data for drug blood plasma concentration. Stoll et al. (2000) chose

the PFR approach, again to model drug absorption and gave good fits to experimental data for 4 different drugs, this approach was novel in that it included multiple length scales. The model takes into account the effect of eddy's upon the dispersion and of the increase in surface area due to *villi*, *microvilli*, and *plicae circulares*, and multiple absorption pathways. Both these approaches are designed for the absorption of drugs and as such do not take into consideration some of the factors which are important in the digestion of food, such as how the physical properties of a meal can affect the gastric emptying rate or the absorption rate.

None of the models in literature so far have look at how the viscosity can affect the mass transfer in the intestinal lumen or how it can influence the gastric emptying rate. Along with this, few models have attempted to take into account any of the digestive systems feedback controls, which will influence the absorption of nutrients. The models presented in this thesis will attempt to address some of these points which as yet have not been included in previous works. This work will take the approach of modelling the stomach as a CSTR and the small intestine as a PFR and look how viscosity could influence the absorption of nutrients, this will be built on to introduce a feedback mechanism as described by Brener et al. (1983) linking the gastric emptying rate to the nutrient bioavailability in the intestinal lumen. A model will also be proposed to link the gastric chymes viscosity the secretion rate of gastric juices and the emptying rate. Finally a population balance approach will be presented to allow for a solid phase of a meal to be included in the models, in a way that is more physiologically relevant that the more black box style approaches that have been carried out before, such as those by Dalla Man et al. (2006) and Kong and Singh (2008).

These models will provide a grounding for future work to develop more comprehensive and physiologically relevant mathematical models of human digestion which could provide some predictive capability and help understand/prevent food related diseases.

2.5 Overview of Mathematical Principles

The following section will present the methods used to solve the equations presented in the later chapters. It will show the explicit forward Euler method and backward finite difference method used to discretise the partial differential equations utilised for the numerical solutions. These methods were chosen to ensure speed of computation, and stability of the solution was ensured using *Von Neumann Analysis*. The chapter also shows the methods used during parameter estimations.

2.5.1 Differential Equations

The work will deal with ordinary and partial differential equations to describe the distribution of nutrients through the digestive system. The Ordinary differential equations will take the form:

$$\frac{dC_s}{\partial t} = -dC_s \tag{2.71}$$

The partial differential equations used in this work will take the generic form of the advection reaction equations:

$$\frac{\partial C(z,t)}{\partial t} = -u\frac{\partial C(z,t)}{\partial z} - RC(z,t) \tag{2.72}$$

Here C will be the concentration of a component in the small intestine at time t, and distance along the intestine z. where $t \in [0, t_f]$, where t_f is the final time of the simulations, and $z \in [0, L]$ where L is the total length of the small intestine. u is the mean velocity of the component along the axial length of the intestine and R is the

reaction rate or absorption rate from the intestine γ is the rate of decay, or in the case where C_s is the concentration in the stomach, the gastric emptying rate. This can be rewritten as the half time of gastric emptying $t_{1/2} = ln(2)/\gamma$.

To solve the equations additional information is required, in the form of the initial and boundary conditions.

Finite Difference Method

The work will focus upon the numerical solutions to the Partial and ordinary differential equations, specifically using the finite difference method to discretise the equation in spatial and temporal dimensions. e.g., taking the forward difference in time and backward difference in space of the advection reaction equation yields the following:

$$\frac{C_m^{n+1} - C_m^n}{k} = -u\frac{C_m^n - C_{m-1}^n}{h} - RC_m^n \tag{2.73}$$

Rearranging the equation yields

$$C_m^{n+1} = (1 - \frac{uk}{h} - Rk)C_m^n + \frac{uk}{h}C_{m-1}^n \tag{2.74}$$

The subscript m represents the spatial position, and h the step size between each position. n represents the temporal position and k the time step between each position.

The finite difference is an approximate of the actual solution, hence along with the discretisation we must define properties which must be satisfied to ensure that the approximate value from the numerical method is in agreement with the actual solution.

To so this three properties must be defined: Convergence, Consistency and Stability.

Convergence, consistency & Stability

A system converges when the approximate solution tends to the exact solution as the step size in both the temporal and spatial discretisation tend to zeros. Defining the exact solution as U, we can define a *discretisation error*, which is the difference between the approximate and actual solution ($U - C$) (Smith, 1978).

The finite difference method can be said to be consistent with the partial differential equation if for any smooth function ϕ multiplied by the difference operator, *P*, the following expression is satisfied at each temporal and spatial point (Strikwerda, 2004):

$$P\phi - P_{k,h}\phi \to 0 \quad as \quad k, h \to 0, \tag{2.75}$$

Further to these we can define the *Lax-Richtmyer Equivalence Theorem* which states that a consistent finite difference scheme is convergent if and only if it is stable (Strikwerda, 2004).

This implies that we can assume the scheme is convergent if it is both consistent and stable, the latter two condition been more easily verifiable.

To assess the stability of a finite difference scheme *Von Neumann analysis* will be used.

2.5.2 Von Neumann Analysis

The *Von Neumann Analysis* uses Fourier analysis to give conditions for the stability of the finite difference method used for the PDE. An example will be given for the advection equation using forward discretisation in time and backward discretisation in space, following the notation and steps in Strikwerda (2004):

$$\frac{\nu_m^{n+1} - \nu_m^n}{k} + a\frac{\nu_m^n - \nu_{m-1}^n}{h} = 0 \tag{2.76}$$

Which can be rewritten:

$$\nu_m^{n+1} = (1 - a\lambda)\nu_m^n + a\lambda\nu_{m-1}^n \tag{2.77}$$

where, $\lambda = k/h$, and the Fourier inversion can then be carried out on ν^n:

$$\nu_m^n = \frac{1}{\sqrt{2\pi}} \int_{-\pi/h}^{\pi/h} e^{imh\xi} \hat{\nu}^n(\xi) d\xi \tag{2.78}$$

adding ν_m^n & ν_{m-1}^n to the equation gives:

$$\nu_m^{n+1} = \frac{1}{\sqrt{2\pi}} \int_{-\pi/h}^{\pi/h} e^{imh\xi} [(1 - a\lambda) + a\lambda e^{-ih\xi}] \hat{\nu}^n d\xi \tag{2.79}$$

This is them compared to the Fourier inversion of ν^{n+1}:

$$\nu_m^{n+1} = \frac{1}{\sqrt{2\pi}} \int_{-\pi/h}^{\pi/h} e^{imh\xi} \hat{\nu}^{n+1}(\xi) d\xi \tag{2.80}$$

It can be concluded that the following formula can be defined:

$$\hat{\nu}^{n+1}(\xi) = [(1 - a\lambda) + a\lambda e^{-ih\xi}] \hat{\nu}^n(\xi) \tag{2.81}$$

Hence, we can define an amplification factor $g(h\xi)$:

$$\hat{\nu}^{n+1}(\xi) = g(h\xi)\hat{\nu}^n(\xi) \tag{2.82}$$

Where, $g(h\xi) = (1 - a\lambda) + a\lambda e^{-ih\xi}$

From theorems presented in Strikwerda (2004) we can say if $g(\theta, k, h)$ is independent of k and h, that the stability can be described as follows:

$$|g(\theta)| \leq 1 \tag{2.83}$$

this implies that to determine the stability the amplification factor is the only thing that need considering.

The next theorem implies that for the following equations:

$$u_t + au_x + bu \tag{2.84}$$

That the system is only stable if the system is stable when $b = 0$.

Taking the example of the following equation:

$$u_t + au_x = 0 \tag{2.85}$$

for forward time and backward spacial discretisation we get the following finite difference scheme:

$$\nu_m^{n+1} = (1 - \lambda)\nu_m^n + \lambda\nu_{m-1}^n \tag{2.86}$$

where, $\lambda = ak/h$, k is the time step, and h is the spatial step.

This allows for the amplification factor to be described as follows:

$$g = [(1 - \lambda) + \lambda e^{-ih\xi}] \tag{2.87}$$

by squaring the amplification factor and using the identities $e^{ix} + e^{-ix} = 2sinx$, and $2sin^2x = 1 - cos2x$, the following expression can be defined:

$$|g|^2 = 1 - 4\lambda sin^2\frac{1}{2}h\xi + 4\lambda^2 sin^2\frac{1}{2}h\xi \tag{2.88}$$

and setting $S^2 = sin^2\frac{1}{2}h\xi$, the following inequality can be defined which must be satisfied to ensure stability:

$$1 \geq 1 + 4\lambda S^2(\lambda - 1) \tag{2.89}$$

for this to be met the following must hold true $\lambda \leq 1$, hence for stability we require the following conditions:

$$\frac{ak}{h} \leq 1 \tag{2.90}$$

From the theorem previously states the advection reaction equation 2.84, will also be stable if the same conditions (equation 2.90) are met.

2.5.3 Parameter Estimation

The parameter estimation allows for a the out put form a model, y, to be optimised against experimental data, y_{meas}, by finding the best values for some parameters θ, to do this an objective function needs to be defined. A common technique used is the least-squared method, where the square of the difference between measured and model output is minimised, so the objective function will take the following form:

$$\min_{\theta} \sum_{i_y=1}^{n_y} \sum_{i_t}^{n_t} \left(y_{meas,i_y}(t_{i_t}) - y_{i_y}(t_{i_t}, \theta)\right)^2 \tag{2.91}$$

Where n_y is the total number of experimental points, and n_t is the total number of time points, and t_{i_y} the time at each measurement point. To compute this the *'lsqnonlin'* function will be used in MATLAB.

This value can be described as the least squared error or sum of squared errors (SSE), from this we can compute two other values, the mean squared error:

$$MSE = \frac{1}{n_y} \sum_{i_y=1}^{n_y} \sum_{i_t}^{n_t} \left(y_{meas,i_y}(t_{i_t}) - y_{i_y}(t_{i_t}, \theta) \right)^2 \tag{2.92}$$

and the root mean squared error:

$$RMSE = \sqrt{MSE} \tag{2.93}$$

Whilst these values give an idea of how a model fits the data, to compare different models with different number of parameters another criterion must be defined, there are a number of approaches to achieve this but in this work the Akakike Information Criterion (AIC) will be used:

$$AIC = n \ln \left(\frac{SSE}{n} \right) + 2p \tag{2.94}$$

This allows for the number of parameters requiring fitting (p) and the number of data point (n) to be taken into account when comparing models, as such if two models have similar SSE, but one requires a greater number of parameters to be fit, the simpler model would give a smaller AIC and as such would be the most efficient model to describe the experimental data.

Chapter 3

In Silico Modelling of Mass Transfer & Absorption in the Human Gut

The following chapter has been published in the *Journal of Food Engineering* Volume 176 in 2016 (Moxon et al., 2016).

The modelling and simulation work was carried out by myself along with the writing of the paper.

Ourania Gouseti reviewed the structure and provided correction to the grammar and spelling.

Serafim Bakalis provided guidance and supervision during the research and writing/correction of the paper.

The paper was also reviewed by two anonymous reviewers prior to publication.

Chapter 3 builds upon works from other authors discussed in the literature review (Chapter 2), to develop a mathematical model for the digestion of food in the human gut. The work used the idea utilised by many authors that the stomach and small intestine can be modelled as a series of ideal reactors and presents a novel approach by linking the absorption rate to the mass transfer in the intestinal lumen, allowing for the viscosity of the meal to influence the absorption of nutrients.

3.1 Abstract

An *in silico* model has been developed to investigate the digestion and absorption of starch and glucose in the small intestine. The main question we are aiming to address is the relative effect of gastric emptying time and luminal viscosity on the rate of glucose absorption. The results indicate that all factors have a significant effect on the amount of glucose absorbed. For low luminal viscosities (e.g. lower than 0.1 Pa.s) the rate of absorption is controlled by the gastric emptying time. For viscosities higher than 0.1 Pa.s a 10 fold increase in viscosity can result in a 4 fold decrease of glucose absorbed. Our model, with the simplifications used to develop it, indicate that for high viscosity luminal phases, gastric emptying rate is not the controlling mechanism for nutrient availability. Developing a mechanistic model could help elucidate the rate limiting steps that control the digestion process.

3.2 Introduction

Understanding digestive processes is important in addressing diet related diseases, such as obesity, which are becoming a major problem all around the world. A World Health Organisation report in 2014 stated that 39% of adults were overweight and 13% were obese; also stating that the obesity rate was most prevalent in the Americas and least in the south-east Asian regions (WHO, 2014). Specifically in the UK around a quarter of adults were classified as obese as of 2014 (HSCIC, 2014); it has been estimated that obesity will cost the UK society £50billion per annum by 2050 (McPherson et al., 2007). In order to address some of the food related diseases and design healthier foods

it is important to understand the behaviour of foods during digestion using *in silico* as well as *in vivo* and *in vitro* studies.

Modelling has been extensively used in a variety of systems e.g., pharmaceuticals (Peng and Cheung, 2009; Stoll et al., 2000), biological systems such as the insulin-glucose system (Makroglou et al., 2006; Pedersen and Cobelli, 2013).Simulation of biological processes allows for investigation into phenomena that are difficult to examine or study in vivo and in vitro. In this work we will be modelling digestion in the gut as a series of ideal reactors, a concept introduced in the late 1980's (Penry and Jumars, 1986, 1987), with wide applications in the area of pharmacokinetics (Ni et al., 1980; Peng and Cheung, 2009; Stoll et al., 2000).

Mathematical models have been developed to investigate the digestion of foods using different approaches: A compartmental approach with a CSTR small intestine was used by Dalla Man et al. (2006) assuming that changes in gastric emptying rate have the largest effect on absorption (Dalla Man et al., 2006), this work showed good agreement with absorption from oral glucose tolerance tests. Bastianelli et al. (1996) simulated the movement and absorption of different nutrients simultaneously with a multiple compartmental approach (Bastianelli et al., 1996), which was able to predict nutrient absorption patterns and transit times. A model developed by Taghipoor et al. (2012) used a system of ODEs to simulate the movement and absorption from a food bolus within the intestine highlighting the effect dietary fibre has on slowing the bolus break down (Taghipoor et al., 2014, 2012).

Despite the fact that mathematical models provide insight into digestion; they typically use parameters that are obtained empirically, which limits their predictive capability.

3.2.1 Starch Digestion

Starch is the largest source of carbohydrate in the human diet (Singh et al., 2010). In the small intestine, α-amylase will convert starch to oligosaccharides, and brush boarder enzymes (e.g., glucoamylase) will hydrolyse the oligosaccharides to glucose, which can then be absorbed. The conversion of oligosaccharide to glucose and absorption of glucose by sodium-dependent glucose cotransporter 1 (SGLT-1) proteins through the epithelium will be rapid and will not be rate limiting (Lentle and Janssen, 2011; Stümpel et al., 2001).

The kinetics of starch hydrolysis by α-amylase has been studied by a number of authors with the amylase substrate isolated from a variety of sources. Both bacterial and human α-amylase have been found to follow Michaelis-Menten kinetics (Ikram-Ul-Haq et al., 2010; Komolprasert and Ofoli, 1991; Satomura et al., 1984; Yankov et al., 1986), although it has also been reported that this is only followed for low substrate concentrations and at high concentrations a modified 1st order kinetics can be used (Komolprasert and Ofoli, 1991). Inhibition of α-amylase by high D-glucose concentrations has been reported on some occasions (Steverson et al., 1984; Yankov et al., 1986), which has been reported to have a large effect at concentration greater than 300 g/L (Yankov et al., 1986), though this is a high concentration that is unlikely to be encountered in vivo.

3.2.2 Gastric Emptying

Gastric emptying rate is often considered to be the rate limiting step in the absorption of nutrients (Hellström et al., 2006; Mourot et al., 1988). The delivery of gastric content to the duodenum is controlled by the pyloric sphincter (Hellström et al., 2006), whilst the stomach acts as a reservoir for consumed food, and mechanically and chemically breaks down the content (Kong and Singh, 2008).

Table 2.3 shows a selection of studies of the gastric emptying rate for different liquid solutions. Gastric emptying is quantified with a half-time (time for half the content to empty the stomach by volume) and calorific emptying rate. These studies were selected as they have a comprehensive description of the physical properties of the fluids and the calorific content.

In Table 2.3 the measurement methods can be separated in 3 groups: breath sampling, aspiration, and imaging (e.g. MRI/Scintigraphy/Sonography). The most common method for measuring gastric emptying rates in a medical setting is Scintigraphy, where meals are labelled with ^{99m}Tc, and distributions of these radio- isomers are taken using gamma cameras (Punkkinen et al., 2006). Punkkinen et al. (2006) compared this to the ^{13}C breath test, where a meal is labelled with ^{13}C and breath samples are taken and the ratio of ^{13}C-^{12}C can be used to calculate the volume remaining in the stomach. The group found that the ^{13}C breath test gives significantly longer emptying half-time than Scintigraphy and that there was no correlation between the half-lives of the two methods (Punkkinen et al., 2006). This could explain why the results by Shimoyama et al. (2007) have longer emptying rates when compared to the rest of the table (also shown in Figure 3.1).

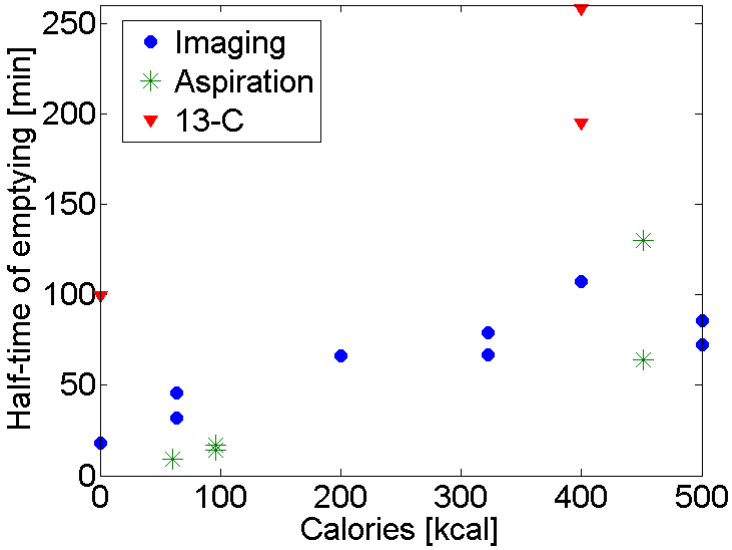

Figure 3.1: plot of half-time of emptying against calories for meals in Table 2.3, different colours represent different methods of measurements, showing that increasing the calorific content of a meal leads to a longer half time of emptying.

Scintigraphy has also shown 70% slower emptying rates than double sampling aspiration, where a dye is added to a meal and samples are taken directly from the stomach via catheter and emptying inferred (Beckers et al., 1992), although this is not evident from the data presented in Table 2.3. Good agreement in measured emptying rates with MRI (Feinle et al., 1999; Schwizer et al., 1992) and ultrasonography (Hveem et al., 1996) are also shown in literature.

Figure 3.1 shows a plot of half-time of emptying against the calorific content of the meal for different measurement methods. As one can see the resulting emptying times depend on the method of measurement. As previously explained the ^{13}C method results in a significantly higher estimation of gastric emptying time; this results in a

large uncertainty on parameters used in models as a large variety of sources have to be considered typically each employing a different method.

As can be seen in Figure 3.1, an increase in calorific content results in an increase of gastric emptying time, but the scarcity of the data points do not allow us to conclude upon the nature of the relationship. This could be explained from observations widely reported in literature of a feedback mechanism from the small intestine (controlled by nutrient sensors) that is thought to be the main controlling mechanism of gastric emptying rate (Brener et al., 1983; Calbet and MacLean, 1997; McHugh, 1983; Shimoyama et al., 2007).

Whilst in Table 2.3 there is a clear trend with emptying rate and the calorific content, the link between the emptying rate and viscosity or volume of meal consumed is not clear. Prior to the initiation of this feedback mechanism, there is an initial rapid emptying rate, which is independent of the nutrient content of the meal. Some researchers suggest that this rate will be controlled by the volume of fluid in the stomach (Brener et al., 1983; Moran et al., 1999), while others point to the effect of viscosity (Marciani et al., 2001b; Shimoyama et al., 2007), with more viscous meals causing greater distension of the antral region relative to the proximal; and also resulting in a great volume of gastric secretions (Marciani et al., 2001b). However, contradictory results on the effect of viscosity on gastric emptying have been reported, as seen in Table 2.3. The effect of gastric secretions could play a key role in determining gastric viscosity (see for example (Marciani et al., 2000)).

The last two results in Table 2.3 indicate the difference in emptying between two meals of the same constitution, one in solid/liquid form and one as a soup. There is

a difference between how solids and how liquids will empty from the stomach, with solids requiring a reduction in particle size, to around 1-2 mm, before they can empty (Hellström et al., 2006). The current work will focus on the ingestion of liquid meals and the gastric processes will not be considered, other than the emptying to the small intestine.

3.2.3 Modelling of Absorption in the Small Intestine

Within the intestinal lumen the chyme (mixture of consumed food and secretions from the digestive system) will be propelled aborally and via peristaltic contractions, which may also provide mixing of the nutrients (Janssen et al., 2007). Segmentation contractions will mix the chyme with no movement axially along the intestine (Barrett et al., 2005). The flow of nutrients along the digestive tract has been studied by numerous authors using computation fluid dynamics (CFD). Studies have been carried out to look at the mixing effects in the stomach (Ferrua and Singh, 2010; Ferrua et al., 2011; Kozu et al., 2010), the flow at the gastroduodenal junction (Dillard et al., 2007), and the flow in the intestine (Love et al., 2013; Nadeem et al., 2012; Riahi and Roy, 2011; Tripathi, 2011a,b,c; Tripathi et al., 2011) . These studies indicate that flow dynamics will affect the movement of nutrients to the luminal wall; this mass transfer can be an important parameter in nutrient bioaccessibility (whether the nutrients are in a form which can be absorbed).

In silico (computer simulated) studies of absorption in the small intestine have been carried out for drug and foods using different methodologies. In pharmacokinetics, two main types of models have been used: non-compartmental and compartmental. Non-

compartmental models are generally developed by fitting a mathematical expression to *in vivo* data, hence the fitted parameters will be accurate only for the system analysed and will not offer any predictive capability. In compartmental models, the system is divided in to compartments each representing a different physiological process; each with different mathematical expressions. A well formulated model should offer a certain amount of predictive capability (Peng and Cheung, 2009).

In literature the small intestine has been modelled as a single compartment (Dalla Man et al., 2006; Di Muria et al., 2010), as multiple compartments (Bastianelli et al., 1996; Yu et al., 1996) or as a plug flow reactor (PFR) (Logan et al., 2002; Stoll et al., 2000).

The model developed by Dalla Man et al. (2006) attempted to simulate an oral glucose tolerance test and a test meal. The intestine was modelled as a continuous stirred tank reactor (CSTR) with an input from the emptying of the stomach which is a function of the mass of glucose in the stomach. The model required the fitting of 6 parameters and had overall a good agreement with experiments ($p<0.005$). However, a more physiologically relevant control for gastric emptying is the sensing of nutrients in the duodenum, followed by the relevant feedback response (Brener et al., 1983; Calbet and MacLean, 1997). In addition, there is no consideration of food properties, which are likely to affect absorption (Gouseti et al., 2014; Tharakan et al., 2010), this will be one of the focus of the models developed in this work.

Yu et al. (1996) compared different compartmental and plug flow models, concluding that the flow profile in the small intestine can be characterised with both a multi-

compartmental model and a plug flow model, but that a single compartmental model, as used by Dalla Man et al. (2006) was inadequate at describing the flow profile.

A multi compartmental model was developed by Bastianelli et al. (1996) for a meal containing a variety of nutrients; the model used 4 compartments described by a series of ordinary differential equations. Although successful in describing digestion of a complex meal, the model does not consider the effect of one component on another (e.g. the effect of fibre on bioaccessibility of nutrients), the effect of nutrients on stomach emptying, nor the spatial location or movement along each compartment (Bastianelli et al., 1996). Another method, used by Stoll et al. (2000), was a plug flow model for the absorption of drugs in the small intestine. This model included the effect of increased surface area due to the folds and projections on the surface of the small intestine, and the effect of eddy rolls, to give good agreement with the absorption and degradation within the systemic circulation system Stoll et al. (2000). The model does not include any gastric disintegration or emptying effects, which might have significant implications on the absorption of nutrients.

The movement and degradation of a bolus in the small intestine was investigated by Taghipoor et al. (2012). The model considered the effect of non-degradable and soluble nutrients; it was further developed to look at the effect of dietary fibre (Taghipoor et al., 2014). This will have an effect on the viscosity and water holding capacity of the bolus, and on the absorption of nutrients (Taghipoor et al., 2014). This highlights the importance of bioaccessibility during digestion.

An all-in-one model would allow full representation of physiological conditions, however this will be at the expense of simplicity, increase the difficulty of implementa-

tion and requiring a large number of parameters, with doubtful advantages over *in vivo* tests. The different factors need indeed to be considered separately, and with their relative importance (Calbet and MacLean, 1997; Hellström et al., 2006; McHugh, 1983).

In this paper a mechanistic approach to the modelling of mass transport and absorption from the small intestine is attempted; focusing on the effect of the delivery of the nutrients to the small intestine from the stomach, the mass transfer (as a function of viscosity of the chyme) within the lumen of the small intestine and the hydrolysis of starch prior to absorption. This study will focus on the use of a plug flow reactor small intestine, assuming a laminar flow and constant mean velocity. In reality the regime of flow will depend on the nature of the chyme; lower viscosity solutions exhibiting turbulent flow, and more viscous solutions displaying laminar flow with large regular vortices (Janssen et al., 2007; Lentle and Janssen, 2008), as a result of wall contractions and curvature of the small intestine. Hence the assumption of laminar flow will likely underestimate the mass transfer of nutrients at particular viscosities and also affect the residence time distribution (Janssen et al., 2007), but the comparison of this parameter to the gastric emptying rate, and hydrolysis rate should still be revealing.

This paper will present three models of increasing complexity. In the first model, mass transfer of nutrients (exemplified by glucose) within the small intestine and through the intestinal wall will be linked with the viscosity of chyme. The effect of gastric emptying on glucose absorption will then be considered in the second model. The third model will include starch hydrolysis, assuming the reaction to follow Michaelis-Menten kinetics.

3.3 Development of Models

The following models (models 1-3) have been developed to investigate different factors that could influence the absorption of nutrients: bioaccessibility within the small intestine, gastric emptying rate and hydrolysis rate.

The models assume that the stomach and small intestine can be described by a series of reactors, specifically a continuous stirred tank reactor (CSTR) for the stomach, which will act as a reservoir and control the emptying of contents only, and a plug flow reactor (PFR) for the small intestine (Figure 3.2).

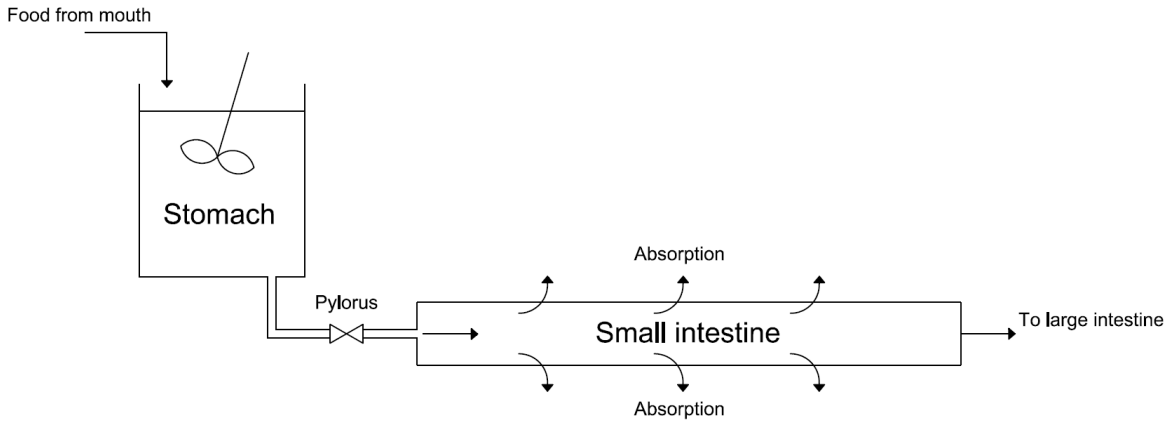

Figure 3.2: Diagram showing layout of CSTR stomach and PFR small intestine.

The models will be developed with increasing complexity, the first looking at the effect of mass transfer within the lumen on absorption of nutrients; the next will include the mass transfer and gastric emptying rate and how these both affect the absorption rate; the final model will look at, mass transfer rate, gastric emptying rate and starch hydrolysis, and how all 3 effect the absorption of nutrients.

3.3.1 Model 1: Glucose Absorption

This first model aims to investigate the effect of mass transfer on glucose absorption in the small intestine; this was modelled as a 1D advection-reaction equation (Logan et al., 2002):

$$\frac{\partial G(z,t)}{\partial t} = -\bar{u}\frac{\partial G(z,t)}{\partial z} - \frac{2f}{r_m}KG(z,t) \tag{3.1}$$

$$Change\ in\ glucose\ mass\ with\ time =$$

$$Movement\ along\ SI\ due\ to\ advection$$

$$- Absorption\ of\ glucose$$

Initial conditions:

$$G(z,0) = \begin{cases} G_0 & \text{if } z = l_0 \\ 0 & \text{otherwise} \end{cases} \tag{3.2}$$

Boundary conditions:

$$\left.\frac{\partial G}{\partial z}\right|_{z=0} = \left.\frac{\partial G}{\partial z}\right|_{z=L} = 0 \tag{3.3}$$

Here $G(z,t)$ is the glucose concentration at time t, and distance along the intestine z, and $\bar{u}$, is the mean velocity along the length of the intestine. The last term is the absorption of glucose, where K, is the mass transfer coefficient, $2/r_m$ is the ratio of surface area to volume for a cylinder and f represents the increase in absorptive surface area due to the folds of the intestinal wall. It is assumed that the volume input is a

bolus and enters the small intestine at position l_0 from the entrance, which is equal the radius of the bolus of entering liquid.

The overall mass transfer coefficient, K, will depend on the mass transfer within the lumen, through the epithelium layer and into the blood (Tharakan et al., 2010). As we are mainly interested in bioaccessibility we will simplify the phenomena and will ignore the effect of transport through the epithelium and blood assuming they are rapid and not rate limiting (Stoll et al., 2000; Wang et al., 2010). Therefore mass transfer coefficient, K is calculated from the relationship between Sherwood ($Sh = Kd/D$), Reynolds ($Re = \rho\bar{u}d/\mu$) and Schmidt ($Sc = \mu/\rho D$) numbers, where d is the mean intestinal diameter, L is the length of the intestine, D is the diffusivity, ρ is the density, and μ is the viscosity. The flow is in the laminar regime (for a water like solution, $Re \approx 3$), and the following empirical relationship is used (Carbonell, 1975).

$$Sh = 1.62 Re^{1/3} Sc^{1/3} \left(\frac{d}{L}\right)^{1/3} \tag{3.4}$$

Rearranging in terms of K gives:

$$K = 1.62 \left(\frac{\bar{u}D^2}{Ld}\right)^{1/3} \tag{3.5}$$

The diffusivity is calculated from the Einstein-Stokes equation, which will depend on the viscosity of the system:

$$D = \frac{K_B T}{6\pi\mu r_0} \tag{3.6}$$

Here K_B is the Boltzmann constant, T is the absolute temperature (310 K), and r_0 is the radius of the diffusing molecule.

Therefore the only parameter that we can control and manipulate will be the viscosity of the food, and from this we can manipulate the mass transfer rate. The mass transfer rate will be inversely proportional to the viscosity to the power of 2/3 i.e.:

$$K \propto \frac{1}{\mu^{2/3}} \tag{3.7}$$

Looking at the effect of protrusions on the surface of the intestine, it can be approximated that the villi increase the surface area by around 10 times relative to a cylinder and the microvilli by around 20 times (Barrett et al., 2005; Stoll et al., 2000). But only around 2% of the surface will be involved with the absorption of glucose, due to the fast speed of the absorption (Lentle and Janssen, 2011), giving an increased surface area of 4 times that of a cylinder. Including the effect of increased surface area from the presence of *plicae circulares* estimated at 3 times (Barrett et al., 2005; Stoll et al., 2000), this will give a value of f as 12. Values for parameters used in the models are shown in Table 3.1.

Table 3.1: Parameter values used in the model with references

Parameter	**Value**	**Reference**
Surface area increase due to folds, villi & microvilli (f)	12	(Barrett et al., 2005; Lentle and Janssen, 2011; Stoll et al., 2000)
Mean Velocity	1.7×10^{-4} m/s	(Stoll et al., 2000)
Length of small intestine	2.85 m	(Stoll et al., 2000)
Radius of small intestine	1.8 cm	(Stoll et al., 2000)
Radius of glucose molecule (r_0)	0.38 nm	(Schultz and Solomon, 1961)
Simulation time	10800 s	
Initial glucose/Starch mass	50g	
Viscosity	0.001- 10 Pa.s	
Emptying half time	2min-2h	
V_{max}	1-25 mM/min	(Fonseca, 2011; Satomura et al., 1984)
K_m	9 mM	(Fonseca, 2011)

The results, typically of glucose absorbed can also be described in terms of calories where 1 g of glucose is 4 kcal.

The equation can also be made dimensionless, glucose was expressed as a fraction of the inlet concentration ($G' = G/G_0$), time was divided by the residence time to give $\tau(= t\bar{u}/L)$, and the distance along the intestine was divided by the length to give $\xi(= z/L)$:

$$\frac{\partial G'(\xi,\tau)}{\partial \tau} = -\frac{\partial G'(\xi,\tau)}{\partial \xi} = -\tau_{transfer} G'(\xi,\tau) \tag{3.8}$$

where

$$\tau_{transfer} = \frac{2fK}{r_m}\frac{L}{\bar{u}} \tag{3.9}$$

This yields the dimensionless number $\tau_{transfer}$ which is the characteristic time of mass transfer, i.e. the mass transfer rate ($2fK/r_m$) multiplied by the mean residence time of passage through the small intestine ($L/\bar{u}$).

3.3.2 Model 2: Stomach Emptying and Intestinal Absorption of Glucose

The gastric emptying rate is thought to be the controlling mechanism in absorption of nutrients (Hellström et al., 2006; Mourot et al., 1988); for this reason a model was built to estimate the overall effect of the gastric emptying and mass transfer of glucose in the small intestine.

This model will treat the stomach as a reservoir for delivery of nutrients to the intestine only and will not consider its effect on the structure (chemical or physical) of

the food. Gastric emptying is modelled as exponential decay, i.e., a liquid solution with no lag phase (Calbet and MacLean, 1997; Hellström et al., 2006), as this model shows a good approximation of the emptying for liquid only meals. The model for the intestine will be the same as for model 1 but with an input from the gastric emptying.

The glucose mass in the stomach was represented by G_S:

$$\frac{dG_s}{dt} = -\gamma G_S \tag{3.10}$$

$$G_s|_{t=0} = G_{S0} \tag{3.11}$$

The model for the small intestine will take the following form:

$$\frac{\partial G(z,t)}{\partial t} \begin{cases} \gamma G_S - \bar{u}\frac{\partial G(z,t)}{\partial z} - \frac{2f}{r_m} KG(z,t) & \text{if } z = l_0 \\ -\bar{u}\frac{\partial G(z,t)}{\partial z} - \frac{2f}{r_m} KG(z,t) & \text{otherwise} \end{cases} \tag{3.12}$$

With initial conditions:

$$G(z,0) = 0 \tag{3.13}$$

and the boundary conditions:

$$\left.\frac{\partial G}{\partial z}\right|_{z=0} = \left.\frac{\partial G}{\partial z}\right|_{z=L} = 0 \tag{3.14}$$

Where G_{S0} is the initial input of glucose to the stomach (50 g) and, γ, is the decay constant, which can be expressed as the half time of emptying, which is a common parameter used to describe the emptying of liquids from the stomach:

$$t_{1/2} = \frac{ln(2)}{\gamma} \tag{3.15}$$

The model can also be made dimensionless in the same way as the advection-reaction equation to give:

$$\frac{dG'_s(\tau)}{d\tau} = -\tau_{emptying} G'_s(\tau) \tag{3.16}$$

where,

$$\tau_{emptying} = \gamma \frac{L}{\bar{u}} \tag{3.17}$$

Here $\tau_{emptying}$ is the characteristic time of gastric emptying and represents the rate of gastric emptying against the residence time in the small intestine. The half emptying times were varied between 10min and 3 h, which is within the range of typical values (seen in Table 2.3). The characteristic time of emptying was varied between 0.5 and 100, and the characteristic time of mass transfer was varied between 0.1 and 100, to see the effect on the fraction of glucose absorbed after the time is equivalent to the residence time.

3.3.3 Model 3: Starch Hydrolysis

In this work we will assume the starch remains intact until it reaches the small intestine, at which point hydrolysis of the starch, following Michaelis-Menten kinetics, will occur and a mass balance on starch and glucose in the small intestine has been carried out. In the small intestine model α-amylase will be in excess, and the ability to hydrolyse will be limited by the bioaccessibility of enzyme to starch, hence will be limited not by amount of enzyme but by the properties of the chyme (Ballance et al.,

2013; Englyst and Englyst, 2005). The effect of salivary α-amylase is not included as the focus of the study is the hydrolysis in the intestine and hence the input is starch only into the stomach at $t = 0$. The model will therefore take a form similar to model 2, with an extra component of starch:

$$\frac{dS_S}{dt} = -\gamma S_S \tag{3.18}$$

$$\frac{\partial S(z,t)}{\partial t} = \begin{cases} \gamma S_S - \bar{u}\frac{\partial S(z,t)}{\partial z} - \frac{V_{max}S(z,t)}{K_m + S(z,t)} & \text{if } z = l_0 \\ \bar{u}\frac{\partial S(z,t)}{\partial z} - \frac{V_{max}S(z,t)}{K_m + S(z,t)} & \text{otherwise} \end{cases} \tag{3.19}$$

$$\begin{aligned} &Change\ in\ starch\ mass\ with\ time = \\ &\qquad Movement\ along\ SI\ due\ to\ advection \\ &\qquad - starch\ conversion\ to\ glucose \end{aligned}$$

$$\frac{\partial G(z,t)}{\partial t} = -\bar{u}\frac{\partial G(z,t)}{\partial z} + \frac{V_{max}S(z,t)}{K_m + S(z,t)} - \frac{2f}{r_m}KG(z,t) \tag{3.20}$$

$$\begin{aligned} &Change\ in\ glucose\ mass\ with\ time = \\ &\qquad Movement\ along\ SI\ due\ to\ advection \\ &\qquad + generation\ of glucose \\ &\qquad - Absorption\ of\ glucose \end{aligned}$$

Initial conditions and boundary conditions are the same as model 2, with input of starch.

These equations can be made dimensionless:

$$\frac{\partial S'(\xi,\tau)}{\partial \tau} = -\frac{\partial S'(\xi,\tau)}{\partial \xi} - \frac{\tau_R S'(\xi,\tau)}{K_{mII} + S'(\xi,\tau)} \tag{3.21}$$

$$\frac{\partial G'(\xi,\tau)}{\partial \tau} = -\frac{\partial G'(\xi,\tau)}{\partial \xi} + \frac{\tau_R S'(\xi,\tau)}{K_{mII} + S'(\xi,\tau)} - \tau_{transfer} G'(\xi,\tau) \tag{3.22}$$

This yields two more dimensionless numbers as well as $\tau_{transfer}$:

$$\tau_R = \frac{L}{\bar{u}} \frac{V_{max}}{G_{S0}} \tag{3.23}$$

$$K_{mII} = \frac{K_m}{G_{s0}} \tag{3.24}$$

τ_R is the characteristic time of reaction, which is the residence time in the small intestine multiplied by the maximum reaction rate scaled with the initial input of starch. K_{mII} is the Michaelis constant normalised with the initial input of starch.

The characteristic time of reaction will be varied from 1 to 25 as the characteristic emptying was varied between 0.5 and 100 and characteristic time of mass transfer was varied between 0.1 and 100 to see the effect on fractional absorption of glucose after the time is equal to the residence time.

3.3.4 Simulations

The equations for each model were simulated in gPROMS (v.3.7.1); the partial differentials were solved using backward finite difference method. All models were simulated over a period of 3 h, similarly to what is used for glycaemic index measurements

(Brouns et al., 2005; Wolever et al., 1991). Graphs were produced using MATLAB (R2014a).

3.4 Results & Discussions

3.4.1 Model 1

The first model investigated the mass transfer of glucose in the small intestine, from an initial input at $t = 0$ of 50 g of glucose solution at different viscosities (20 simulations for viscosities ranging 0.001 Pa s and 10 Pa s). The lower viscosity corresponds to viscosity of water, while the higher viscosity would be relevant to honey. Figure 3.3(a) shows the amount of absorbed glucose against time. The initial rate of absorption decreases as the majority of glucose is absorbed, the effect being more pronounced at low viscosities. The results in terms of the rate of calories absorbed can be seen in Figure 3.3(b). For low viscosities one can see an initial high rate of absorption as the luminal glucose is absorbed. From Figure 3.3(a), it appears that by around 1 h, about half of the 50 g input of glucose has been absorbed and by around 3 h about 80% has been absorbed. It should be noted that *in vivo* experiments show that nutrients are absorbed are generally completely absorbed in the proximal small intestine (Weber and Ehrlein, 1998), this would imply 100% absorption by around 2 hours after input, and as this is a non viscous glucose solution we would expect faster absorption still, hence the results seem to underestimate the overall absorption rate when compared to that expected *in vivo*.This will result to a lower amount of glucose in the lumen, and a lower absorption gradient, which explains the decrease in the absorption rate for the

low viscosity solution. When higher viscosity solutions were used the absorption rate stays almost constant over the 3 h simulated. This is due to the low mass transfer rate resulting in only a small percentage of the luminal glucose being absorbed. In Figure 3.3(c) the effect of viscosity on absorbed glucose after 3 h is shown. Figure 3.3(c) indicates that at low viscosities (1 mPa s) glucose is absorbed to a high extent (80% of input), and as the viscosity increases the amount of glucose absorbed decreases. For viscosity higher than 0.1 Pa s, the total absorbed glucose is less than 10% of the input and does not significantly reduce with viscosity. Figure 3.3(d) is a dimensionless representation of Figure 3.3(c), i.e. glucose absorbed versus viscosity/rate of mass transfer. The curve has a sigmoidal shape, showing a rapid increase between $\tau_{transfer}$ values of 0.1 and 3, corresponding to viscosity values of about 0.2 Pa s and 1 mPa s.

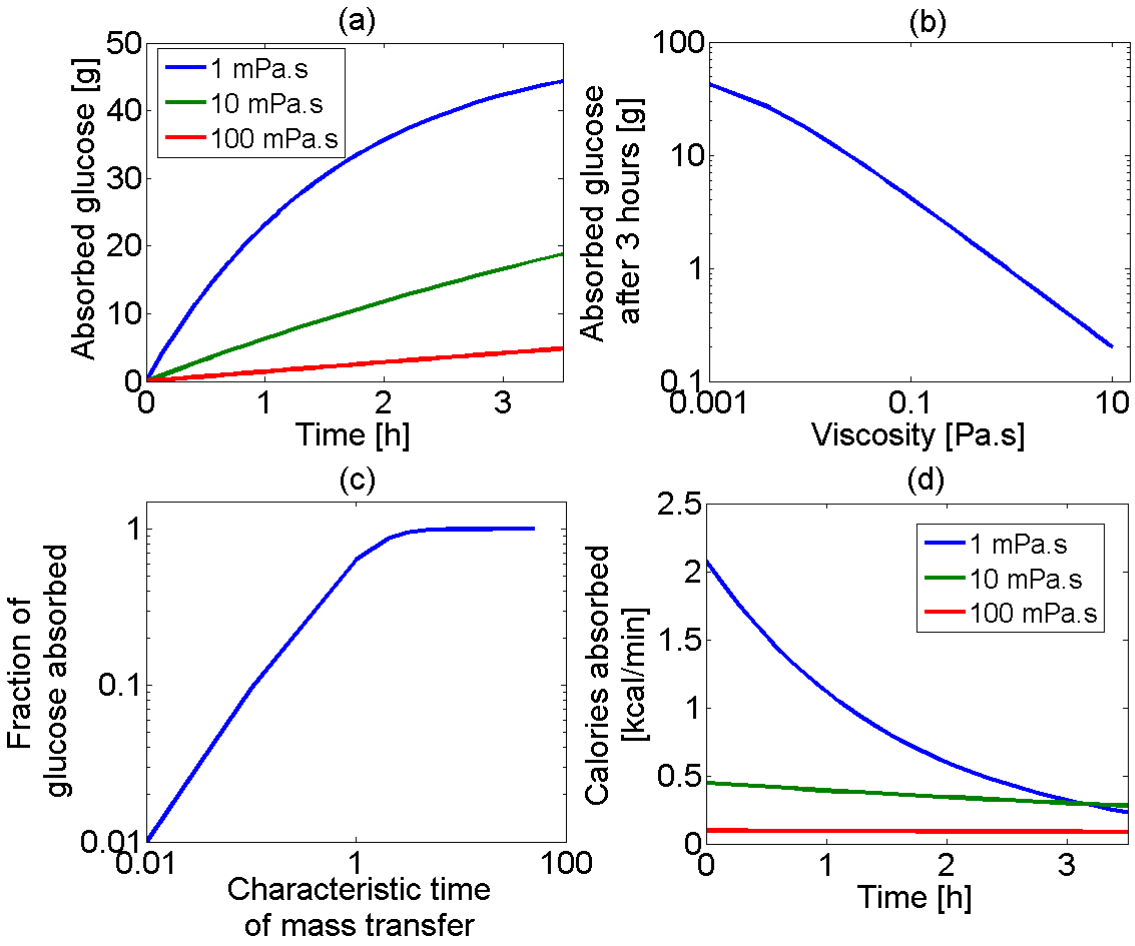

Figure 3.3: (a) the absorption curves for glucose solutions at different viscosities; (b) graph showing the total absorbed glucose after a 3 h period for solutions of different viscosities (log scale); (c) the fraction of glucose absorbed for the non-dimensionilised model against the characteristic mass transfer coefficient(log scale); (d) the rate at which calories are absorbed at different viscosities.

At low values of $\tau_{transfer}$, i.e., rate of absorption slow compared to the residence time, little absorption of glucose occurs; as $\tau_{transfer}$ increases an increase in absorbed glucose is observed. As the value of $\tau_{transfer}$ reaches 1, i.e., the rate of mass transfer is

similar to the rate of advection along the length of the intestine, a plateau occurs with total absorption of the fed glucose.

These results indicate that the mass transfer coefficient within the lumen (determined by luminal viscosity) may have a large effect on the absorption of nutrients in the small intestine especially when mass transfer is significantly limiting the rate of absorption typically at viscosity values greater than 0.1 Pa s. Similar relation- ships have been seen in vivo, for example, Ellis et al. (1995) showed a non-linear relationship between zero shear viscosity of the chyme (measured in the jejunum) and absorption of nutrients in pigs, also indicating an inverse linear relationship between absorption over a 4 h period and concentration of guar gum in the meal (Ellis et al., 1995). (Takahashi et al., 2009) showed how the disappearance of glucose in the small intestine of rats is inversely proportional to the viscosity (Takahashi et al., 2009), in this work 3 different viscosities were used and so there is not enough evidence to extrapolate these models. Fitting these results to a power law curve the absorption was found inversely proportional to the viscosity to the power of around 0.45; this is lower than the relationship suggested in the present model (see equation (3.7)). This difference could be due to the added motility of a functioning gut, when digesting materials of high viscosity which is not included in this model. Due to secretions in the stomach and intestine the viscosity is unlikely to be constant with time, which is another limitation of the current model, but the trends here are consistent with those reported in the literature. Leclère et al. (1994) took a different view and speculated that the observed changes in blood glucose etc. from different viscosity meals are mainly due to the effect of the viscosity on stomach emptying rather than any mass transfer resistance within the small intestine, which

the current results show. Model 2 will be used to compare the emptying rate and mass transfer rate to test this hypothesis.

Overall in this work the parameters used were obtained from literature and the results were within the range of order of magnitude seen with in vivo data from literature see for example Dalla Man et al. (2006). Validation of similar *in silico* digestion models can be challenging as availability rather than postprandial glucose data would be required. As part of on going work we are aiming to make best use of existing in vivo data in the literature to validate our models. In vitro studies though demonstrate some agreement with the results presented here. Tharakan et al. (2010) showed a decrease in absorption with viscosity, pointing to an increase in diffusion resistance or decreased mixing efficacy as an explanation. A 50% decrease in absorption was seen when the guar gum was added at 0.5% compared to a starch mix with no guar gum. Gouseti et al. (2014) showed similar results for the absorption of glucose *in vitro* from model solutions for a range of food hydrocolloids. Others show similar trends (Sasaki and Kohyama, 2012; Singh et al., 2010; Slaughter et al., 2002), whilst speculating that the viscosity modifiers may have additional effects on the digestion process such as encapsulation of starch molecules, thus reducing bioaccessibility (Sasaki and Kohyama, 2012), or direct inhibition of digestive enzymes (seen with Guar Galactomannan) (Slaughter et al., 2002). The results here seem to agree with many of the experimental observations but the present model does not include any mixing effects, e.g., via segmentation or peristalsis. These are likely to increase the mass transfer rate and hence increase the absorption rate (Gouseti et al., 2014; Tharakan et al., 2010), and subsequently this could reduce the effect of viscosity upon the absorption rate. In future work the effect

of mixing could be included in the mass transfer coefficient by investigating how segmentation/peristaltic mixing will affect the empirical relationship between Sherwood, Reynolds, and Schmidt numbers.

3.4.2 Model 2

The second model expanded on model 1 by including the effect of gastric emptying, on glucose absorption. The input at $t = 0$ is into the stomach, and not into the intestine; the stomach then feeds the intestine. Figure 3.4(a) shows the estimated emptying for glucose solutions for 3 different emptying half-times (15 min, 30 min and 1 h shown). Increasing the half-time results in a slower emptying rate, by definition. Figure 3.4(b) shows the associated glucose absorption in the small intestine. The total absorbed has a sigmoidal shape. For times smaller than 15mins the rate of absorption is low as expected from the small amount of glucose in the lumen (more than 50% glucose still been in the stomach). This is equivalent to an induction time. This is followed by an almost linear increase as more glucose enters the intestine and is available to be absorbed. The rate of absorption decreases after the majority of luminal glucose is absorbed. As the half-time of emptying increases, the induction time decreases and the rate of absorption decreases. Figure 3.4(c) is a contour plot showing absorption of glucose versus emptying times (characteristic time of emptying) and viscosities (characteristic time of mass transfer). This plot can be separated into 4 regions: (1) the bottom right shows an area where the emptying rate is limiting, and greater characteristic time of emptying will result in greater absorption of glucose and vice versa; (2) the bottom left region shows an area where both emptying rate and mass transfer rate will be rate limiting; (3) the top

left shows the area where mass transfer rate will be limiting only; and (4) top right area shows the area where near maximum absorption is reached (these regions are shown more clearly in Figure 3.5).

The characteristic mass transfer time was varied from 0.1 to 100. The values of 0.1 and 3.4 corresponding to viscosities of 0.2, 10 3 Pa s, respectively; in this range of viscosities we would expect that mass transfer can be the rate limiting step. The higher values of characteristic mass transfer rates are in regime of effective and rapid mixing, i.e. one where mass transfer values are very large, e.g. $K = 1 \times 10^{-6}\ m/s$ The characteristic time of emptying was varied between 0.5 and 100; where the value of 3.2 and 100 resulted in half emptying time of 1 h and 2 min respectively. The lower value of 0.5 was included to investigate what happens for slow emptying and fast intestinal transit, corresponding to a 2 h emptying half-time and 1.5 h (Read et al., 1986) intestinal residence time.

In this work we will incorporate published research to understand the effect of gastric emptying (Brener et al., 1983; Calbet and MacLean, 1997; Marciani et al., 2000, 2001b; Shimoyama et al., 2007), using exponential decay to model the stomach emptying (Brener et al., 1983; Calbet and MacLean, 1997; Hellström et al., 2006). For reasons of simplicity the effect of secretions is not included in this model (Marciani et al., 2000, 2001b).

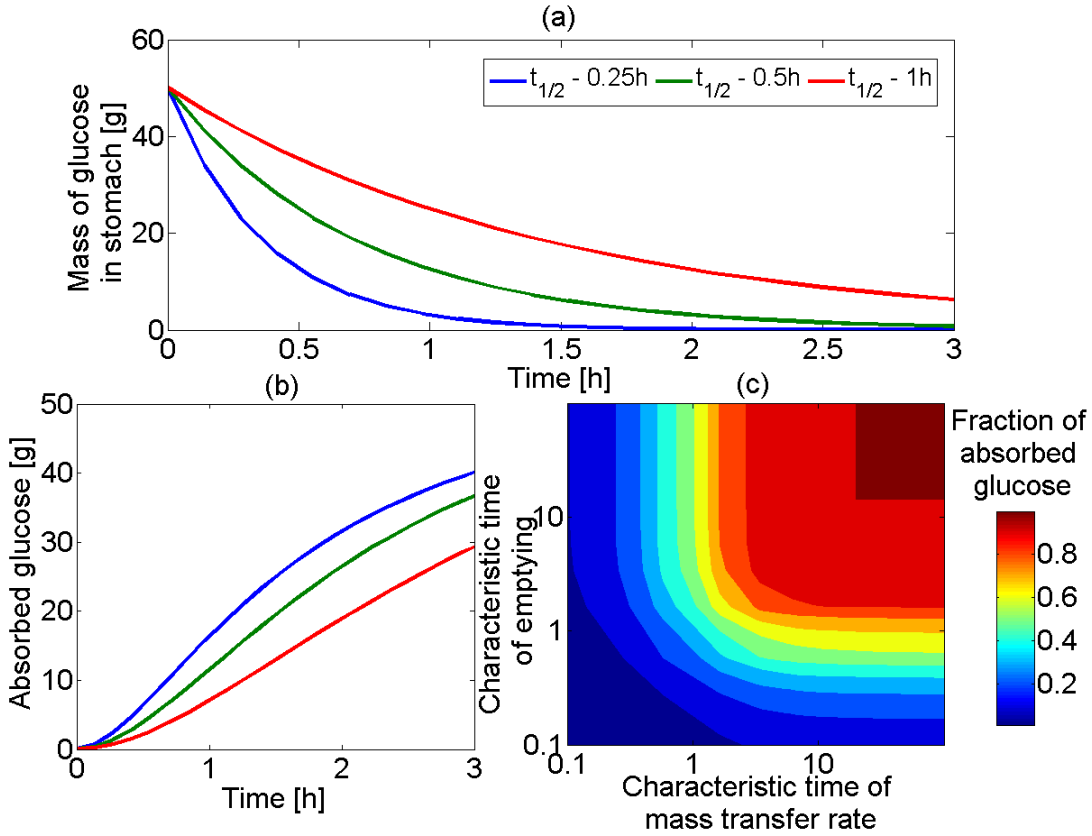

Figure 3.4: (a) mass of glucose in stomach over time with different half-time's of emptying and viscosity of 1 mPa s, (b) the absorbed glucose against time for 3 different gastric emptying half-time's, (c) contour plot of the characteristic mass transfer, against the characteristic emptying time on log-log scale, colour representing the fraction of glucose absorbed.

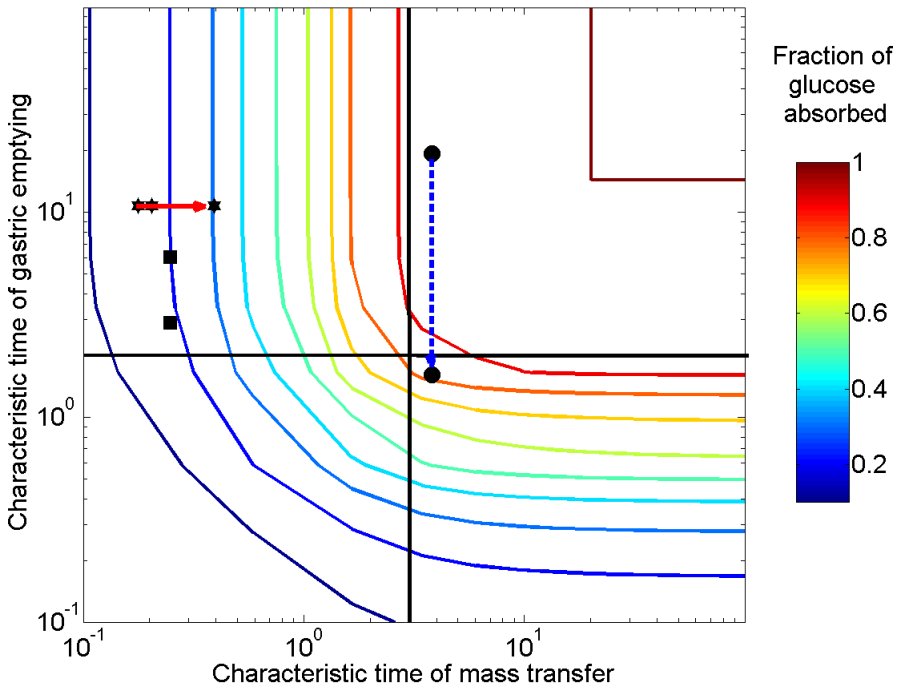

Figure 3.5: Contour plot from Figure 3.4 (c) with plots from literature (★) (Marciani et al., 2000), (■) (Marciani et al., 2001b), (●) from the model.

The two square data points (Marciani et al., 2001b) represent low and high nutrient meals with similar viscosities. One would expect that they will have similar fractional absorption of glucose, even with a change in gastric emptying rate, as absorption is controlled from mass transfer. The majority of the data in Table 2.3 for liquid meals will appear into the upper left region of Fig. 5, indicating that the total absorption after around 3 h should be mass transfer limited.

The final set of points connected by a blue dotted arrow indicates how solutions, with similar initial viscosities (1 mPa s), would be affected by increasing the gastric emptying half-time from 10min to 2 h. In this case the system will see little effects in the total glucose absorption until it crosses the black horizontal line (around a half-time

of 1 h). A further increase in the gastric emptying half-time will result in a shift to a gastric emptying limited region, which will cause a reduction in the fraction of glucose absorbed. Overall for relatively high viscosity food systems it appears that the fraction of glucose absorbed after 3 h is not controlled from gastric emptying rate, as with half-times of less than 90min (a characteristic time of emptying around 2), the system will be in the upper left region of Figure 3.5, limited by the mass transfer coefficient.

3.4.3 Model 3

Model 3 incorporates the effect of starch hydrolysis to produce glucose on Model 2. In Figure 3.6(a) absorbed glucose is plotted against time for different rates of hydrolysis, V_{max}. One can see that the increasing V_{max} results in an increase in glucose absorption and decrease of lag phase (the initial slow absorption region). This is expected as the faster the starch is hydrolysed to glucose the faster glucose can be absorbed. However, increasing chyme viscosity will also affect the bioavailability of starch for reaction, or enzyme kinetics. In Figure 3.6(b) contour plots of glucose absorbed for different characteristic reaction rates against characteristic emptying and mass transfer are shown.

The planes show similarities to Figure 3.4(c), where the plot of characteristic emptying and transfer rate showed four regions. In Figure 3.6(b), at low characteristic reaction rates there is little change in absorption as either emptying or mass transfer are changed, i.e., very little of the starch is hydrolysed to glucose, but increasing the reaction rate moves the system away from being reaction limited and the other parameters have a greater effect on glucose absorption, at around a characteristic reaction rate of 25, the starch is hydrolysed very quickly and behave similar to the Figure

3.4(c), where the input is purely glucose. The two slices in the middle, V_{max} = 7.1 mmol/min(Satomura et al., 1984) and V_{max} = 14.1 mmol/ min (Fonseca, 2011), show results for reaction kinetics taken from literature, and it can be seen that the reaction rate can be limiting if these rates are seen in vivo.

Each of these parameters is currently independent of the others, but in reality they are likely coupled. Changes in viscosity are likely to affect the emptying and mass transfer of nutrients as previously stated, as well as mass transfer of the enzymes. In addition, It is also important to consider other effects of food ingredients e.g., nutrient encapsulation by thickeners or direct enzyme inhibition by additives (Sasaki and Kohyama, 2012; Slaughter et al., 2002).

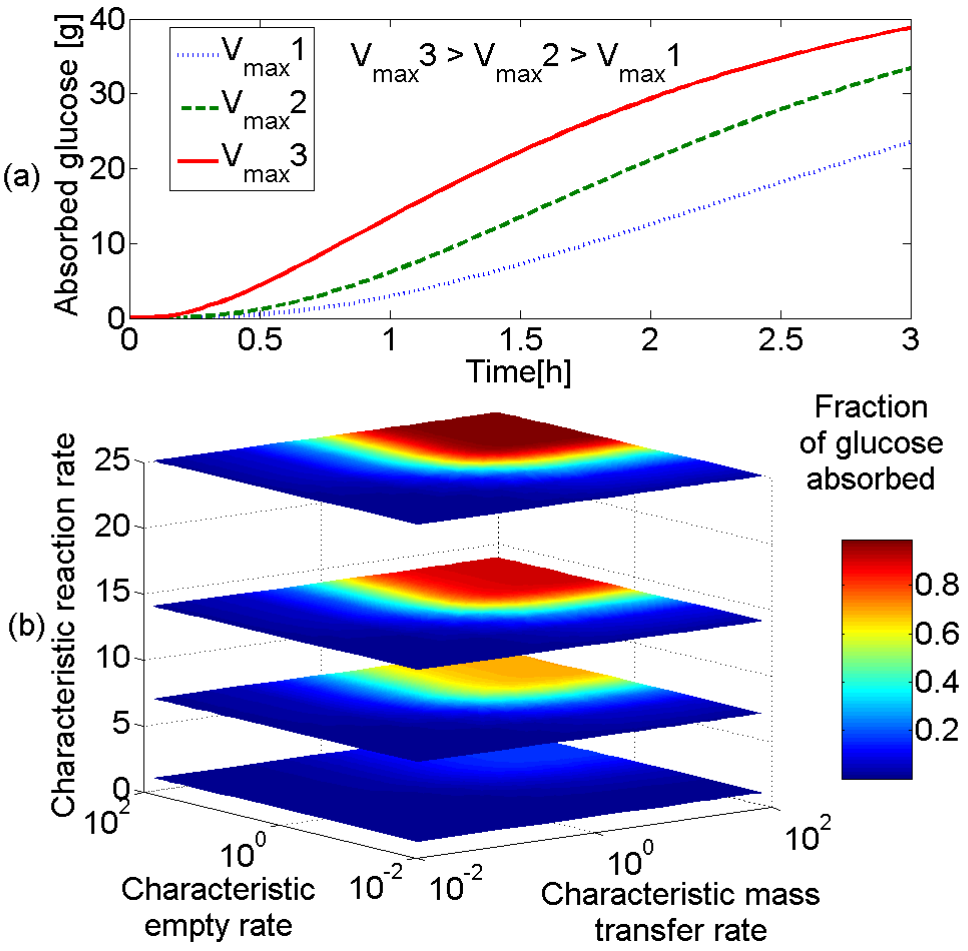

Figure 3.6: (a) absorption of glucose with time for systems with different starch hydrolysis rates (gastric emptying half-time 20min, viscosity = 1 mPa s, V_{max} = 4, 9 and 16 mmol/ min), (b) contour plot showing the effect of gastric emptying rate, mass transfer rate and reaction rate for hydrolysis on absorption of glucose.

3.5 Conclusion

Mathematical models to describe in vivo digestion were developed and used to examine the relative effect of gastric emptying, mass transfer and reaction rate limitations in the small intestine. Within the assumptions of the models the results indicate that

for gastric emptying half-times less than 1 h the viscosity/mass transfer rate is the limiting factor for the amount of glucose absorbed after 3 h. If the emptying half-time is greater than 1 h, both the gastric emptying and mass transfer rates can influence the absorption depending on the viscosity. If the mass transfer rate is faster than 1×10^{-7} m/s (i.e. luminal viscosity of 1 mPa s), the amount absorbed in 3 h is not limited by the mass transfer, and only by the gastric emptying rate. Starch hydrolysis reaction rates, when both the mass transfer and gastric emptying are fast and not limiting, can have a pronounced effect. The reaction kinetics for starch hydrolysis from literature showed around 25% difference in absorption when used in the model. Further development of the models is required to understand some of the controlling mechanisms as well as comparison with in vivo data to obtain confidence in the validity of the results.

Chapter 4

Effect of Chyme Viscosity & Nutrient Feedback Mechanism on Gastric emptying

Chapter 4 is taken from the paper published in *Chemical Engineering Science* volume **171** in 2017 (Moxon et al., 2017). The work was carried out in collaboration with KU Leuven, with funding from the Erasmus+ Qsafe project.

The modelling and simulation as well as writing of the chapter was carried out by myself.

Philippe Nimmegeers provided advice and recommendations upon the implementation of the feedback model, sensitivity analysis, and Monte-Carlo analysis and also reviewed the manuscript. Further work is planned where Philippe will build upon the model presented in this chapter and carry out an Optimal Experimental Design procedure.

Dries Telen provided advice and recommendations upon the implementation of the feedback model, sensitivity analysis, and Monte-Carlo analysis and also reviewed the manuscript.

Jan Van Impe provided advice and recommendations upon the implementation of the feedback model and also reviewed the manuscript.

Chapter 4 builds upon the model developed in Chapter 3. The overall aim of Chapter 4 is to show how the viscosity of a liquid meal can influence not only the intestinal mass transfer but also the gastric processes, and link the gastric emptying rate to the absorption rate through a feedback mechanism. This mechanism has been identified by many researchers and discussed in Chapter 2 but never implemented in a mathematical model. Along with this a model for the secretion of gastric juice is developed, similar to those discussed in Chapter 2 but assumes that the rate of secretion is influenced by the gastric chyme viscosity. The emptying rate from the stomach is also studied and linked to the meal properties allowing for the parameter γ, introduced in Chapter 3 and assumed constant, to be linked to the meal properties/gastric properties.

4.1 Abstract

A comprehensive mathematical model of the digestive processes in humans could allow for better design of functional foods which may play a role in stemming the prevalence of food related diseases around the world. This work presents a mathematical model for a nutrient based feedback mechanism controlling gastric emptying, which has been identified *in vivo* by numerous researchers. The model also takes into account the viscosity of nutrient meals upon gastric secretions and emptying. The results show that modelling the nutrient feedback mechanism as an on/off system, with an initial emptying rate dependent upon the secretion rate (which is a function of the gastric chyme viscosity) provides a good fit to the trends of emptying rate for liquid meals of low and high nutrient content with varying viscosity.

4.2 Introduction

Numerical modelling of the digestive system has been carried out from both a pharmacokinetic (Di Muria et al., 2010; Peng and Cheung, 2009; Stoll et al., 2000; Yu et al., 1996), and a food science perspective (Bastianelli et al., 1996; Dalla Man et al., 2006; Logan et al., 2002; Moxon et al., 2016; Penry and Jumars, 1986, 1987; Taghipoor et al., 2014, 2012). The general approach is to break the digestive system into compartments which can be described as ideal reactors. The stomach is typically described as a Continuous Stirred Tank Reactor (CSTR), whereas the small intestine has been described as a single CSTR, multiple CSTRs in series, or as a Plug Flow Reactor (PFR). Most of these models take only the dosage of the nutrient or drug into account when modelling

the absorption, ignoring the physical properties of the meal, such as viscosity, and the interactions with the digestive system or other meal components. Here we will present a simple model to describe the influence of viscosity upon gastric processes (e.g., Marciani et al. (2001b) etc.) and the effect of the nutrient based feedback mechanism upon gastric emptying (e.g., Brener et al. (1983) etc.). The aim is to develop a model which takes into account physical and chemical properties of the meal and can provide a greater understanding of food digestion. This could help in the development of functional foods to combat diet related diseases, such as obesity and type-2 diabetes etc., which are becoming increasingly more prevalent in modern society (Jew et al., 2009; Popkin, 2006).

4.2.1 Gastric Emptying

The presence of a nutrient based feedback mechanism, also referred to as 'duodenal Brake', has been observed by numerous researchers such as (Brener et al., 1983; Calbet and MacLean, 1997; McHugh and Moran, 1979; Shahidullah et al., 1975), by measuring gastric emptying rate with intraduodenal nutrient secretions. This mechanism allows for the pyloric sphincter to control the emptying of gastric content into the duodenum depending upon the amount of nutrient already present in the proximal small intestine- ensuring a constant rate of calories per minute entering the small intestine- and the nutrient type (Calbet and MacLean, 1997). Similar to the tongue the sensing of nutrients within the intestine will be via taste receptors, such as the T1R family of receptors allowing for the sensing of sugars (Depoortere, 2014; Young, 2011). The stimulation of these sensors induces the secretion of the hormone CKK, which acts

to decrease the gastric emptying rate and increase satiety (Depoortere, 2014), and/or slow gastric emptying via stimulation of the vagal nervous system (Young, 2011).

Whilst nutrient content will have an effect upon the gastric emptying rate other meal properties will also have an influence. The volume of a meal has been shown to speed up gastric emptying (Hunt and Stubbs, 1975). The viscosity of the chyme can also have an effect upon the gastric emptying rate, with some experimental results showing higher viscosities increase the gastric emptying rate of nutrient meals (Shimoyama et al., 2007; Vist and Maughan, 1995), while other show the opposite (Marciani et al., 2001b; Yu et al., 2014). For non-nutrient meals, it has been shown that the gastric volume over time shows little variation with the viscosity of the meals input (with a 1000 times increase in zero shear viscosity), but that the level of secretions will be much greater with higher viscosities- resulting in large drops in the viscosity of the chyme (Marciani et al., 2000).

This work will build upon a model previously developed in Moxon et al. (2016) (Chapter 3). The aim is to demonstrate the viscosity of a liquid meal affects the mass transfer of nutrients within the intestine, and will influence the gastric emptying rate via a feedback mechanism. Further to this a model for the secretion of gastric juices is proposed, assuming the rate of secretion is influenced by the gastric chymes viscosity, and that the emptying rate previously assumed constant (γ) (Moxon et al., 2016), is affected by the meal and gastric properties. The work will attempt to fit model outputs to experimental data and gain numerical values for the constants used in the model from the experiments.

4.3 Model Structure

A model will be presented building upon the work in Chapter 3 (Moxon et al., 2016), which assumed the stomach can be modelled as a continuous stirred reactor, and small intestine as a plug flow reactor and look at how gastric emptying rate a intestinal lumen mass transfer rate can influence the absorption of nutrients. Most models assume gastric emptying work will link the gastric emptying rate and luminal mass transfer rate by introducing a nutrient based feedback mechanism observed from literature (Brener et al., 1983). Secretion in the stomach can be initiated via 3 different phases (Di Mario and Goni, 2014): a cephalic phase, due to processes prior to arrival of the food in the stomach (e.g., taste); a gastric phase, due to the presence of food in the stomach; and an intestinal phase, via a feedback mechanism from the content of the small intestine. A secretion model will focus on how meal properties might affect the gastric phase of secretion (the phase inducing the highest volume of secretions (Di Mario and Goni, 2014)) and the influence of secretions upon the chyme viscosity, which will play a role in the gastric emptying of the meal. A schematic of the model is shown in Figure 4.1. The work will further introduce a secretion model, focusing on how meal properties might affect the *gastric phase* of secretion and the influence of secretions upon the chyme viscosity, which will play a role in the gastric emptying of the meal.

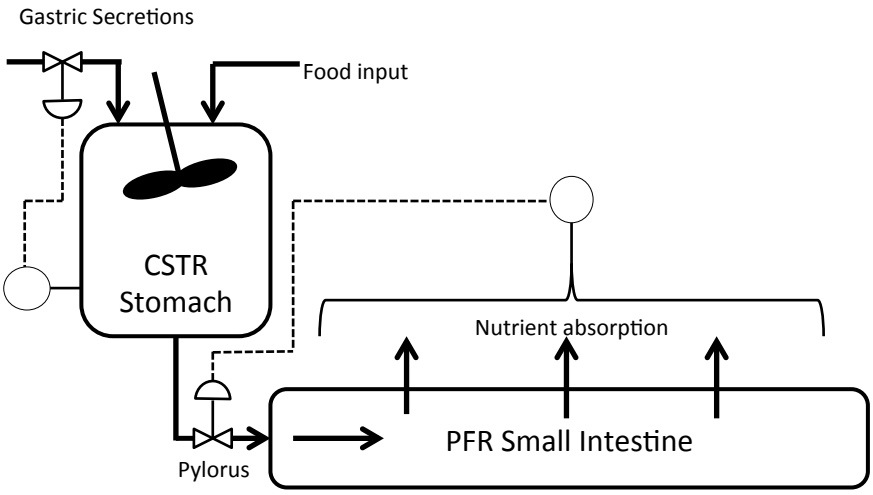

Figure 4.1: Schematic of the processes occurring in the stomach and small intestine which will be modelled. The absorption rate from the small intestine will control the pyloric sphincter, and the secretions will be controlled via properties of the food in the gastric compartment.

4.3.1 Model Equations

The model presented will look only at liquid meals, with a mass of nutrient ($Stom_{N0}$ $[g]$) entering the stomach at $t = 0$. The basic structure of the model will be taken from previous work (Moxon et al., 2016). The stomach will be modelled as a continuous stirred tank reactor with the output emptying into the duodenum over the time period $t \in [0, t_f]$, where t_f is the final measurement time. The mass of nutrient in the stomach is represented as $Stom_N$:

$$\frac{dStom_N(t)}{dt} = -\gamma\, Stom_N(t) \tag{4.1}$$

$$Stom_N(0) = Stom_{N0} \tag{4.2}$$

Where γ is the gastric emptying rate in s^{-1}. It is assumed that the meal is consumed rapidly and that negligible gastric emptying or dilution of gastric content will occur

before the whole meal is consumed. This assumption is more relevant for low viscosity liquid meals, which are consumed more rapidly than high viscosity meals (Marciani et al., 2001b).

The mass of nutrient in the small intestine will be modelled as a 1-D advection-reaction equation, assuming the limiting factor in the absorption of nutrients will be the mass transfer rate within the intestinal lumen. This approach has been taken by others when looking at drug or food absorption (Logan et al., 2002; Stoll et al., 2000). It was shown by Yu et al. (1996) to give a good description of the intestinal transit time, much better than assuming a single compartment, and similar to assuming 7 CSTR compartments. The mass of nutrient in grams $(SI_N(z,t))$ will be modelled along the temporal domain and spatial domain, $z \in [0, L]$, where z is the position along the length of the intestine in meters, and L is the total length of the small intestine (2.85m (Stoll et al., 2000)), and position $z = 0$ represents the position of the pyloric sphincter:

$$\frac{\partial SI_N(z,t)}{\partial t} = \begin{cases} \gamma\, Stom_N(t) - \bar{u}\, \frac{\partial SI_N(z,t)}{\partial z} - K_a\, SI_N(z,t) & \text{if } z = l_0 \\ -\bar{u}\, \frac{\partial SI_N(z,t)}{\partial z} - K_a\, SI_N(z,t) & \text{Otherwise} \end{cases} \tag{4.3}$$

$$SI_N(z,0) = 0 \tag{4.4}$$

With the following Neumann boundary conditions:

$$\left.\frac{\partial SI_N}{\partial z}\right|_{z=0} = \left.\frac{\partial SI_N}{\partial z}\right|_{z=L} = 0 \tag{4.5}$$

The advection term $\bar{u}$ will be the mean velocity (1.7×10^{-4} (Stoll et al., 2000)). K_a is the absorption constant of the nutrients in the intestinal lumen, linked in previous work to the mass transfer coefficient in the lumen (Moxon et al., 2016), but will be estimated from experimental data in the work.

The mass entering at time t, to the small intestine from the stomach will be assumed to enter as a spherical bolus of effective radius l_0, and it will be assumed that to be classed as in the small intestine it must be a distance along the small intestine equal to the to that radius, l_0.

The absorption rate of nutrients from the intestinal lumen, will be modelled as the integral of the reactive terms from Equation 4.3 over the length of the intestine:

$$A(t) = K_a \pi r^2 \int_0^L \frac{SI_N}{V} dz \tag{4.6}$$

4.3.2 Feedback Mechanism

A feedback mechanism will be introduced to the model developed in Chapter 3 (Moxon et al., 2016). It will be assumed that the mechanism will be mediated by the bioaccessibility of the nutrient in the intestinal lumen (Depoortere, 2014) and that this controls the rate at which gastric chyme empties. Hence here the feedback mechanism is triggered by the rate of absorption, described by Equation 4.6. From literature (Brener et al., 1983; Calbet and MacLean, 1997) it seems that the mechanism maintains a constant rate of calories emptied from the stomach, and the model will assume the mechanism acts as an on/off switch, acting instantaneously. A maximum absorption rate, A_{max}, will be set, and if this rate is exceeded the gastric emptying rate, γ, will be set to zero:

$$\gamma = \begin{cases} 0 & \text{if } A(t) > Amax \\ \\ \gamma_0 & \text{otherwise} \end{cases} \tag{4.7}$$

To ensure smoothness Equation 4.7 can be approximated to:

$$\gamma = \gamma_0 \left[1 - \left(\frac{1}{1 + \exp(\tau_A (A(t) - A_{max}))} \right) \right] \tag{4.8}$$

The term τ_A is set to a value of $5 \times 10^6\ g/s$ to ensure that the function behaves in the same way as the logical one. A physiological interpretation and greater understanding is left for future work.

4.3.3 Secretion Model

Data on gastric chyme viscosity was taken from Marciani et al. (2000) which measured the gastric response of non-nutrient meals of different viscosities. Experiments were conducted for four fluids of different viscosities, and Echo-planar MRI was used to assess the volume remaining in the stomach and viscosity of the gastric chyme. Nasogastric tubes were also used to take samples from the stomach and measure the viscosity of gastric chyme.

The model will assume the gastric content is perfectly mixed and that secretions are a function of viscosity only. The viscosity of the meal will be assumed to be a function of the concentration of thickener present. The assumption of perfect mixing is more accurate for the low viscosity solutions than for the higher viscosity solutions, and for two phase meals it has been shown that the solid phase resides in the proximal stomach for long periods of time, when compared to liquid phases (Collins et al., 1991), as such this assumption may not be applicable to a two phase meal. Results shown in Marciani et al. (2001b) for the dilution of highly viscous meals highlight that dilution is much greater at the outer edge of the chyme bolus initially, with greater dilution towards the centre taking more time. This can also be seen via the variation in viscosity measurement by Marciani et al. (2000); for the high viscosity solution (initially 11 Pa.s) the measured viscosity in the stomach (after 12 min) varied between 1 and 8.5

Pa.s, whereas the variation was smaller for the consumption of 2 Pa.s meal (0.9-2.0 Pa.s). The assumption of perfect mixing will therefore lead to more accurate results when considering the emptying of low viscosity meals, but should still provide insight into the emptying of higher viscosity liquid meals. However when looking at solid components separate compartments may be required to account for the distribution between proximal and antral regions of the stomach.

The relationship between the concentration of locust bean gum (LBG) and viscosity was found from the initial measurements, and the fit carried out using MATLAB curve fitter application. The most reasonable fit was found using a power law, but normal meals are likely to have more complex rheological properties.

$$\mu = a_L {C_{LBG}}^{b_L} \tag{4.9}$$

From this equation the concentration of locust bean gum (C_{LBG}) in the stomach was calculated to give the correct initial viscosity and this was used in the simulations, and constant $a_L = 2\ [Pa.sL/g]$ and $b_L = 4.21\ [-]$.

The rate of secretions into the gastric compartment have been shown to increase with the viscosity of a meal (Marciani et al., 2000, 2001b), and that this could be due to the effect of gastric distension which has been shown to increase the secretion rate of gastric acid (Grötzinger et al., 1977). It is then assumed that the secretion rate will be a function of the viscosity of digesta in the stomach:

$$K_{sec} = \lambda_s \mu^b + S_b \tag{4.10}$$

Where λ_s and b are constants to be evaluated and S_b is the basal secretion rate, i.e., that occurring with no stimulation.

To describe the gastric compartment we must add two more components to the original gastric model (Equation 4.2), one for the mass of LBG in the meal ($Stom_{LBG}$), to allow viscosity calculations, and one for the non-nutrient liquid ($Stom_{liq}$), which will have an input from the secretions.

$$\frac{dStom_{liq}}{dt} = K_{sec}(\mu) - \gamma\ Stom_{liq}(t) \tag{4.11}$$

$$\frac{dStom_{LBG}}{dt} = -\gamma\ Stom_{LBG}(t) \tag{4.12}$$

$$C_{LBG} = \frac{Stom_{LBG}(t)}{Stom_{liq}(t)/\rho_w} \tag{4.13}$$

Where ρ_w is the density of the non-nutrient liquid (assumed to have the properties of water). The total mass in the stomach will be:

$$Stom_{tot} = Stom_N + Stom_{liq} + Stom_{LBG} \tag{4.14}$$

Evaluating the secretion rate and viscosity of the gastric chyme allows the initial gastric emptying rate (γ_0 in Equation 4.8) to be evaluated as a function of the chymes properties. The initial rapid rate of emptying has been linked to the volume in the stomach (Brener et al., 1983; Moran et al., 1999), and the viscosity (Kusano et al., 2011; Marciani et al., 2001b; Shimoyama et al., 2007). But in the results of Marciani et al. (2000), varying the viscosity of non-nutrient meals resulted in negligible variability in gastric half life, but did increase the secretion rate.

To determine which of these factors are important in the initial rapid emptying phase, a number of different hypotheses for the dependence of the parameter γ_0 were

tested. The following equations were defined to look if the volume, viscosity or secretion rate or combination best describes the emptying:

$$\gamma_0 = m_\mu \mu + m_s V_{tot} \tag{4.15}$$

$$\gamma_0 = m_s V_{tot} + C_1 \tag{4.16}$$

$$\gamma_0 = m_\mu \mu + C_1 \tag{4.17}$$

$$\gamma_0 = m_{sec} K_{sec} + C_1 \tag{4.18}$$

$$\gamma_0 = m_{sec} K_{sec} + m_s V_{tot} \tag{4.19}$$

Here V_{tot} is the total volume in the stomach ($Stom_{tot}/\rho_w$), μ is the gastric viscosity, and K_{sec} is the gastric secretion rate. $m_\mu[1/(Pa.s^2)]$, $m_s[1/(m^3.s)]$, and $m_{sec}[1/g]$ are the rate constants of gastric emptying as a function of the viscosity, gastric volume, and gastric secretion rate, respectively, and C_1 is a constant emptying rate independent of the three factors. For nutrient meals the overall emptying rate will depend upon the feedback mechanism (equation 4.8).

A parameter estimation will be carried out using the following equations against experimental data from Marciani et al. (2000), and the Akaike Information Criterion (AIC) will be used to evaluate which of the models gives the best description of the experimental results:

$$AIC = n \ln\left(\frac{SSE}{n}\right) + 2p \tag{4.20}$$

Where n is the number of experimental data points, p is the number of parameter to be fit and SSE is the sum of squared errors.

The model assumes that the reduction in the viscosity of the gastric content is due to the dilution of the thickener in the gastric compartment, though it should be noted

that there will also be dilution due to saliva. The effect of digestive enzymes (salivary α-amylase and proteases) will also influence the viscosity of gastric chyme (De Wijk et al., 2004).

4.3.4 Methods

Sensitivity Analysis

To analyse how the model outputs vary with respect to the estimated parameters a sensitivity analysis can be carried out. In this work a simple finite difference approach will be used to evaluate the sensitivity:

$$\frac{\partial f}{\partial \theta_i} = \frac{f(\theta_i + \theta_i \varepsilon) - f(\theta_i)}{\theta_i \varepsilon} \tag{4.21}$$

Where f is the model output and θ_i is a parameter which is changing by a fractional perturbation of ε. To look at the relative effect and compare systems with different input masses etc. the sensitivities will be normalised with the nominal value of the parameter and the input into the model for the different experiments (f_0). All Sensitivities quoted will take the following general form:

$$S^* = \frac{\partial f}{\partial \theta_i} \frac{\theta_i}{f_0} \tag{4.22}$$

Monte Carlo Analysis

A Monte Carlo Analysis will be carried out to assess the quality of the parameters estimated. This will involve applying random noise to the experimental measurements over a number of iterations (5,000) to assess how the parameter estimates respond to these changes. Histograms showing the distribution of the parameter values will be

used to assess the quality of the estimates. The analysis will allow for the experimental noise to be included in the parameter estimates and allow calculation of variance in model parameters, which could be induced due to variation between people, or time of day (circadian cycle) etc.

4.4 Results & Discussion

This section presents and discusses the results of the models developed. Firstly the feedback mechanism (Equation 4.8) will be presented on its own, with parameter estimations against 3 different sets of experimental data, those of Brener et al. (1983), Calbet and MacLean (1997), and Vist and Maughan (1995), a sensitivity analysis will be carried out on the estimated parameters followed by Monte Carlo analysis. Then the secretion model (Equations 4.9-4.19) will be applied to a non-nutrient meal (Marciani et al., 2000), and parameters evaluated, followed by the combination of the two models and parameter estimation from experimental data (Marciani et al., 2001b), to show how both gastric secretions and nutrient feedback will play an important role in the gastric emptying rate.

4.4.1 Feedback Mechanism

Parameter Estimation

A parameter estimation was carried out for γ_0, A_{max}, and K_a, along with this the input mass ($Stom_{N0}$) was allowed to vary to take into account experimental noise at t=0. The parameter estimations were carried out using the *lsqnonlin* function in MATLAB

Table 4.1: Estimated parameters for simulations of different experimental results, (HP - high polymer concentration)

	Conditions	$Stom_{N0}$ (g)	γ_0 (s^{-1})	A_{max} (g/s)	K_a (s^{-1})	**Experimental data**
a	15g input	15.03	1.2×10^{-3}	-	-	(Calbet and MacLean, 1997)
b	20g input	20.82				
c	50g input	54.334	9.23×10^{-4}	0.007	9×10^{-4}	(Brener et al., 1983)
d	100g input	98.95				
e	24g input	24.74				
f	112.8g input	114.28	9.22×10^{-4}	0.01	1.7×10^{-3}	
g	24g input (HP)	23.98				(Vist and Maughan, 1995)
h	112.8g input (HP)	112.83	8.98×10^{-4}	0.01	4.2×10^{-4}	

with experimental data from 3 different sources with different conditions (conditions and optimal parameter values are shown in Table 4.1). The model outputs (using model Equations 4.1-4.8), at optimal parameter values, and experimental results for the temporal change in gastric nutrient content after a meal has been consumed are shown in Figures 4.2 & 4.3. It is observed that in plots (a) and (b) in both figures, the emptying curve for the glucose solutions can be described as an exponential function of time. This is due to the mass of glucose in the small intestine not reaching a sufficiently high level to trigger the feedback mechanism for sustained periods of time with Figure 4.2 (b) and Figure 4.3 (a) triggering the mechanism for a short period of time around 15 minutes. Table 4.1 shows the fitted values for the emptying rate. The differences in values could be due to one of the following factors not taken into account in the current model: different volumes of the liquid meal (Hunt and Stubbs, 1975), different gastric secretion

rates due to the composition of the meal (Marciani et al., 2000), different rheological properties (Marciani et al., 2001b; Shimoyama et al., 2007), and variation between those tested, some of these factors (Viscosity and secretion rate) will be studied later.

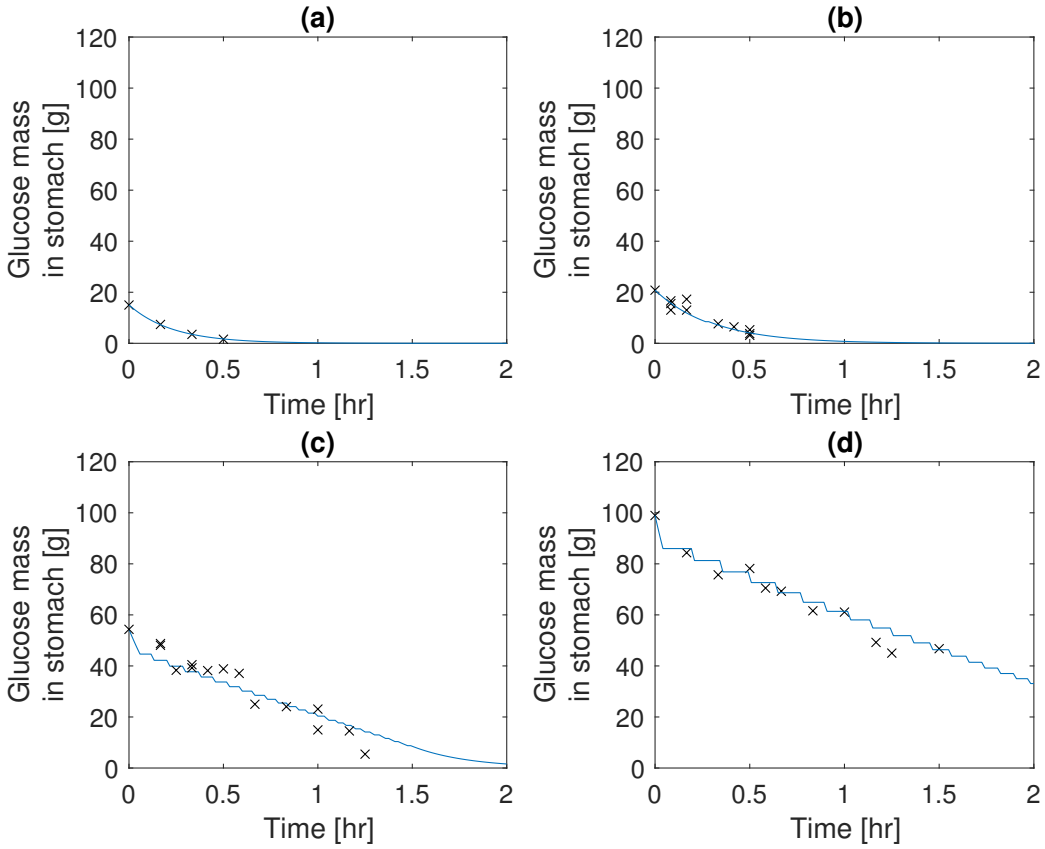

Figure 4.2: Model output & experimental results for emptying of different glucose solution from the stomach, solid lines represent the simulated results and dots represent experimental data. (a) 15g initial mass (Calbet and MacLean, 1997), (b) 20g initial mass (Brener et al., 1983), (c) 50g initial mass (Brener et al., 1983), and (d) 100g initial mass (Brener et al., 1983)

Increasing the initial mass of glucose in the meal leads to an emptying which can be described as linear, after an initial rapid empty period; this is observed both in the simulated and experimental data plots (c) and (d) in both Figures. Unlike the data of plots (a) and (b), the mass of glucose in the small intestine increases to a level which is

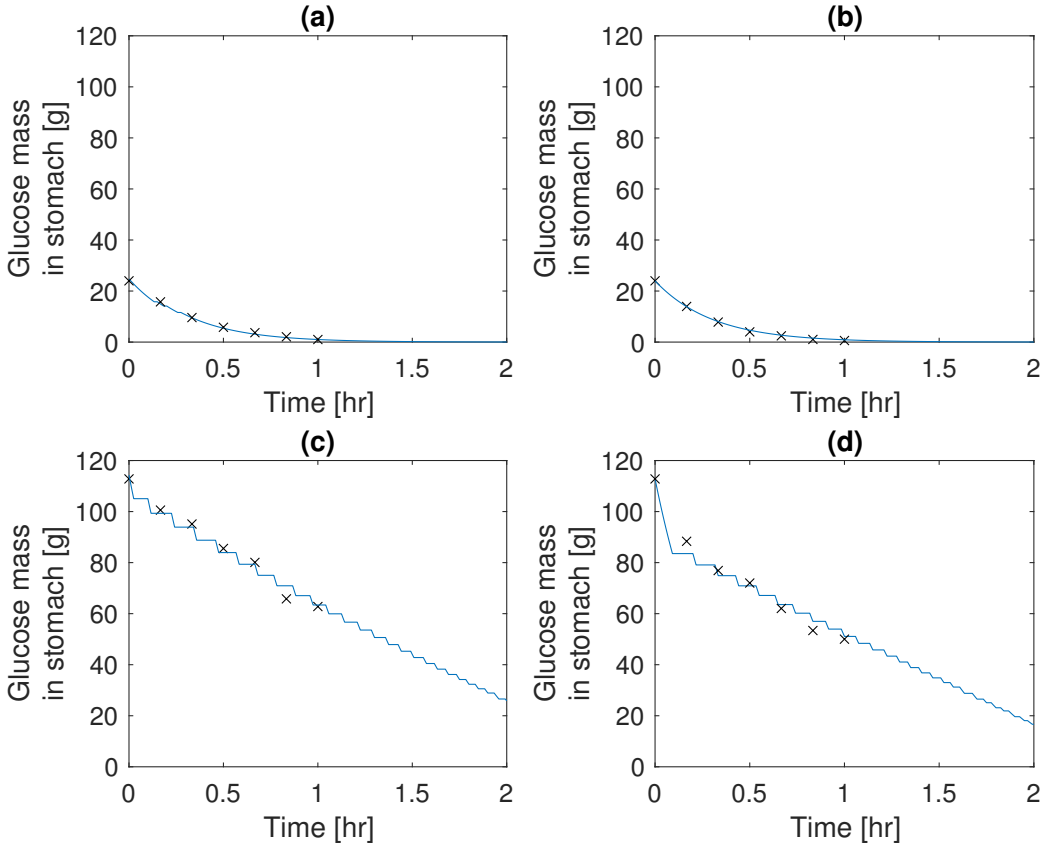

Figure 4.3: Model output & experimental results for emptying of different glucose solution from the stomach, with high and low polymer and glucose, solid lines represent the simulated results and dots represent experimental data from Vist and Maughan (1995). with initial masses (a) 25g initial mass, low viscosity, (b) 25g initial mass, high viscosity, (c) 112.8g initial mass, low viscosity, and (d) 112.8g initial mass, high viscosity

able to stimulate the feedback mechanism over longer periods of time, this leads to the step like decrease in gastric content mass seen in the simulations (c) and (d) of Figures 4.2 and 4.3. The behaviour gives the constant emptying rate of calories described by Brener et al. (1983) & Calbet and MacLean (1997) amongst others. Due to the nature of the numerical solution the number of temporal discretisation points will have an effect upon the step like nature of the simulations.

Sensitivity Analysis

The effect of the parameters γ_0, A_{max}, and K_a upon the mass within the stomach postprandially was analysed using a sensitivity analysis. Small perturbations were applied to the parameters and the outputs compared using a finite difference approach. To do this data from Table 4.1 was used as the nominal values and a perturbation (ε) of 1% applied to the parameters. Figures 4.4, 4.5 and 4.6 show the sensitivity of the gastric content to the initial gastric emptying rate (γ_0) and the maximum absorption rate (A_{max}), and intestinal lumen mass transfer rate, respectively. Plots (a)-(g) in each of the Figures correspond to the labels in Table 4.1 for the different input conditions for the meals.

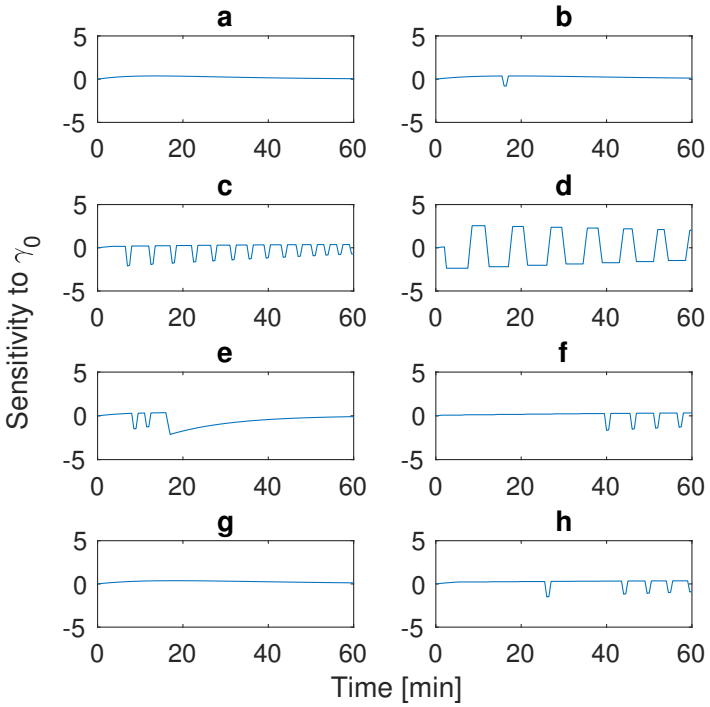

Figure 4.4: Sensitivity analysis of the 8 different experimental conditions shown in Table 4.1 with respect to the parameter γ_0

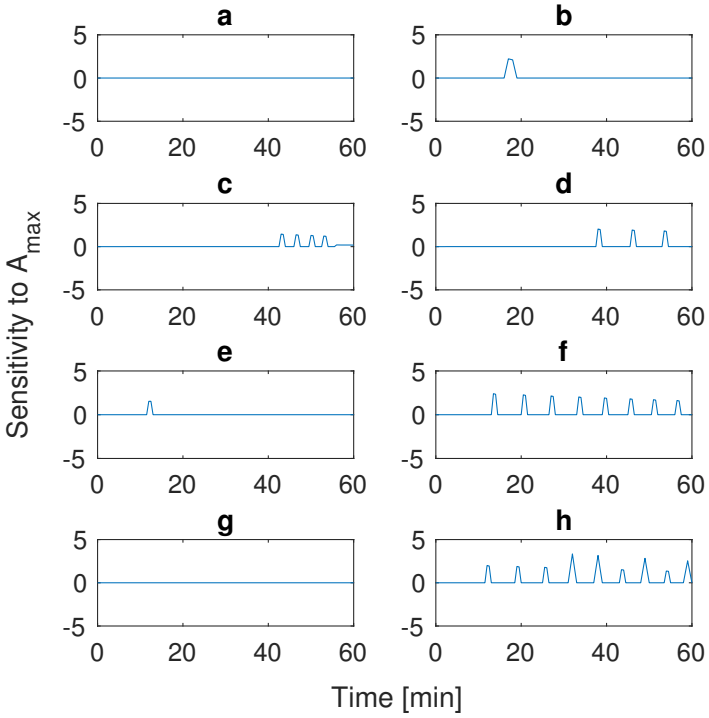

Figure 4.5: Sensitivity analysis of the 8 different experimental conditions shown in Table 4.1 with respect to the parameter A_{max}

The sensitivity of the emptying to the parameter γ_0 is shown in Figure 4.4. The low nutrient simulations plots (a) and (g) do not initiate the feedback mechanism as the mass of glucose does not reach high enough levels in the small intestine to allow the triggering if the feedback mechanism, consequently the system empties exponentially with time. For plots (b) and (e), the feedback mechanism is initiated for a short period of time, seen from the spike in plot (b) and two spikes in plot (e) before the sensitivity plots return to behaving similar to those where the mechanism is not initiated (plots (a) and (g)), this is due to the glucose levels in the small intestine reach high enough levels to ensure the bioavailability is high enough to trigger the feedback mechanism shortly before availability falls. With the high nutrient meals (plots (c), (d), (f), and (h)), one can see a deviation from the zero point along with spikes occurring due to the

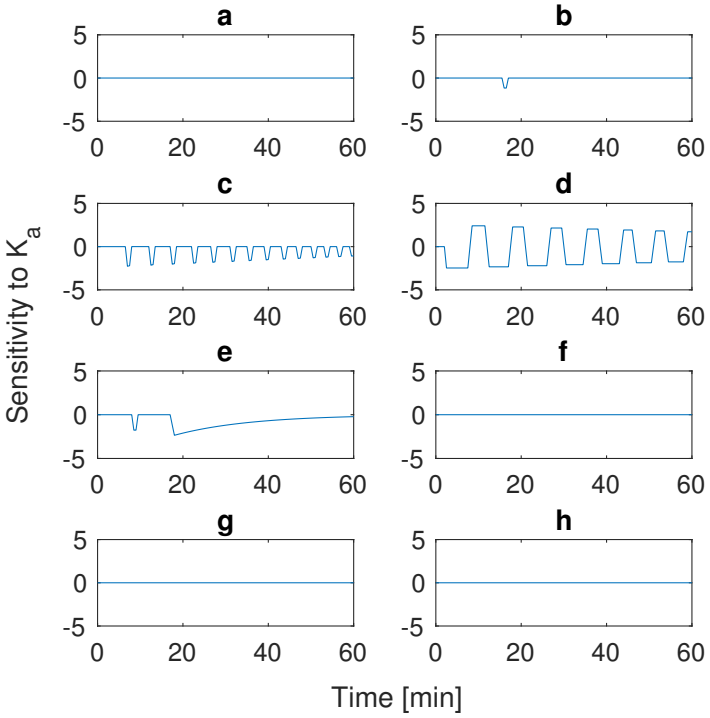

Figure 4.6: Senstivity analysis of 8 different experimental conditions shown in Table 4.1 with respect to the parameter K_a

feedback mechanism initiating, this is due to the bioavailability in the small intestine been maintained at a high level, this is seen later in plots (f) and (h) due to the higher viscosity meals taking longer to stimulate the feedback mechanism.

The sensitivity to parameter γ_0 seems to be exacerbated when the feedback mechanism is initiated. Increases in emptying rate could result in the subsequent increase in absorption rate that triggers the feedback mechanism and results in the increase in sensitivity. This is seen at the beginning of plot (e), where the increase in mass of nutrients due to the faster emptying rate (1% increase) triggers the feedback mechanism, but after around half the mass has emptied from the stomach the availability in the lumen will drop and the absorption rate will not reach the maximum again so the sensitivity reduces back to what would be expected during exponential emptying with time.

For low nutrient content meals the feedback mechanism is not initiated, hence the system will show no sensitivity to the parameter A_{max}, which can be seen in Figure 4.5, plot (a) and (g). As the amount of nutrient increases we start to see an effect. Looking at plot (b) we see a spike as the feedback mechanism initiates for a short amount of time before returning to zero. With plots (e) and (g) we see the effect of viscosity upon the sensitivity to A_{max} the high viscosity solution does not trigger the feedback mechanism, hence no sensitivity to A_{max} but the lower viscosity does leading to a peak in sensitivity and deviation from zero. At the higher nutrient contents (plots (c), (d), (f), and (h)) characteristic spikes can be seen due to the initiation of the feedback mechanism before falling back down to zero; hence the average rate of emptying will be maintained the same, with slight differences when the mechanism is initiated.

Figure 4.6 shows the sensitivity to the absorption rate. This shows similarities to the sensitivity to A_{max}, where for low glucose inputs (plots (a) and (g)) the stomach volume has no sensitivity to the absorption rate as the feedback mechanism is not initiated, this is also seen in plots (f) an (g), where the high nutrient content and high absorption rate means the feedback mechanism is initiated and the same point independent of the small perturbations in the absorption rate. Plots (b) and (e) show sensitivity similar to those for A_{max} where we see spikes before tending back to zero, and Plots (c) and (d) show sensitivity to the absorption rate similar to that of the A_{max} values. This is due to the rate being close to the maximum rate, so small changes mean the feedback mechanism is initiated at different points resulting in a similar sensitivity profile to the A_{max} sensitivity.

Table 4.2: Experimental standard deviation (Vist and Maughan, 1995)

Time [min]	10	20	30	40	50	60
Condition f	16.1	9.7	9.7	11.1	12.4	10.6
Condition h	9.7	6.0	9.7	14.3	16.6	16.1

Monte-Carlo Simulations

The quality of the parameter estimations were analysed using a Monte Carlo simulation. The data used for the simulation was from Vist and Maughan (1995), and two of the experimental conditions were chosen to analyse: (i) high glucose and low polymer (HGLP), Table 4.1 condition (f), and (ii) high glucose high polymer solutions (HGHP) Table 4.1 condition (g). These two data sets were chosen to ensure the feedback mechanism is triggered during emptying (high glucose) and to highlight the effect of changes in mass transfer rate (low and high viscosity). Random noise was added to the experimental data. This noise was taken from the range of maximum deviation from the mean experimental results from the repetitions. The initial emptying rate (γ_0), the feedback point (A_{max}) and the absorption rate (K_a) were estimated, with a total of 5,000 iterations carried out. The results are plotted as histograms in Figures 4.7, with plots (a)-(c) showing the parameter distributions for the low polymer solution, and plots (d)-(f) showing the plots for the high polymer solutions.

It would be expected that parameters which are insensitive to the experiment noise to show little variation across the iterations, giving a high number of occurrences at the same value. Parameters which are sensitive to the experimental noise would be expected to show a distribution of values.

From Figure 4.5 plots (a)-(c) it can be seen that there is little variation in the parameter estimates, indicting the estimations are insensitive to the experimental noise.

For parameter A_{max} (plot (b)), the results can be compared with the sensitivity analysis, Figure 4.5 plot (f). Small perturbations in the parameter manifest in slight changes in when the feedback mechanism initiates, but quickly equalises back to the control state.

We can postulate that for low viscosity high glucose meals, when the glucose enters the small intestine it will be in amounts which will initiate the feedback mechanism very shortly after consumption and that changes in the value have little effect upon the emptying rate. This is also seen for the value of K_a (plot (c)).

Plot (a) showing the distribution of the γ_0 estimations shows a more Gaussian distribution than the insensitive parameters A_{max} and K_a.

The high viscosity values behave differently when experimental noise is introduced. The meals will take longer to initiate the feedback mechanism due to the reduced bioaccessibility of intestinal nutrients. Reduced bioaccessibility results in a lower absorption rate, which is closer to the maximum rate (A_{max}), therefore in Figure 4.5 the spikes occur at a greater frequency than in the lower viscosity higher nutrient meals; hence plots (d)-(f) shows a more Gaussian distribution of the parameters values from the Monte Carlo simulation.

The estimated values for the parameters for low and high polymer content can be seen to be different. This could be explained by phenomena which have not been considered in the model so far. The effect of secretions upon the viscosity of the meal is not considered; it is expected that due to these secretions the viscosity will be dynamic,

changing over time. The effect of secretions is likely to have a greater impact upon the high polymer solutions, as high viscosity meals have been shown to stimulate greater rates of secretion (Marciani et al., 2000). This is looked at in greater detail in the following section.

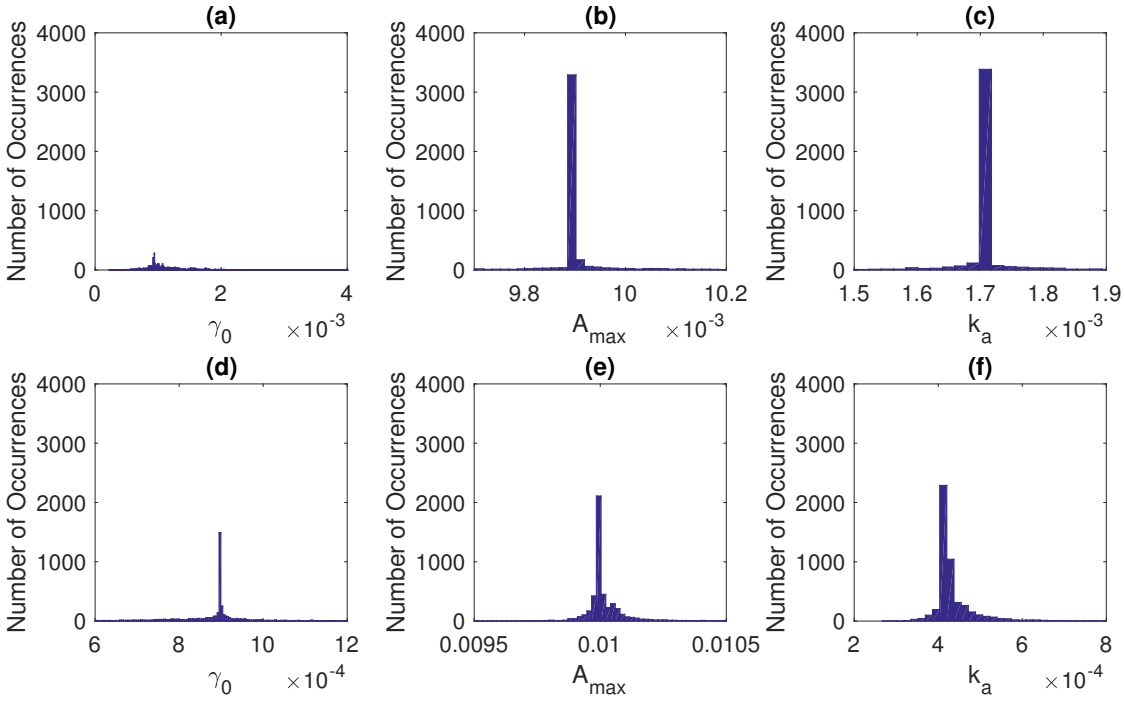

Figure 4.7: Parameter Histograms from Monte Carlo simulation with a total of 10,000 iterations using data from Vist and Maughan (1995), plots (a)-(c) for low viscosity solutions with high glucose levels (condition f), and plots (d)-(f) for high viscosity solutions with high glucose level (condition h).

4.4.2 Non-Nutrient Meal Secretions

Using data from Marciani et al. (2000) a model selection was carried out to determine which of the Equations (4.15:4.19) best describes the experimental results when used along with Equations 4.9-4.13 to describe gastric processing, using the *lsqnonlin*

function in MATLAB. The objective function used was the sum of the squared differences between viscosity values (normalised by the initial viscosity) and the half time of gastric emptying for all 4 sets of experimental data (shown in Equation 4.23, where i is the experimental data set (total n), and j is the sampling points (total m). $\mu_{0,i}$ and $liq_{0,i}$ are the initial viscosity and liquid load for each experiment, and subscripts exp and sim, represent experimental data and model output, respectively). The Akaike Information Criterion (AIC) was calculated for each of the models and used to compare them.

$$Obj = \sum_{i=1}^{n}\sum_{j=1}^{m}\left(\frac{\mu_{exp,i,j} - \mu_{sim,i,j}}{\mu_{0,i}}\right)^2 + \sum_{i=1}^{n} 2\left(0.5 - \frac{Stom_{tot}|_{t=t_{1/2,i}}}{liq_{0,i}}\right) \tag{4.23}$$

The model with the lowest AIC, or information loss used Equation 4.18 to describe the emptying as a function of the secretion rate. Comparing the likelihood ($\exp((AIC_{min} - AIC_i)/2)$), the model utilising Equation 4.17 describing the emptying as a function of viscosity is 0.9 times as likely as Equation 4.18. But as Equation 4.18 takes into account both the effect of viscosity and the change in volume (due to secretion) this model was chosen as a more physiologically relevant approach and will be used for further work.

The parameter values for the optimised model using Equation 4.18 to describe the initial gastric emptying rate (Equation 4.8) are shown in Table 4.3. The results of the optimal solution are shown in Figure 4.8. This shows the simulated and experimental zero shear viscosity measurements from the gastric region. The values all show good fit to the experimental results and fall within the experimental variation. The higher viscosity solutions cause greater secretion rates, which in turn cause a greater reduction in the chyme viscosity. Figure 4.9 also shows that the normalised stomach volumes have

Table 4.3: Optimal parameter values for non-nutrient meal secretion with the Upper and lower bound for parameter estimations calculated from 5000 iteration Monte Carlo simulation.

	m_{sec}	C_1	λ_S	b	S_b
$\bar{\boldsymbol{\theta}}_{\boldsymbol{i}}$	0.0025	6.58×10^{-4}	0.018	1.5	0.018
$\bar{\boldsymbol{\theta}}_{\boldsymbol{i}} + \mathbf{2}\boldsymbol{\sigma}_{\boldsymbol{i}}$	0.0174	8.38×10^{-4}	0.0621	2.2	0.028
$\bar{\boldsymbol{\theta}}_{\boldsymbol{i}} - \mathbf{2}\boldsymbol{\sigma}_{\boldsymbol{i}}$	3.27×10^{-4}	4.69×10^{-4}	0.0014	0.2	0.0014

similar gastric half times for all four solutions, corresponding to what was seen in the *in vivo* work (Marciani et al., 2000). It should be noted that the experimental variation is large (especially at high viscosities), which may be due to the poorer mixing reported at high viscosities (Marciani et al., 2000), and as such there will be a large variability in the parameter values after running the Monte Carlo simulation show a large variance (Table 4.3)

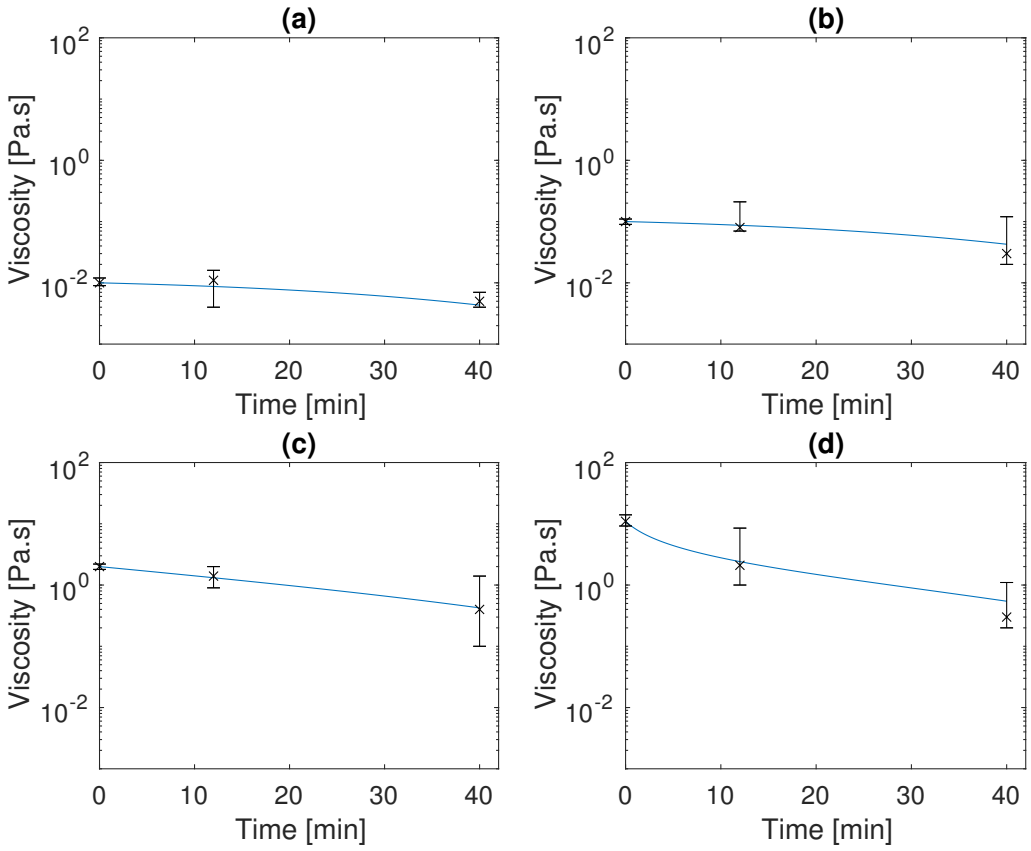

Figure 4.8: Viscosity profiles for 4 different input viscosities. Solid line shows model output (using Equation 4.18), crosses and error bars show the values from literature in vivo data (Marciani et al., 2000).

Using the parameter values from Table 4.3 as an initial guess, a Monte Carlo simulation was carried out using random experimental data points taken from the values between the extrema of the experimental variability. From this the variance in the parameter values over 5000 iterations were calculated. The parameter variance was assuming normal or log-normal distribution depending upon visual inspection parameter histograms. Using this variance an upper and lower limit for further parameter estimation was defined as $\bar{x} \pm 2\sigma$, to take into account 95% of the values estimated from the Monte Carlo simulation. These bounds are shown in Table 4.3.

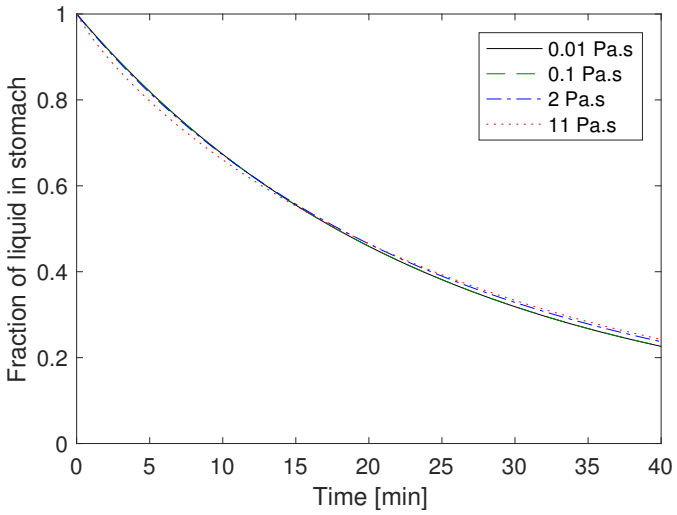

Figure 4.9: Volume profiles for 4 different input viscosities.

4.4.3 Nutrient Meal With Secretions & Feedback

The feedback model (Equation 4.8) and secretion model were then combined to look at the effect of secretion and nutrient feedback mechanism upon gastric emptying of a liquid nutrient meal. Experimental data was taken from Marciani et al. (2001b), which looked at emptying of nutrient meals of different viscosities, modified by addition of LBG, therefore Equation 4.9 can be used to predict the change in gastric viscosity with concentration. Although the experimental meals contained different sources of nutrient (63% lipid and 27% carbohydrate), it was assumed in the model that the nutrients behaved the same and required no enzymatic hydrolysis to be absorbed through the gut epithelium. The nutrient meals had a calorific content of 323kcal and the control meals had a calorific content of 64kcal.

A random initialisation used to obtain model parameters values with the upper and lower bounds of the parameter estimations chosen from the mean of the parameter

values from the non nutrient meal plus/minus 2 times the standard deviation ($\bar{\theta}_i \pm 2\sigma_i$) from Table 4.3. The parameter value of K_a was assumed constant along the length of the intestine (*in vivo* this will likely change due to intestinal secretions and mixing induced by intestinal wall motility) and estimated from the experimental results. To ensure the stability of the system a finer temporal step was required compared to the feedback only model; and in the current form of the model implies a faster feedback response. This was due to the stiffness of the modified equations; i.e., the parameter values are different orders of magnitude in size, and hence due to the chosen discretisation scheme smaller step sizes are required.

Due to the variability between different people etc. each data set was run separately, with the value for K_a was consistent for each viscosity value.

The optimal parameter values for the different meals are showing in Table 4.4, and Figure 4.10 shows the gastric content against time for the different meals:

- The low viscosity nutrient meal (plot (a)) stimulates the feedback mechanism and empties in a linear fashion.

- The high viscosity meal (plot (b)), there is an initial lag period where little change in the gastric content occurs due to the high level of secretions, this is followed by an emptying period until the feedback mechanism initiates and a slight plateau is seen. The plateau can be explained by the reduction in bioaccessibility (lower mass transfer rate) leading to higher nutrient concentration in the lumen before the feedback mechanism is initiated.

- The control meals, with low nutrient content, do not initiate the feedback mechanism, and the emptying rate is controlled by the viscosity and secretion rate (Equation 4.18).
  - The low viscosity control meal (plot (c)) shows a typical exponential emptying curve.
  - The high viscosity control (plot (d)) a slight lag phase can be observed again at the beginning of the curve due to the higher rates of secretions.

The parameter values estimated for these models all fall within the range found from the Monte Carlo simulation of the non nutrient meals (Table 4.3). The main difference in the results are given by changes in the parameter K_a. There is an order of magnitude difference in the value of K_a for the low and high viscosity solutions, and the is assumption of the model is that the parameter will be a function of the mass transfer in the lumen and hence expected to change with viscosity of the meal (Moxon et al., 2016) (Chapter 3). There are smaller variations in other optimal parameter values. Parameters b, λ_S, and S_b from Equation 4.10 show some variability, with b having a lower value for the higher viscosity meals. This may result from the equation used to describe the viscosity values with LBG concentration (Equation 4.9). This equation was fitted from data in Marciani et al. (2000) with a maximum viscosity of 11 Pa.s, whereas the high viscosity in the second data set (Marciani et al., 2001b) had a viscosity closer to 30 Pa.s, but no LBG concentration data. There could also be an additional mechanism stimulating the secretion other than the model proposed linked to the viscosity. The cephalic phase of secretion is not taken into account in this model, which would add secretions due to the anticipation of food and/or the sensing of nutrients in the mouth.

This phase could explain the higher value of parameter b for low viscosity nutrient meal compared to low viscosity control meal, and may also be affected by the viscosity of the meal. The value C_1 also shows some variability which may imply other phenomena, as well as viscosity and volume change, which could influence the emptying rate.

It should be noted that during the parameter estimation of the two control meals, the value of m_{sec} reached the lower bound and the value of λ_S reached the upper bound. Low m_{sec} values imply slow emptying ,whereas high λ_S values imply high secretion rates, which in turn imply faster emptying. As the bounds used in this model were taken from estimates of secretions for non-nutrient viscous meals, they may not be applicable to meals with nutrients present, as there are likely additional mechanism present which are not considered in the model, e.g., the nutrient content of the meal influencing the gastric secretion rate.

Table 4.4: Optimal parameter values for different meals (Marciani et al., 2001b), where LVN - is low viscosity nutrient meal, HVN- is high viscosity nutrient meal, LVC- is low viscosity control meal, and HVC- is high viscosity control meal.

Parameter	A_{max}	m_{sec}	C_1	λ_S	b	S_b	K_a
LVN	1.04×10^{-2}	3.66×10^{-4}	6.77×10^{-4}	4.05×10^{-2}	1.08	0.57×10^{-2}	9.80×10^{-3}
HVN	0.98×10^{-2}	3.48×10^{-4}	4.74×10^{-4}	6.17×10^{-2}	0.40	1.51×10^{-2}	2.89×10^{-4}
LVC	1.00×10^{-2}	3.27×10^{-4}	4.69×10^{-4}	6.21×10^{-2}	0.67	2.13×10^{-2}	9.80×10^{-3}
HVC	1.01×10^{-2}	3.27×10^{-4}	5.86×10^{-4}	6.21×10^{-2}	0.42	2.34×10^{-2}	2.89×10^{-4}

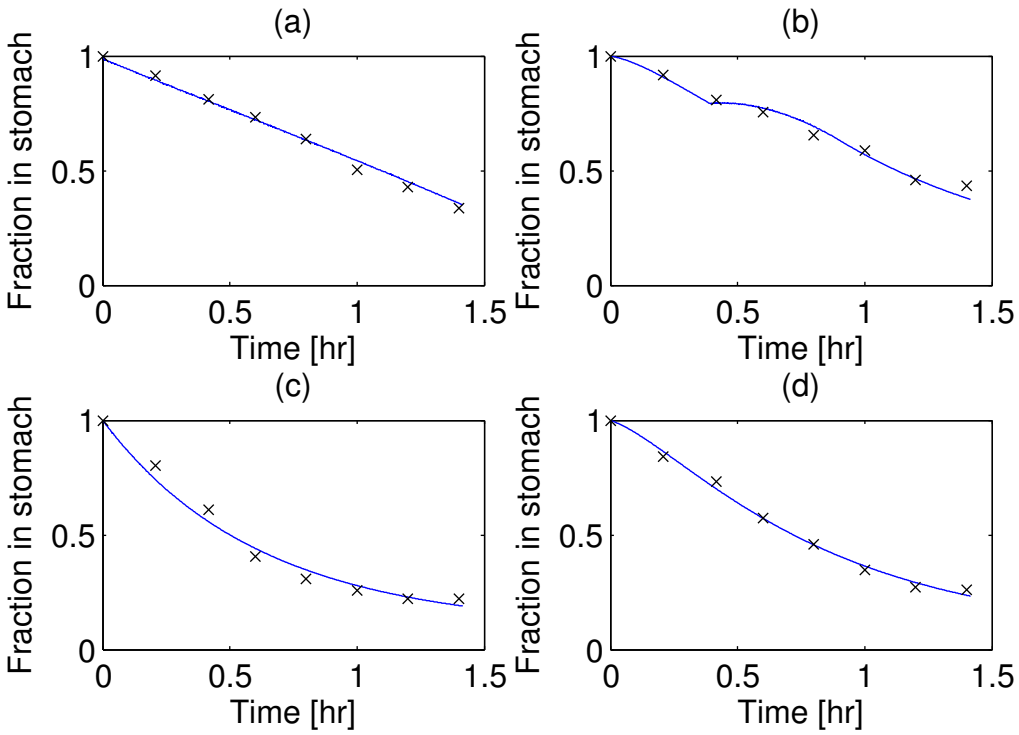

Figure 4.10: Gastric content after meal normalise against input volume, for (a) low viscosity nutrient meal, (b) High viscosity nutrient meal, (c) low viscosity control meal, (d) high viscosity control meal. solid line representing simulated results and crossed in vivo data (Marciani et al., 2001b)

Figure 4.11 shows simulations with (a) the optimal parameter values for the LVN from Table 4.4 for 3 different inputs of glucose: 20g, 40g, and 80g, (b) is simulated with parameters for HVN from Table 4.4 for the same glucose inputs, (c) the 40g simulation with LVN parameters with the initial feedback point and final feedback point marked with vertical lines, (d) same as (c) for the 80g simulation from HVN parameters. In plot (a) the effect of the feedback mechanism can be seen clearly, with the 20g curve not initiating the mechanism, the 40g curve initiating the feedback almost straight away, until around 30 minutes (highlighted in plot (c)) when the absorption rate drops (most

of the glucose already absorbed), and is no longer high enough to stimulate the feedback mechanism, hence the emptying returns to a more exponential pattern. The highest glucose solution (80g) initiates the feedback mechanism and the curve follows a straight line over the whole 80 minute simulation period.

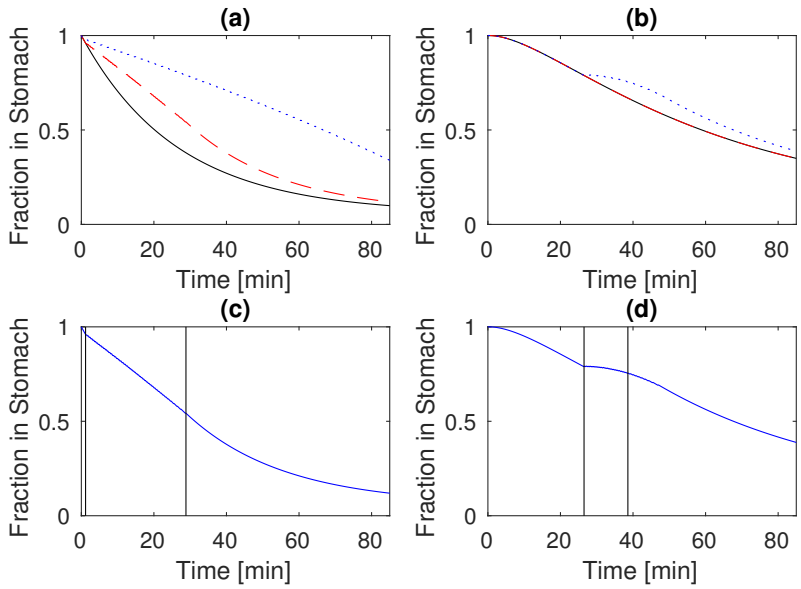

Figure 4.11: Predictions of Gastric responses for (a) low viscosity meals using parameters from LVN in Table 4.4, and (b) high viscosity using parameters from HVN in table 4.4, for each set of parameters simulation was ran at initial glucose mass of 20g (solid line), 40g (dashed line), and 80g (dotted line), (c) shows the 40g low viscosity solution with vertical lines indicating when the feedback mechanism initiates and when it finally stops, (d) shows the 80g high viscosity solution with vertical lines indicating when the feedback mechanism initiates and when it finally stops

For the high viscosity values in plot (b) neither the 20g nor the 40g solutions initiate the feedback mechanism and hence follow the same curve, the 80g solution however does trigger the mechanism just before 30 minutes causing the emptying to slow, but

the absorption rate quickly drops to levels below that which would trigger the feedback mechanism and the emptying goes back to similar behaviour as the lower nutrient level solutions, this is highlighted in plot (d).

The ability to predict the temporal changes in the gastric viscosity could allow for better predictions of hormone release, such as *Gastrin* or *Ghrelin*, and be important in predicting a meals effect upon satiety, where more viscous meals reduce appetite (Marciani et al., 2000). Along with this, understanding the viscosity of intestinal chyme will allow better understanding of the secretion rate of incretins, which will be a function of intestinal nutrient bioaccessibility (Baggio and Drucker, 2007), and will play a role in the secretion of insulin.

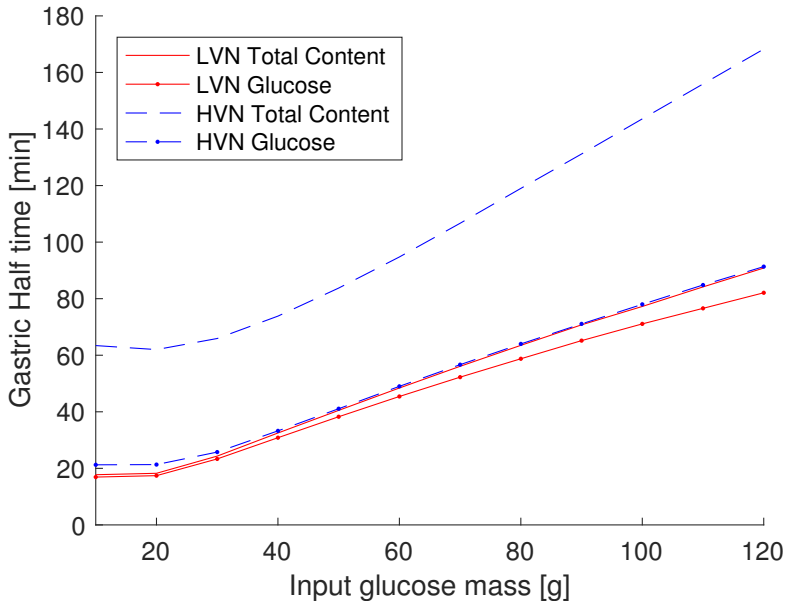

Figure 4.12: Prediction of the half time for the whole gastric content and the half time for the glucose input only were calculated at different initial glucose inputs, but constant volume. Parameters used in the model were taken from Table 4.4 for the optimal parameter values for the LVN and the HVN meals

The effect of viscosity on the half emptying time was studied using the predicted parameters from Table 4.4 for the LVN and HVN meals, with the results shown in Figure 4.12. The plots show the time for half the initial glucose content to empty for each set of parameters when different initial glucose loads are used with constant liquid volume, and the time for the gastric content to reach half the initial volume for the different glucose inputs. For all the plots, when the input mass of glucose is increased the half empty time also increases, with a larger difference in the half emptying time for the high viscosity meal compared to the lower viscosity meal. This is partly due to the increase in secretions expected with higher viscosity meals. This curve may have implications on the way gastric emptying is measured. Scintigraphy, for example, will label a particular component, e.g., glucose, and measure the amount in the gastric compartment, of this component only (Hveem et al., 1996). In contrast Marciani et al. (2000) use MRI, which will measure the entire gastric content. As such for high viscosity meals, the large volumes of secretions may lead to underestimation of the rate at which the nutrients (glucose in this case) are emptying.

4.5 Conclusion

The paper presents a mathematical model to describe the gastric emptying rate of nutrient liquid meals of varying viscosity (shown in appendix). To achieve this an attempt was made to model the nutrient initiated feedback mechanism present between the proximal small intestine and the pyloric sphincter The results indicate that with the estimation of two parameters: an initial emptying rate (γ_0) and a feedback cut off point (A_{max}), the model can produce simulations to show the differing trends between

low and high nutrient meals. This model was developed further to take into account the gastric secretions induced through meal viscosity and the subsequent effect on the parameter γ_0, this model predicted the increased secretion rate due to gastric chyme viscosity and subsequent rapid reduction in the viscosity values. The Monte Carlo analysis highlighted the variability in the parameter values which stem from the difference between individuals amongst other factors, which need to be considered when modelling the digestion of food. Including the model for gastric secretions and the influence on the emptying rate along with a nutrient feedback mechanism gave a model able to predict closely the gastric curves found for high and low nutrient meals of varying viscosity.

The models presented will go someway towards providing predictive capability for the emptying of viscous, nutrient-rich, liquid meals, further work will look at validation of the absorption rate. Used in conjunction with models already available in literature for glucose-insulin system would allow for the prediction of postprandial plasma glucose curves and design of food tailored for different glycemic responses.

Chapter 5

Oral Glucose Tolerance Test

The modelling and simulation in the chapter along with the writing was carried out by myself.

Peter J. Fryer reviewed the chapter.

Serafim Bakalis offered advice and reviewed the chapter.

Chapter 5 takes the feedback model developed in Chapter 4 and adds a delay term. The model is validated against data from literature showing the rate of glucose appearance in the plasma after consumption of a glucose solution. Chapter 5 highlights that the assumptions presented in Chapters 3 and 4 are reasonable and that with the right amount of information about the meal and physiology, predictions of absorption rates for liquid meals can be made from the model.

5.1 Introduction

Chapter 5 will take the models developed in Chapters 3 (Moxon et al., 2016) & Chapter 4, which look at the gastric emptying and nutrient absorption of liquid meals and validate the models against experimental data gathered from literature measuring the rate of glucose absorption after the oral consumption of a glucose solution. The aim is to show the predictive capability of the mathematical models for simple meals.

5.2 Experimental data

The experimental data will be taken from 3 different sources, (Anderwald et al., 2011; Dalla Man et al., 2006; Wachters-Hagedoorn et al., 2006). This data shows the rate of appearance of glucose in the subjects plasma, measured using a [^{13}C]-glucose tracer following the method outlined in Dalla Man et al. (2004). This provides the opportunity to validate the model of the digestive system without having to include a model of the blood glucose and insulin, which would add extra complexity and uncertainty.

The experiments used either a 75g oral solution of glucose (Anderwald et al., 2011; Dalla Man et al., 2006), or a 55g oral solution of glucose (Wachters-Hagedoorn et al., 2006). The rate of appearance of glucose in the plasma after the meals have been consumed are shown in Figure 5.1. The 55g input has a smaller peak absorption rate but after the maximum shows a steady reduction in rate, but looking at the two 75g inputs we see a higher peak followed by a more step like drop, which is more apparent

in the data from Dalla Man et al. (2006), this could be explained by the presence of the nutrient feedback mechanism.

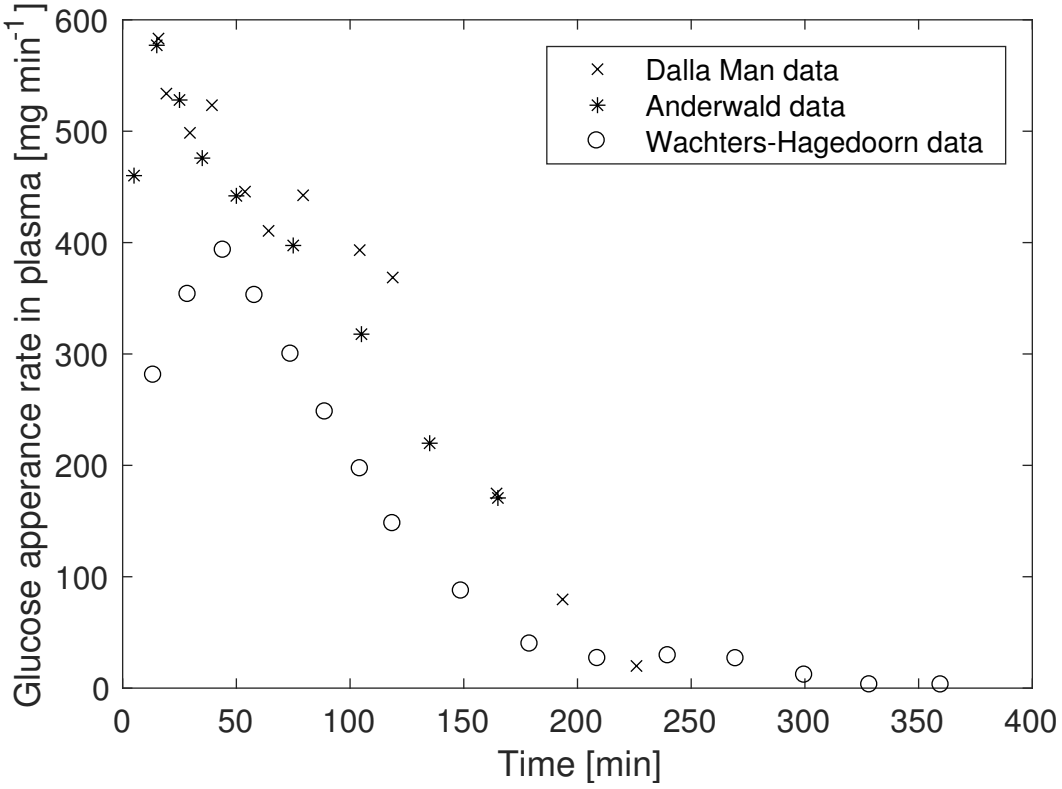

Figure 5.1: Rate of glucose appearance in plasma after the oral consumption of a glucose solution. Data from three sources (Anderwald et al., 2011; Dalla Man et al., 2006; Wachters-Hagedoorn et al., 2006)

5.3 Model

The model will take the same form as from Section 3.3.2, which looks at the emptying of a CSTR stomach into a PFR Small intestine, and like this the model will be made dimensionless. To this model the feedback mechanism developed in Section 4.3.2 will be added. The schematic of this model is shown in Figure 5.2. The model in dimensionless form will be as follows:

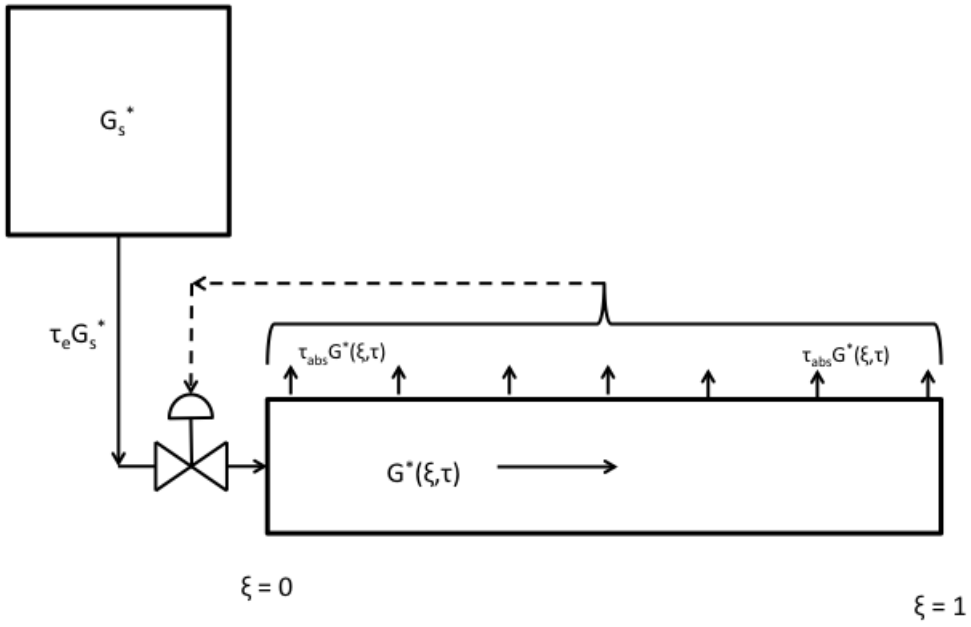

Figure 5.2: Schematic of the gastric and small intestinal compartments in dimensionless form with a feedback mechanism

Stomach

$$\frac{dG_s^*}{d\tau} = -\tau_e G_s^* \tag{5.1}$$

$$G_s^*|_{t=0} = 1 \tag{5.2}$$

Small Intestine

$$\frac{\partial G^*}{\partial \tau} = \begin{cases} -\frac{\partial G^*}{\partial \xi} - \tau_{abs} G^* + \tau_e G_s^* & \text{if } \xi = \xi_0 \\ -\frac{\partial G^*}{\partial \xi} - \tau_{abs} G^* & \text{otherwise} \end{cases} \tag{5.3}$$

Glucose Absorption Rate

$$G^*_{abs} = \tau_{abs} \sum_{\xi=0}^{1} G^* \tag{5.4}$$

Glucose Rate of Appearance

$$Ra^* = f_a \tau_{abs} \sum_{\xi=0}^{1} G^* \tag{5.5}$$

where $\tau = t\frac{\bar{u}}{L}$, $\xi = \frac{z}{L}$, and the model gives two dimensionless numbers, characteristic absorption rate τ_{abs} ($= Kf\frac{2}{r_m}$), and the characteristic gastric emptying rate, τ_e ($= \gamma\frac{L}{\bar{u}}$). The convective mass transfer rate is calculated from Equations 3.5 and 3.6. L is the length of the small intestine, and $\bar{u}$ is the mean axial velocity along the length of the small intestine.

The rate of appearance of glucose (Equation 5.5) will be difference from the absorption of glucose (Equation 5.4), due to the fact that not all the glucose absorbed will appear in the plasma, this is expressed as the fraction, f_a, which can be given the value of 0.89 (Dalla Man et al., 2004) for glucose absorption.

To take into account the feedback mechanism we must make Equation 4.8 dimensionless, which will take the following form:

$$\tau_e = \tau_{e,0}\left(1 - \left(\frac{1}{1 + \exp(\tau_a(G^*_{abs} - A^*_{max}))}\right)\right) \tag{5.6}$$

Where $\tau_{e,0}$ is the characteristic initial emptying rate ($= \gamma_0\frac{L}{\bar{u}}$), and A^*_{max} is the normalised maximum absorption rate ($= \frac{A_{max}}{G_0}$).

In reality it is unlikely that there will be an instantaneous feedback mechanism, but that the feedback will occur after a delay. Therefore we can build upon what was presented in Chapter 4, by redefining Equation 5.6:

$$\tau_e = \tau_{e,0}\left(1 - \left(\frac{1}{1+\exp(\tau_a(G^*_{abs}(\tau - \tau_{delay}) - A^*_{max}))}\right)\right) \tag{5.7}$$

with the new parameter τ_{delay}, which is the amount of time before the increase in absorption rate above A^*_{max} initiates the pyloric response of inhibiting the emptying of gastric content. The effect in adding the delay to the model is shown in Figure 5.3, with the feedback taking longer to trigger for the delayed signal and the pylorus remains in the off position for longer. It also removes the influence of the time step upon the feedback mechanism, which occurs when no delay is used, this was discussed slightly in Chapter 4, where the finer step were required for numerical stability in one of nutrient meal model, which altered the feedback response. With the feedback delay included the choice of step size will not influence the model outputs with respect to the feedback.

5.3.1 Parameter Values

The parameters f, and r_0 will be the same as those quoted in Table 3.1. It will be assumed that the viscosity of the solution when in the intestinal lumen will be equivalent of that of water ($\mu = 0.001Pa.s$) and the value of τ_a, $\bar{u}$, L, r_m, will be the same as those used in Chapter 4. Hence we require a value from literature for A_{max}, γ_0, and τ_{delay}.

We can assume the value of A_{max} will be equal to the rate of empty from the stomach in kcal per minute when the feedback mechanism is initiated defined by Brener et al. (1983), this gives us a value of A_{max} of $0.53\ g/min$.

The initial emptying rate (γ_0) will be assumed constant and the same as non-nutrient liquid meals (Marciani et al., 2000), which have a half time of emptying of around 18 minutes, which corresponds to an emptying rate of $0.04\ min^{-1}$.

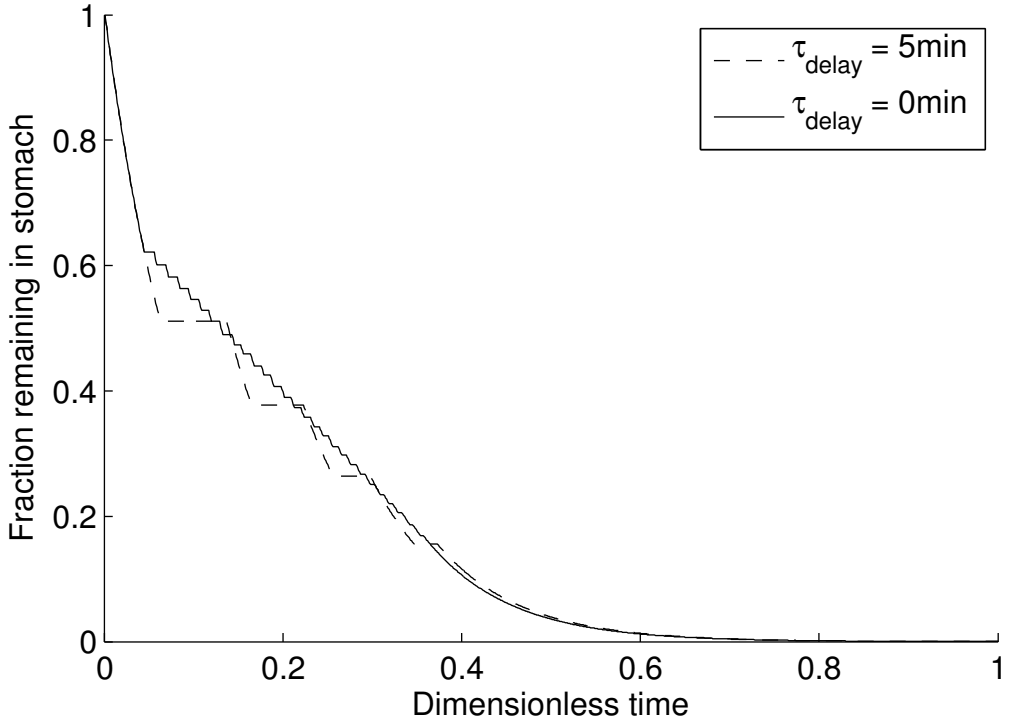

Figure 5.3: Fraction of 100g glucose solution remaining in stomach when the delay in feedback is set to 0min and 5min

The delay time was inferred from literature (Heddle et al., 1988b; Rayner et al., 2000). Treacy et al. (1990) showed that the pyloric contractions can be linked to the gastric emptying rate in pigs. Rayner et al. (2000) showed that the number of occurrences and pressure of pyloric contractions for an intraduodenal infusion of glucose at 2kcal/min, resulted in a increase between 5 min to a peak around 15 minutes, before the pressure drops sharply, but the number of occurrences remains at a similar elevated level.

Work by Heddle et al. (1988b) highlights the nutrient based feedback mechanism, where dextrose sensed in the duodenum or proximal jejunum stimulates isolated pyloric pressure waves and increases the pyloric pressure. The results show the change from

basal pyloric pressure is similar and relatively small in the first 5 minutes for 10%, 15%, and 25% dextrose solution infused into the duodenum at a rate of 4 ml/min, but the change is greater for higher concentration solutions between 5-10 minutes. From these we can infer that the presence of sugars within the duodenum increases the pyloric contraction rate and pressure, with a larger change seen after 5 minutes of intraduodenal sugar infusion. This work will assume that the feedback mechanism will operate with a delay of 5 minutes, and for comparison simulations will also be run as in Chapter 4 with zero delay. The parameters are shown in dimensionless form in table 5.1.

Table 5.1: Table showing the dimensionless parameters used for simulations to compare with experimental data

	Condition 1	**Condition 2**	**Condition 3**	**Condition 4**
$G_0[g]$	75	55	75	55
$\tau_{e,0}$	10.76	10.76	10.76	10.76
τ_{abs}	4.54	4.54	4.54	4.54
τ_{delay}	0	0	0.0179	0.0179
A^*_{max}	1.99	2.71	1.99	2.71

5.4 Results

From the results shown in Figures 5.4 & 5.5 it can be seen that the feedback mechanism is only initiated for the 75g inputs and not for the lower glucose inputs. The sim-

ulated curve for the 55g input glucose follows closely to the experimental data points with a similar time at which the maximum rate occurs and maximum rate, though seems to overestimate the experimental results. Figure 5.4 shows the curves with no delay in signal, the simulated results for the 75g input shows a more rapid increase, plateauing when the feedback mechanism initiates. The peak is lower for the model output that the experimental data, but the terminal phase behaves in a similarly to the experimental data.

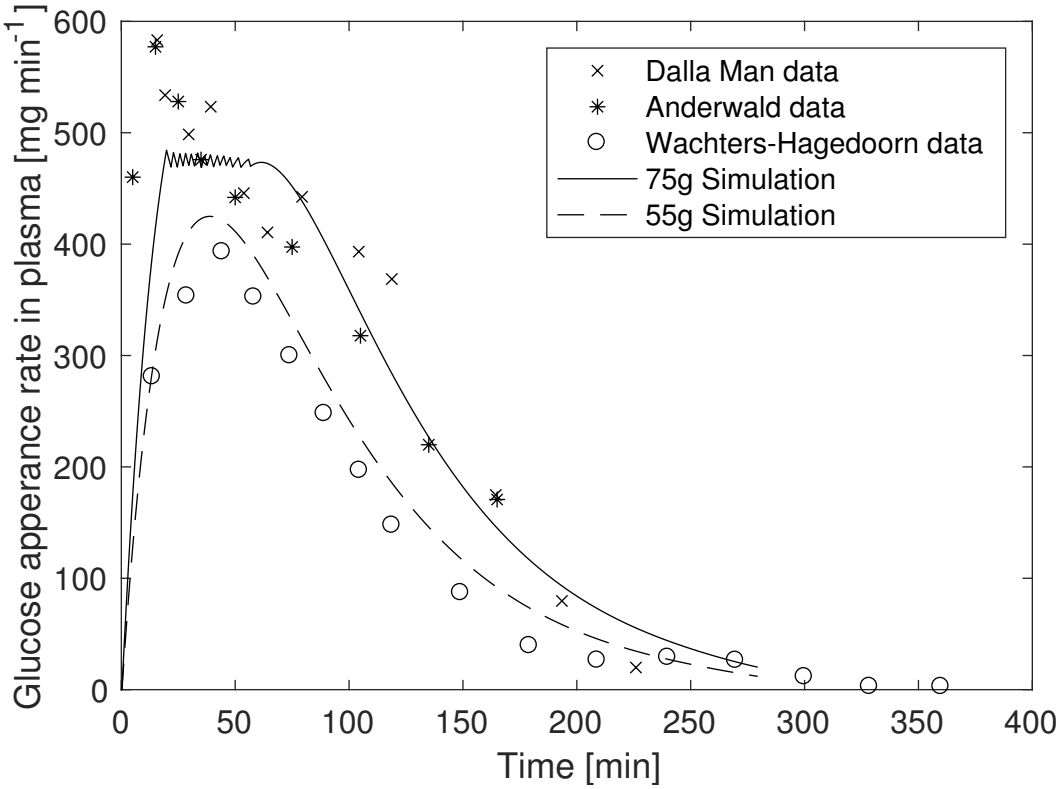

Figure 5.4: Rate of Appearance of glucose in plasma after the consumption of glucose solution, simulated with a 55g (condition 2) glucose input and 75g (condition 1) glucose input, assuming feedback mechanism acts instantaneously. Experimental data from Anderwald et al. (2011); Dalla Man et al. (2006); Wachters-Hagedoorn et al. (2006)

The 75g simulation in Figure 5.5 shows a different response, with an initial peak in absorption rate at a similar time as experimental data, but under estimating the maximum rate. This is followed by a second lower peak, where the feedback mechanism is again initiated, and a final third smaller peak is seen before the rate of glucose absorption drops due to the reduction in the concentration gradient, i.e., less glucose available in the intestinal lumen.

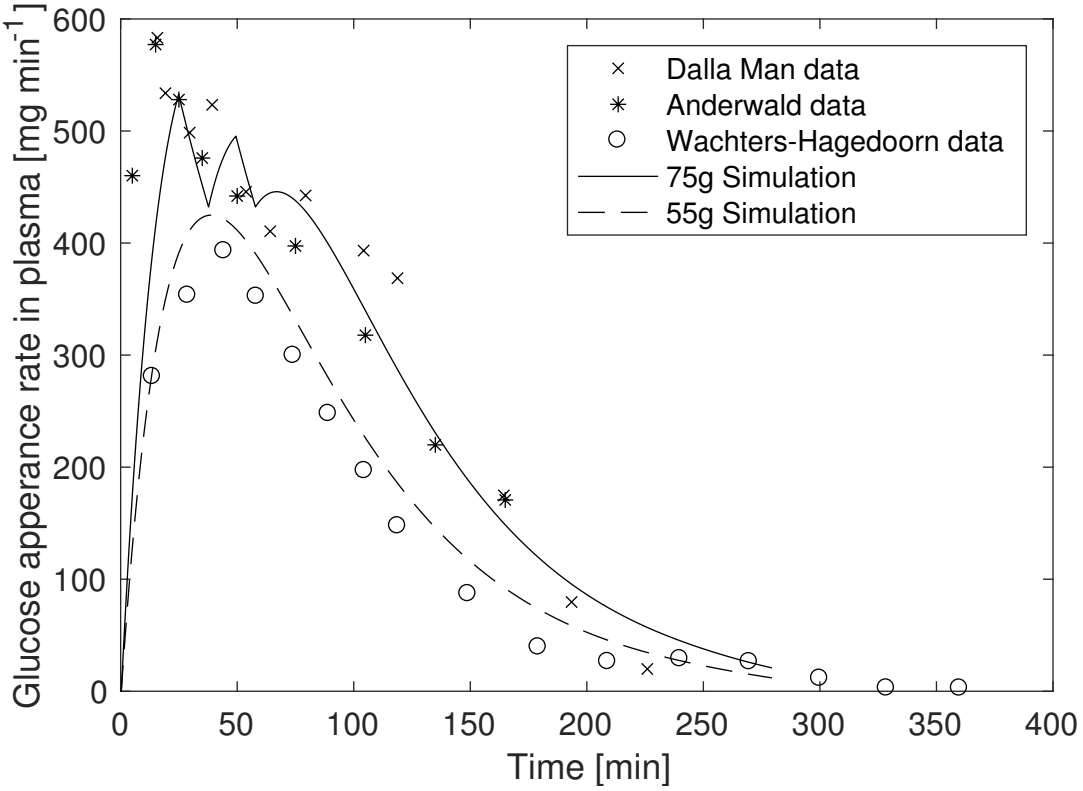

Figure 5.5: Rate of Appearance of glucose in plasma after the consumption of glucose solution, simulated with a 55g (condition 4) glucose input and 75g (condition 3) glucose input, assuming feedback mechanism has a delay of 5 minutes. Experimental data from Anderwald et al. (2011); Dalla Man et al. (2006); Wachters-Hagedoorn et al. (2006)

5.4.1 Smoothing peaks

Assuming the feedback response behaves like a step function (i.e., when $\tau_a \to \infty$), the emptying f the stomach switches on and off quickly if no delay, or more slower if there is a delay, but one still sees a step like decrease in the fraction remaining in the stomach, and peaks and troughs in the absorption rate, these are faster and tighter with no delay (Figure 5.4) or slower but deeper when one considers a delay in signalling (Figure 5.5). One way to correct for this and smooth out the feedback response is to consider the expressions in Equations 5.6 & 5.7 as logistical distributions were we define A_{max} as the mean and τ_a can be defined as a function of the standard deviation of that mean. For a physiological interpretation of this we can assume there is a mean value at which point receptors will signal, but there will be receptors stimulated before this value and some which take greater stimulus to respond, which we can define with the standard deviation σ, and τ_a can be defined as:

$$\tau_a = \frac{\pi}{\sqrt{3}(\sigma/G_0)} \tag{5.8}$$

As the deviation tends to zeros, the value of τ_a tends to infinity, and the feedback mechanism will behave as a step function, but for standard deviation values greater than zero, the feedback will be smoother. The effect of varying the standard deviation on the gastric emptying and the rate of absorption is shown in Figure 5.6. When the value is increased from zeros, the steps of the gastric emptying and the spikes in the rate of appearance are smoothed, the peak in the rate of appearance is also lower.

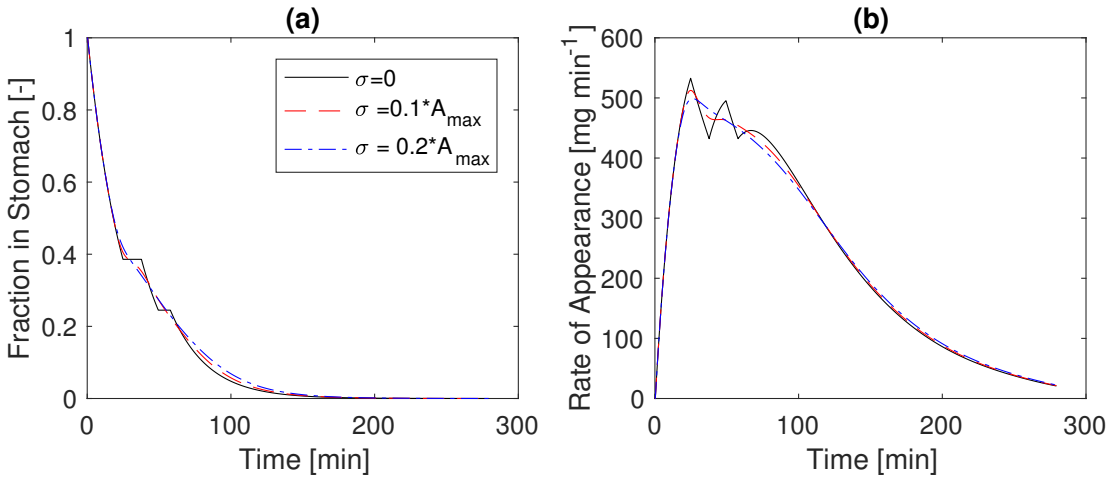

Figure 5.6: Effect of varying the standard deviation of the A_{max} value in Equation 5.8, upon (a) the fraction of meal remaining in the stomach, and (b) the rate of glucose appearance in the plasma, after the consumption of 75 g glucose solution.

5.4.2 Effect of Viscosity

The model was run with variations in the small intestinal chyme viscosity to see what influence this would have, the model was run with a high τ_a value assuming the feedback behaves as a step function, and also with a standard deviation of $0.25A_{max}$. Three different viscosities were simulated: 0.001 Pas (τ_{abs} =4.54), 0.002 Pas (τ_{abs} =2.85), and 0.004 Pas (τ_{abs} =1.80). Absorption rates could not be found in the literature for OGTT with variation in viscosity so could not be validated and it was assumed that the viscosity is constant along the length of the intestine and does not affect the gastric emptying (the model developed in Chapter 4 for gastric secretions was not implemented). It can be seen in Figure 5.7 that the viscosity will have a large effect in the current state of the model. The reduction in mass transfer rate means that the increase in absorption rate is slower and the peak rate is small, such that increasing the viscosity from 0.001 Pa.s to 0.002 Pa.s means that the maximum rate of absorption is no longer high enough

to trigger the feedback mechanism. But with higher viscosities the terminal phase of the curve is shallower so there is a lower but longer period of absorption. One can also see the effect of assuming a step like feedback (plot (a)) and assuming there is some variance (plot (b))

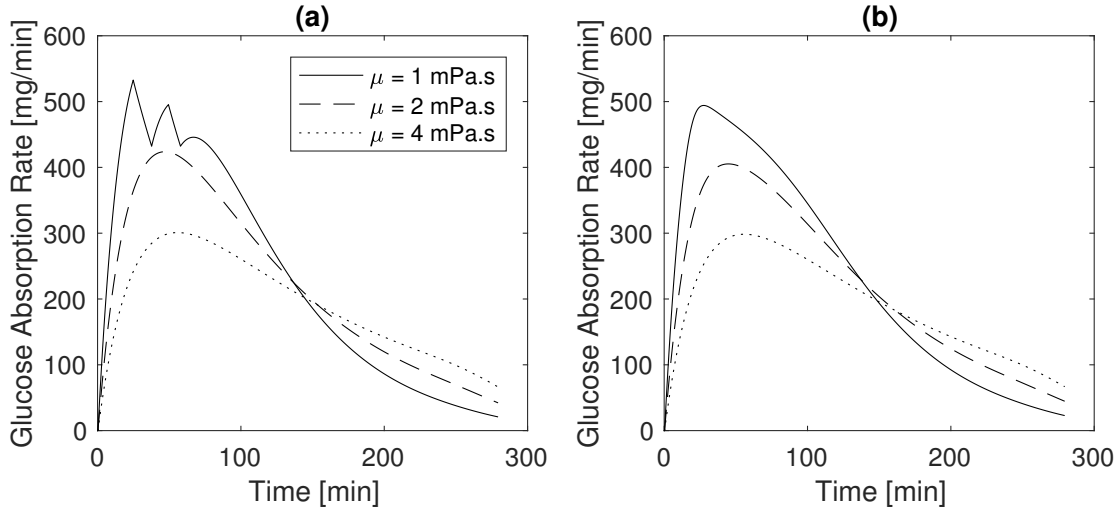

Figure 5.7: Glucose absorption rate with variations in the chyme viscosity, for an input of 75g of glucose. Plot (a) assumes a step like function $\sigma = 0$ in Equation 5.8, and plot (b) assumes the feedback is smoother with a value of $\sigma = 0.25A_{max}$ in Equation 5.8

5.5 Discussion & Conclusion

This work shows that using values from literature assuming a CSTR stomach and PFR small intestine with a nutrient based feedback mechanism as described by Equation 5.7 can provide close predictions to the rate of appearance of glucose into the plasma. But there are limitations to how we can extrapolate. The data from literature on rate of glucose appearance in the plasma is limited; in these two cases glucose solutions of different initial glucose concentrations, up to a value of 75g of glucose ($\approx$ 300kcal),

were used to validate the model,however this calorific content is low compared to an average meal and additional data would be required to understand if the assumptions made here hold true for higher calorie meals.

The mass transfer rate in the model is calculated from Equations 3.5 and 3.6, which rely upon the chyme viscosity (assumed to be that of water). Most viscous liquid nutrient drinks (e.g., milkshakes, smoothies) will have an initial viscosity greater than that of water. The effect of increasing the chyme viscosity is shown in Figure 5.7, which show that small increases can have a large effect upon the absorption rate, similar to that seen *in vitro* (Gouseti et al., 2014), but data is not available to validate these changes nor was the effect of secretions upon the viscosity implemented. The viscosity is likely to drop dramatically in the stomach due to gastric secretions and processing (Marciani et al., 2000) but it is unlikely to be diluted down to that of water over the time frame of the maximum peak ($\approx$30 min) seen in Figure 5.5. Therefore data from liquid meals with higher initial viscosity would be required to validate the use of Equations 3.5 and 3.6.

Gut wall contractions will likely play an important role in nutrient mass transfer in the intestinal lumen (Lentle and Janssen, 2008). *In vitro* experiments have shown that segmentation contractions can increase the mass transfer by over 20% (Gouseti et al., 2014). The current model does not attempt to implement the mixing induced by segmentation and peristalsis, and hence the Reynolds number calculated from the mean flow velocity is low- compared to *in vivo* observations- as pointed out by Lentle and Janssen (2008). Incorporating peristalsis and segmentation into models has been done using a computational fluid dynamics (CFD) approach in both the small intestine (Love

et al., 2013; Tripathi, 2011a) and the stomach (Ferrua and Singh, 2010, 2011), but this approach is computationally expensive and could prove difficult to validate. Along with this the results from CFD may not be accurate reproductions of what happens *in vivo*, for example Love et al. (2013) achieved a maximum Reynolds number of 160, which is comfortably within the laminar regime, and does not reflect the residence time distributions seen by Janssen et al. (2007), which show the gut wall contractions are able to move the chyme in to the turbulent regime. A simpler approach could be through an empirical formulation of the Reynolds number during segmentation and/or peristaltic contractions and an understanding of the frequency and strength of these contractions, or taking into account the curved nature of the intestine which will significantly increase the mass transfer (Carbonell, 1975).

The dynamic nature of the chyme viscosity would also require modelling, this has been attempted in Section 4.3.3 for gastric secretions, but has not been attempted for the intestinal secretions which would be linked in part to the pH of the gastric chyme, and the type and amount of calories entering the duodenum (Keller and Layer, 2005).

Chapter 6

Towards a 2-Phase Model of Digestion

The modelling and simulation as well as the writing of this chapter was carried out by myself.

Peter J. Fryer reviewed the chapter.

Serafim Bakalis offered advice and reviewed the chapter.

The previous chapters (3-5) of this thesis have focused on the postprandial processes occurring after the consumption of liquid carbohydrate meals. However, most meals consumed will contain a mixture of nutrients along with a variety of textures and be multiphase. The different phases and components will all behave differently in different parts of the gut. Chapter 6 aims to address this by implementing a population balance on the stomach to model the disintegration of solid though the mechanisms described by Kong and Singh (2009) and discussed in Chapter 2, along with a model for the disintegration of solids in the small intestine. This will be implemented along with the

models for liquid parts of the meal developed in Chapters 3-5, and the nutrient based feedback mechanism developed in Chapters 4-5. The models produced will be able to simulate the digestion of a solid meal with a liquid drink. The model developed is validated against data for the gastric emptying of solid meals from literature.

6.1 Introduction

When considering a solid meal there is likely a liquid part consumed with it; once in the stomach a sieving mechanism will initiate, whereby the liquid phase of the meal, or secretions to the stomach will be able to pass through the pyloric sphincter to the duodenum, the maximum diameter of the pylorus opening is around 2mm (Keet, 1962). The solid particles with diameter greater than that of the pyloric opening will remain in the stomach to allow the grinding mechanism to reduce the particle size before allowing passage through the pylorus (Marciani et al., 2012). This process of gastric sieving will mean that low nutrient liquid will empty quickly (e.g., water) and solids which contain the nutrients will remain in the stomach.

The idea of a nutrient feedback mechanism has been discussed widely in literature (Brener et al., 1983; Calbet and MacLean, 1997; McHugh and Moran, 1979; Shahidullah et al., 1975); which shows the presence of a mechanism whereby nutrients in the small intestine are sensed by taste receptors and signal the pyloric sphincter to control the amount of gastric content which empties. Chapter 4 developed a model for this mechanism and it was validated against data from oral glucose tolerance tests in Chapter 5.

Solids will be broken down in the stomach by two methods: *Fragmentation*, where a particle will break into several large pieces and *Erosion*, where the the particles surface will wear away (Kong and Singh, 2009). Which method dominates will depend upon the initial properties of the particles, the force applied to them in the stomach, and how their properties change overtime due to the forces and secretions in the stomach.

Studies have been carried out showing how meals of the same composition but in different forms i.e., solid meals and blended soups have different gastric emptying rates and glycaemic responses (Clegg et al., 2013; Marciani et al., 2012). In this work a model for the breakdown of solid in the stomach and small intestine will be proposed to build on previous models for liquid meals outlined in Chapters 3-5 and in Moxon et al. (2016) to investigate how solid breakdown and gastric sieving mechanisms play a role in the gastric emptying and absorption of nutrients.

6.2 Model Formulation

The model is made up of two compartments: Stomach & small intestine. Building on work done in previous Chapters 3-5 (Moxon et al., 2016).

6.2.1 Stomach

For solid particles to empty from the stomach, they must have a diameter below 1-2mm (Kong and Singh, 2008). Larger particles will not empty but will undergo size reduction. To model this a population balance will be carried out on particle of different sizes, for n=1,2,...,k, where r_1 is the largest particle size (size of bolus delivered from swallowing), and r_k is the smallest particle size, and dr is the is the change in particle size between each class. Particle of size r_k will be the only particles which can empty, and will not undergo further size reduction within the stomach. There will be N_n particles in each class, where $\sum_{n=1}^{k} N_n(t)$ is the total amount of particles in the stomach at time, t, where $t \in [0, t_f]$ and t_f is the total simulation time. The mass of particles in

each class will be m_n, where $\sum_{n=1}^{k} m_n(t)$, is the total mass in the stomach at time, t. The movement from one class to the other will be by either fragmentation or erosion. The models are based on previous work by (Fan and Srivastava, 1981).

Fragmentation

Particle of size, r_n, undergoing fragmentation will break into 2 particles of equal size, $r_{f,n}$, plus a number, $X_{f,n}$, of particles of size r_k, according to a mass balance. The rate that this process will occur will be defined as $P_{f,n}[1/s]$. To ensure continuity of mass, $r_{f,n}$ must be equal to one of the sizes in the vector r_n.

We say the radius of the fragmented particles is equal to the radius of the parent particle r_n divided by 1.3, then rounded down to the nearest value of r_n. Hence the daughter particles will have radius r_{n-j}, and the mass balance to determine the number of particle of r_k will take the form:

$$X_{f,n} = \frac{(r_n^3 - 2r_{n-j}^3)}{r_k^3} \tag{6.1}$$

Erosion

A particle of radius r_n will reduce its size by one class, r_{n-1}, during the erosion process. This will occur at an erosion rate defined as $P_{e,n}[m/s]$, and the extra mass will move to the smallest class, r_k, where the number, $X_{e,n}$ will be determined by the following mass balance:

$$X_{e,n} = \frac{(r_n^3 - r_{n-1}^3)}{r_n^3} \tag{6.2}$$

Both fragmentation and erosion will occur during the gastric period, and the rate of each occurring will depend on the meal properties. In the model it will be assumed, for

simplicity, that the rate at which these processes occur will remain constant, and system assumed to be a Markov process (i.e., the particle have no memory and secretions have no effect upon the processes).

Particle balance

With both mechanism taking place the balance on the number of particles in each class will take the following form:

$$\frac{dN_n}{dt} = \begin{cases} -\frac{P_{er}}{dr}N_n - P_f N_n & \text{if } n = 1 \\ -\frac{P_{er}}{dr}N_n - P_f N_n + \frac{P_{er}}{dr}N_{n-1} + 2P_f.N_{n-j} & \text{if } n > 1 \ \& \ n < k \\ \sum_{n=1}^{k-1} N_n(\frac{P_{er}}{dr}X_{er} + P_f X_f) + \frac{P_{er}}{dr}N_{k-1} + 2P_f N_{k-j} - \gamma N_k & \text{if } n = k \end{cases} \tag{6.3}$$

For the case of class k, which contains the smallest particle size, r_k, along with input from erosion and fragmentation process there will be gastric emptying at the rate γ. Where γ will be a function of the bioaccessable nutrients & nutrient types in the small intestine.

Liquid

During the gastric processing of solid meals a gastric sieving mechanism will occur (Marciani et al., 2012). Liquid will empty from the stomach whilst the solid particles will remain until the size of the particle is less than a minimum (around 1-2mm in diameter (Kong and Singh, 2008)). Hence the equations for the liquid part of the meal in the stomach will have the following form:

$$\frac{dW_{stom}(t)}{dt} = -\gamma W_{stom}(t) \tag{6.4}$$

6.2.2 Small Intestine

The model will assume a particle enters the small intestine with size r_k, containing a nutrients which require breakdown prior to absorption (e.g., starch) (S_b), where S_b is the amount of energy in kcal. As the particle propagates along the length of the small intestine the size will reduce. Soluble nutrients in the particle will move into the bulk fluid, it is assumed that water absorbed by the particle will facilitate the release, in the intestinal lumen (S_a), here it can be accessed by the enzymes, which will break the macro nutrient down to absorbable nutrients (G) (or nutrients which will be hydrolysed at the brush border, which is assumed not to be rate limiting (Weber and Ehrlein, 1998)) these nutrients will move to the intestinal epithelium where they can be absorbed. There will be a total of 6 PDEs representing the system, one for each of the following components:

- Number of particles, $N_{SI}(z,t)$
  - Particles will enter the small intestine from the stomach and move along the length due to advection, the size of the particles will reduce but the number will not increase/decrease only move along the length.
- Nutrients in bolus, $S_b(z,t)$
  - The non-absorbable nutrients will be contained in the bolus, it will move into the lumen at rate K_d depending upon the size of the bolus and the amount of swelling the bolus undergoes (amount of water in the bolus)
- Accessible nutrients, $S_a(z,t)$

  - nutrients in the lumen can be hydrolysed by enzymes, this will occur by Michaelis-Menten kinetics

- Absorbable nutrients, $G(z,t)$
  - Products of the enzymatic hydrolysis of Accessible nutrients (S_a) which can be absorbed, this is assumed to be limited by the mass transfer rate of the nutrients in the intestinal chyme (see Chapter 3).

- Water in bolus, $W_b(z,t)$
  - Its is assumed that the disintegration of the bolus in the intestine is facilitated by the absorption of water/ intestinal fluids.
  - The movement into the bolus will depend upon the surface area of the bolus and the rate gradient between water in the bolus and in the chyme

- Water in lumen, $W_l(z,t)$
  - Water will be introduced through secretions into the intestine as well as from the meal.

The system can be expressed with the following partial differential equations:

$$\frac{\partial N_{SI}(z,t)}{\partial t} = -u\frac{\partial N_{SI}(z,t)}{\partial z} \tag{6.5}$$

$$\frac{\partial S_b(z,t)}{\partial t} = -u\frac{\partial S_b(z,t)}{\partial z} - K_d\frac{S.A._b(z,t)}{V_b(z,t)}W_b(z,t)S_b(z,t) \tag{6.6}$$

$$\frac{\partial S_a(z,t)}{\partial t} = -u\frac{\partial S_a(z,t)}{\partial z} + K_d\frac{S.A._b(z,t)}{V_b(z,t)}W_b(z,t)S_b(z,t) - \frac{V_{max}S_a(z,t)}{K_m + S_a(z,t)} \tag{6.7}$$

$$\frac{\partial G(z,t)}{\partial t} = -u\frac{\partial G(z,t)}{\partial z} + \frac{V_{max}S_a(z,t)}{K_m + S_a(z,t)} - K_aG(z,t) \tag{6.8}$$

$$\frac{\partial W_b(z,t)}{\partial t} = -u\frac{\partial W_b(z,t)}{\partial z} + K_W\frac{S.A._b(z,t)}{V_b(z,t)}\left(W_l(z,t) - W_b(z,t)\right) \tag{6.9}$$

$$\frac{\partial W_l(z,t)}{\partial t} = -u\frac{\partial W_l(z,t)}{\partial z} - K_W\frac{S.A._b(z,t)}{V_b(z,t)}\left(W_l(z,t) - W_b(z,t)\right) + W_{sec} \tag{6.10}$$

The PDEs require boundary and initial conditions. The introduction of bolus into the small intestine is assumed to occur at the position equivalent to the radius of the bolus entering, i.e., r_k, , hence at $z = r_k$ the PDEs for starch in the bolus and number of bolus will take the form:

$$\frac{\partial N_{SI}(r_k,t)}{\partial t} = -u\frac{\partial N_{SI}(r_k,t)}{\partial z} + \gamma N(t,k) \tag{6.11}$$

$$\frac{\partial S_b(r_k,t)}{\partial t} = -u\frac{\partial S_b(r_k,t)}{\partial z} - K_d\frac{S.A._b}{V_b}W_b(r_k,t)S_b(r_k,t) + \gamma m(t,k) \tag{6.12}$$

It will also be assumed that the non-nutrient liquid entering into the W_l component of the small intestine will enter at the same position, taking the following form:

$$\frac{\partial W_l(r_k,t)}{\partial t} = -u\frac{\partial W_l(r_k,t)}{\partial z} - K_W\frac{S.A._b}{V_b}\left(W_l(r_k,t) - W_b(r_k,t)\right) + \gamma(t)S_W(t) + W_{sec} \tag{6.13}$$

Whilst the derivatives w.r.t. time for the other PDEs will be set to zero.

The equations will all be given the same Neumann boundary conditions equal zero, e.g.,

$$\left.\frac{\partial N_{SI}}{\partial z}\right|_{z=0} = \left.\frac{\partial N_{SI}}{\partial z}\right|_{z=L} = 0 \tag{6.14}$$

The secretion of water into the intestinal chyme (W_{sec}) is simplified. It is assumed that it occurs at a constant rate, and that it enters at the beginning of the intestine. The rate is assumed to be 3.5ml/min, which is calculated from the estimated daily secretion of 2500ml of water into the intestine (Barrett et al., 2005) and the assumption that this occurs during the processing of 3 meals, each for around 4 hours (12 hours per day).

Absorption rate

The absorption rate from the small intestine will depend upon the amount of absorbable nutrients (G) in the small intestine. The rate of absorption will be defined as:

$$A_{rate}(t) = \sum_{z=0}^{L} K_a G(z,t) \tag{6.15}$$

The absorption rate constant K_a can be further defined as a function of the chymes viscosity, as in previous work (Moxon et al., 2016), where it is assumed the convective mass transfer rate, K, is the limiting factor in the absorption and we get the following expression:

$$K_a = \frac{2f}{r_{SI}} K \tag{6.16}$$

6.2.3 Feedback Mechanism

The rate at which the gastric content can empty γ is a function of the absorption of the nutrients from the small intestine, this was defined Chapter 4:

$$\gamma = \gamma_0 \left(1 - \frac{1}{1 + \exp\left(-\tau_a \left(A_{rate}(t) - A_{max}\right)\right)}\right) \tag{6.17}$$

6.3 Experimental Data

To validate the model, and obtain values for some of the parameters, experimental data from literature will be used. The data used will be for the gastric emptying rate of solid meals from the stomach and will take the form of fraction of gastric content remaining after a meal is consumed. The first set of data from Urbain et al. (1989), is for the consumption of an egg meal, where the egg was consumed in 3 different states:

Homogenised, cubed with diameter 2.5mm, and cubed with diameter 5mm. The meal was 100ml of the egg, 300ml of water, and 2 slices of toast; giving a total of 318kcal. To include this in the current model only the cubed egg was used in the model and it was assumed that the calorie sources (proteins, carbohydrates, and fats), behaved the same and could be modelled as a single component in the meal, this assumption is based on the fact that the gastric emptying rate is linearly dependent upon the calorific density of a meal (kcal/ml) (Calbet and MacLean, 1997; Hunt and Stubbs, 1975), and that the absorption of carbohydrates, fats and proteins in the jejunum of mini pig was found to occur at the same rate when measured in terms of energy (kcal) (Weber and Ehrlein, 1998). It was also assumed that the calories from the meal were all from the eggs, and that the toast nor water provided any calories. A final assumption was on the processing of the toast, as the diameter of the egg was known and toast unknown- this was eaten normally as opposed to the pre-diced egg- it was assumed this had no effect upon the gastric and small intestinal processes which the egg undergoes.

The second set of data used (Siegel et al., 1988) looks at the gastric emptying of a liver meal and an egg meal. The liver and egg were labelled with Tc-99m-sulphur colloid with the liver cut into 0.5cm cubes and having a total mass of 260g and calorific content of 243kcal, while the egg was cooked until it was solid and eaten as toast with a total mass of 142g and calorific content of 270kcal. Along with the liver a drink of water was also consumed, this was labelled with In-111-DTPA and a total volume of 300ml consumed. This allowed for the solid and liquid part of the meal to be visualised simultaneously.

It will be assumed that the meals are homogenous in content, and that the egg meal from Siegel et al. (1988) is entirely egg and the particle size distribution of the meal entering the stomach can be described from by that of masticated egg white (Jalabert-Malbos et al., 2007).

6.4 Results & Discussions

To estimate the values of parameters a least square mean method was used from the *lsqnonlin* function in MATLAB with experimental data from (Urbain et al., 1989). The parameters which are to be estimated are: the erosion rate (P_e), the fragmentation rate (P_f), the initial emptying rate (γ_0), the maximum absorption rate (A_{max}), mass transfer rate of water into the bolus (K_w), the mass transfer rate of nutrients in the chyme (K_a), and the rate of release of starch form the bolus (K_d). This experimental procedure used eggs which were cooked into a homogenous solid and cut into cubes of 2.5mm and 5mm, participants were asked to swallow without chewing, so it will be assumed that the particles arrive in the stomach at the initial sizes. These were assumed to be spherical particles of the same volume and an equivalent radius was calculated accordingly and parameter estimation carried out simultaneous for both particle size with the results shown in Figure 6.1.

The parameter estimates for the Urbain et al. (1989) results are shown in Table 6.1. It can be seen that assuming the same parameter values for the egg meal with only the input particle size changing allows for the model output to follow the same trend as the experimental data, with a RMSE value of 0.018 (shown in Figure 6.3). The small particles seem to breakdown and empty quicker leading to a faster initialisation of the

feedback mechanism, this can be seen in the characteristic step like decrease in stomach content, which is more apparent in the 2.5mm cube meal.

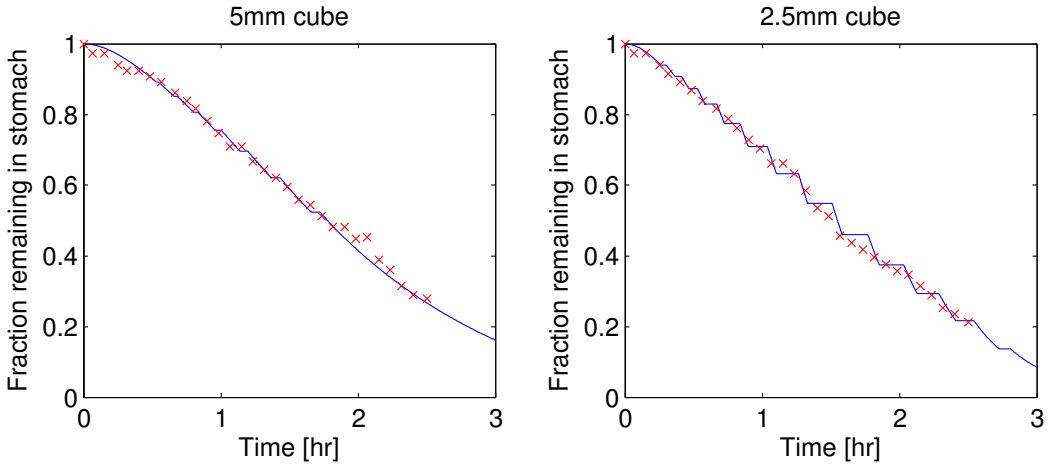

Figure 6.1: fraction of meal remaining in the stomach for two different egg meals, one with initial particle size of 5mm and a second with initial particle size of 2.5mm, experimental data from Urbain et al. (1989) shown with red crosses, model output shown with solid blue line.

Table 6.1: Optimal Parameter values for egg meals of input size 2.5mm^3 and 5mm^3 from experimental data by Urbain et al. (1989)

$P_e[m/min]$	$P_f[1/min]$	$K_d[m/min\ g_{water}]$	$K_w[m/min]$	$K_a[m/min]$	$A_{max}[kcal/min]$	$\gamma_0[1/min]$
7.7×10^{-6}	6.5×10^{-3}	4.1×10^{-5}	2.5×10^{-5}	0.35	1.50	0.41

The results were then used with the data from Siegel et al. (1988), the parameter values were kept the same as the optimal values from the Urbain et al. (1989) parameter estimation (Table 6.1) and the input size was take from literature for the particle size distribution of egg white after mastication (Jalabert-Malbos et al., 2007).

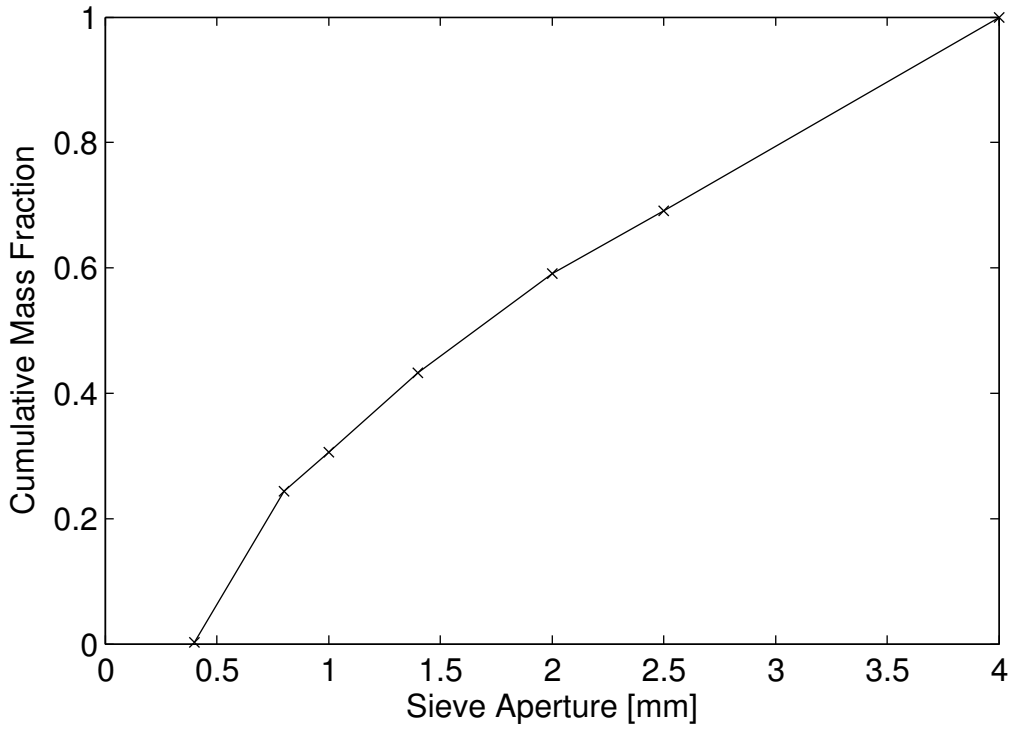

Figure 6.2: Cumulative mass of egg white remaining on different sieve apertures after mastication (Jalabert-Malbos et al., 2007).

The model output quickly initiates the feedback mechanism, unlike the experiments by Urbain et al. (1989) the meal undergoes mastication before swallowing which will produce a particle size distribution (shown in Figure 6.2), containing around 30% of particles below 1mm in diameter and thus will be able to pass through the pylorus without further disintegration. These will pass into the small intestine and the carbohydrate will become bioaccessible before been absorbed. Due to the quick initiation the emptying of the solid portion follows a linear step like emptying over the 2.5 hour period, following the same trend as the experimental results with a RMSE of 0.027. The liquid portion of the meal empties in a more exponential pattern similar for both the model output and experimental data, but the model seem to overestimate the experimental

data slightly, this results in a RMSE value of 0.043. The liquid curve also highlights the effect of gastric sieving with around 20% of the liquid portion of the meal emptying before the feedback mechanism initiates compared to a much smaller percentage of the solid meal emptying.

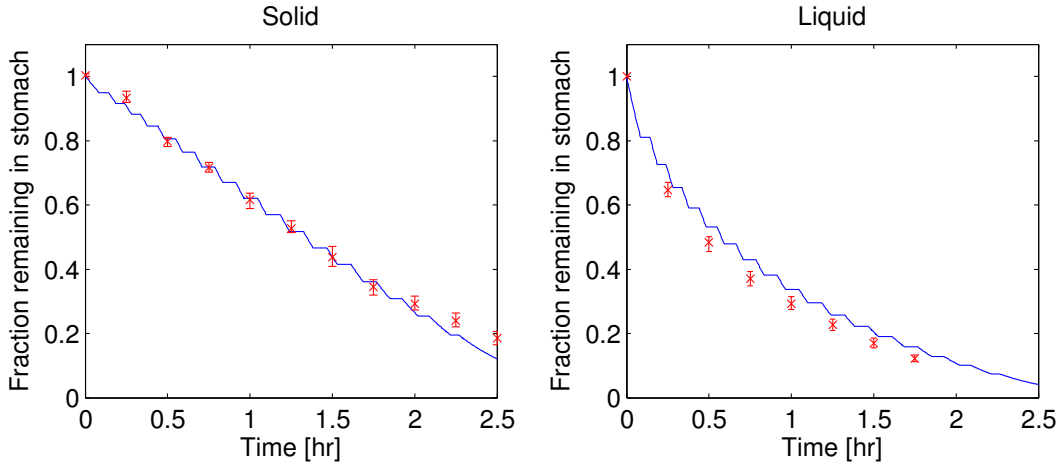

Figure 6.3: Fraction of meal (Solid and liquid components) remaining in the stomach with red crosses showing experimental results from Siegel et al. (1988), the solid lines show the model output with parameter taken from the estimates for the Urbain et al. (1989) egg meals.

This highlights how a population balance can be used to estimate the gastric emptying rate of solid meals. the meals used had a low calorific content compared to an average meal (270kcal and 320 kcal), but in both meals the main source of these calories was consistent (eggs), and parameters estimated from one of the sources was able to predict closely the emptying curve of the other source with only the description of the input particle sizes differing.

The parameter values are therefore mainly linked to the meal type. The breakdown in the stomach will be a function of the cohesive forces, and as highlighted by Kong and Singh (2009) these will determine whether the breakdown is controlled by ero-

sion or fragmentation. The rate is likely dynamic and will change depending upon the interactions of the food particles and secretions, and how these change the particles structure, for example through the hydrolysis of peptides, or effect of gastric acid upon the particles (Van Wey et al., 2014). The breakdown rate rate for rice during *in vivo* experimentation on pigs was calculated at around 2.3-3.5^{-3} min^{-1} for brown rice and 23.7-16.2$\times 10^{-3}$ min^{-1} for white rice (Bornhorst et al., 2015), which are in similar orders of magnitude as the P_f values calculated for the egg meal. Once in the small intestine it is assumed that the particle size at the boundary (pyloric sphincter) is the same for all particles entering (r_{min}), and hence any further breakdown will be independent of the mastication profile or the rates of erosion and fragmentation, these will only affect the delivery of solids to the small intestine and not the structure; but K_d and K_w will be a function of the physical properties of the meal (assumed unchanged due to the gastric processing), and also the amount of water. This is a simplification assuming that the water will cause swelling and aid breakdown of the food, but other secretions could play a role here.

The mass transfer rate in the intestinal lumen, K_a, will be a function of the chyme properties and the solid content of the meal, i.e., increase in viscosity of the liquid phase and increase in solid fraction (which would increase the effective viscosity) would reduce the mass transfer rate and also affect the flow regime, low viscosity chymes will likely be characterised as turbulent with different eddy sizes, but more viscous chymes exhibit laminar flows with large eddy (Janssen et al., 2007). The gastric secretions will play a major role in reducing the effective viscosity of the meal (Marciani et al., 2000).

The parameter A_{max} will not be affected by the physical properties of the meal, but will be linked to the nutrient type (Calbet and MacLean, 1997), with carbohydrates (Heddle et al., 1988b), lipids (Heddle et al., 1988a), and proteins (Soenen et al., 2014) shown to increase the number of IPPW (isolated pyloric pressure waves) with intraduodenal infusion of the nutrients, this increase in the number of IPPW can be linked to the inhibition of gastric emptying (Treacy et al., 1990). Here we assumed that all the nutrients behave the same, when considered in terms of energy (kcal), this was show to be an accurate assumption through the work of Weber and Ehrlein (1998), who showed absorption rate was the same for fats, carbohydrates, and proteins when considered in terms of energy. The model here also assumes that the hydrolysed of the nutrients occurs in the small intestine, with the kinetics associated with pancreatic α-amylase (Fonseca, 2011). This assumption is not correct for proteins and lipids as it ignores the break down of proteins and lipids which will occur within the stomach, facilitated by the secretion of gastric enzymes, but allows greater simplicity for the modelling of the population balance. The estimated value of 1.5 kcal/min gives a good order of magnitude agreement with the expected rates of gastric emptying when the feedback mechanism is active, Brener et al. (1983) measured this at 2.14 kcal/min, and Weber and Ehrlein (1998) measured rate of flow into the jejunum at around 1.3 kcal/min.

The parameter γ_0 is also likely affected in some way by the meal properties, for viscous liquid meals, good agreement with experimental data was found when linked to the chyme viscosity and the secretion rate (as shown in Chapter 4), both of these would affect the distension of the stomach, which is also likely affected by the solid volume fraction of a meal. The density of solid pellets of the same size has been shown to affect

the emptying rate (Meyer et al., 1988), this may be due to the internal cohesive forces and how the pellets are disintegrated or could be influenced by where the particles are in the stomach, with some data showing that the solids will initially sit in the fundus before moving towards the antrum (Bürmen et al., 2014). Though this is not considered in the current model where it is assumed that the solids are uniformly mixed and each part of the stomach behaves the same (stomach assumed to be a CSTR).

To analyse the effect of different foods a second meal of liver was modelled using data from Siegel et al. (1988), again the results are displayed as solid and liquid components and are highlighted in Figure 6.4, with the parameters shown in Table 6.2. The liver was cut into 5mm cubes, though not stated in the experimental procedure it is assumed that the cubes are not chewed but swallowed intact, and therefore the initial bolus size in the stomach will be the equivalent spherical diameter, it is also assumed that the calories are all within the solid phase of the meal.

One of the key differences between the egg and liver meal is that the liver meal does not initiate the feedback response as quickly nor is it as sustained. Both meals have a similar erosion rate from the model, but the liver undergoes fragmentation more easily, still the emptying rate is slower due to a lower value of γ_0. However in the small intestine it seems the bioaccessibility is lower, with lower K_d and K_w values, along with a K_a value around an order of magnitude lower, meaning the simulated mass transfer rate within the intestinal lumen is slower for the liver than for the egg meal; this is the main reason why the feedback mechanism is not initiated. But as the results are only fit against the gastric emptying rate, and no data was available for this meal to validate

against the absorption rate it is not possible to say with certainty that this is what is occurring *in vivo*.

Table 6.2: Optimal Parameter values for liver meal gastric emptying Siegel et al. (1988) data

$P_e[m/min]$	$P_f[1/min]$	$K_d[m/min\ g_{water}]$	$K_w[m/min]$	$K_a[m/min]$	$A_{max}[kcal/min]$	$\gamma_0[1/min]$
7.7×10^{-6}	4.6×10^{-2}	2.0×10^{-5}	1.5×10^{-5}	3.7×10^{-2}	0.14	1.7×10^{-2}

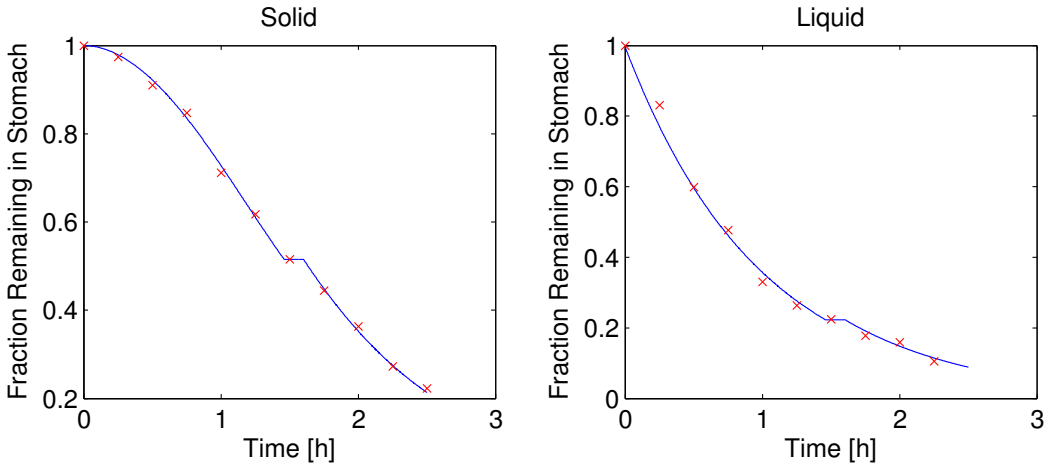

Figure 6.4: Model emptying output and Experimental results (Siegel et al., 1988) for liver and water meal, split into solid and liquid phases.

6.5 Conclusion

The work shows that the gastric emptying of solid meals can be modelled using a population balance with parameters which offer some physiological relevance, as opposed to current models where fitted parameters have no physiological interpretation (Bürmen et al., 2014; Kong and Singh, 2008, 2009; Siegel et al., 1988). The model assumes the gastric breakdown occurs by either fragmentation or erosion, the rates of

which will be linked to the meal properties. The model also assumes that the emptying rate is linked to the feedback mechanism developed in Chapters 4 & 5, which in turn will be a function of the bioaccessibility of the nutrients in the lumen. The bioaccessiblity will be controlled by the release of the nutrients from the particles entering from the stomach, which will be linked to the swelling and disintegration of these particles, and also the mass transfer rate of the nutrients through the luminal chyme. Currently the model assumes that the solid phase of the meal behaves homogeneously, though in reality it is likely that a meal will have multiple components behaving differently. Though with an understanding of the particle size distribution from mastication, and the meal type the model does offer some predictive capability. More work is required to understand the breakdown of the particles in the small intestine, and give more confidence to the model and parameters chosen to represent this section of digestion.

Chapter 7

Conclusion

This work has presented multiple models looking at how different meals behave postprandially; highlighting the importance of both luminal mass transfer and the gastric emptying rate of meals upon the absorption of nutrients. One of the main hypotheses of this work (as with other works from literature e.g., (Penry and Jumars, 1986, 1987; Stoll et al., 2000)) is that the human gut can be described as a series of reactors, in this case the stomach is described as a CSTR and the small intestine as a PFR. The processes which occur in these reactors will be linked to the properties, both physical and chemical, of the meal. To add to the complexity of the system there are numerous feedback mechanisms to allow for the digestive system to control how the nutrients are absorbed, e.g., the effect of nutrient sensing in the small intestine upon the gastric secretion rate (Di Mario and Goni, 2014), or upon the gastric emptying rate (Brener et al., 1983; Calbet and MacLean, 1997). Some of these processes were implemented in the model, such as the 'Duodenal brake' (nutrient based feedback mechanism), and show how the luminal mass transfer is likely linked to the rate of gastric emptying allowing the body to control, for example, the glycemic response to a meal.

The model implemented in Chapter 4 showed how a simple on/off feedback mechanism can describe the gastric emptying rate of viscous liquid, nutrient meals, and that along with the feedback mechanism, the viscosity could be linked to the secretion rate for the *Gastric phase* of secretions showing good estimates of the gastric viscosity changes compared to *in vivo* results by Marciani et al. (2000); and the parameter defined for the initial (or rapid) gastric emptying rate (γ_0) can be linked to the rate of secretion and the viscosity of the meal. This highlights how these simple models linked to the meal properties can be used to describe the gastric emptying rate for simple liquid

meals. The viscosity changes in the stomach were linked to the concentration of Locust Bean Gum, this simplified assumption provided a good fit, but a better understanding of how the gastric secretions reduce the viscosity is still required to apply the model to other meals with other thickener systems.

The model developed in Chapter 4 was used in Chapter 5 to predict the glucose absorption rate for two different initial inputs of glucose, in this case a delay was also implemented in the feedback mechanism- i.e,. the mechanism is not instantaneous. This showed that without fitting any parameters (all parameters estimated from literature) that the absorption rate can be predicted for standard OGTT meals. The effect of increasing the viscosity could not be validated due to the lack of literature data, but it is likely that to describe high viscosity meals the mass transfer rate will have to be linked to the effect of gut wall motility, with this having the effect of increasing the mixing. This could be done through experimental observation and production of an empirical formula or through the coupling of the model to a fluid dynamics model of the small intestine e.g., (Love et al., 2013), although the latter option would likely be computationally expensive.

In Chapter 6 the model was developed further to include the input of a 2 phase meal, this allows for the gastric emptying and absorption of a solid meal to be modelled. To do this a population balance was implemented in the stomach, and a swelling/shrinking core model was implemented in the small intestine. Fitting of 7 parameters to data on the gastric emptying rate of egg meals which were cubed to two different sizes and swallowed whole gave a good fit, the model along with these parameter values were then validated with a separate set of data for an egg meal which required an estimation

of the input size, this was taken from a particle size distribution of masticated egg whites (Jalabert-Malbos et al., 2007). This again provided a close approximation of the experimental results, and the parameters can be linked to the physical properties of the meal e.g., fragmentation and erosion rate in the stomach, or meal composition, e.g., A_{max}. Though there are still limitations to the model, and the effect of gastric and intestinal secretions require implementing along with a model for the rate of these secretions.

A model for gastric secretions induced from consumption of a solid meal could take a similar form to that presented in Chapter 4 for viscous liquid meals. The effective viscosity of the chyme would be a function of the viscosity of the continuous liquid phase and the volume fraction of the solid particles, assuming the solids behave as a suspension of spheres and are homogeneously mixed this could be linked to models for concentrated suspensions of spheres in literature, e.g., Beenakker (1984). This is working with the assumption that the *Gastric phase* of gastric secretions, which contributes the largest volume of secretions (Di Mario and Goni, 2014), is induced (at least in part) as a result of gastric distension (Grötzinger et al., 1977). The antrum distension has been linked to the viscosity of the meal (high viscosity, greater distension) (Marciani et al., 2001b) and to the perception of satiety (Hveem et al., 1996; Marciani et al., 2001b; Santangelo et al., 1998). Unlike liquid meals the solid initially reside in the fundus before moving to the antrum (Meyer et al., 1988), hence further work may require an extra gastric compartment to represent the fundus and antrum separately, this would require greater understanding of the meal physical properties and how they are affected by the gastric processes and secretions as the spatial distribution of solids is likely linked to the den-

sity of the solid particles (Meyer et al., 1988), and currently it is assumed that the meal is homogenous and evenly mixed in either phase.

The work presented in this thesis builds upon previous literature work assuming the human gut can be described by a series of reactors, the work unlike others in literature (as far as the author knows) makes the assumption that the limiting factor of intestinal absorption is the mass transfer of nutrients in the lumen, further work is required to include the effect of gut wall motility upon this mass transfer coefficient and validate the terms used at high viscosities. This work also takes the approach of linking the gastric emptying rate to the bioaccessibility of nutrients within the intestine, something which has be observed and tested *in vivo* but has so far not been implemented in mathematical form.

There are many areas for future development of the model, as previously stated further work is required to implement an understanding of intestinal wall motility upon the mass transfer of intestinal chyme, to develop a more global approach to the effect of secretions upon the viscosity of gastric chyme and develop a model for intestinal secretions, and implement this with the 2 phase model developed in Chapter 6.

One of the main area in which the work could be developed in the future is thorough the coupling of the glucose absorption with literature or new models for the plasma glucose-insulin dynamics. A simple approach to this could be coupling with a minimal model for an oral input of glucose (Breda et al., 2001; Dalla Man et al., 2005), though there are drawbacks to using the minimal model approach, some of these are outlined in literature such as the fact that an equilibrium is not achievable with the minimal model and that the solutions are not bounded (Li et al., 2001). To move away from the minimal

model some authors have used differential equations with delay terms, the stability of these equations was confirmed for intravenous glucose tolerance test (IVGTT) (De Gaetano and Arino, 2000; Li et al., 2001). A similar approach to this could be taken for OGTT, and coupled with the models developed in this thesis to provide a prediction of blood glucose levels after a meal is consumed, and if the glucose-insulin model is stable it would ensure and accurate output for a large range of different absorption profiles.

Bibliography

Anderwald, C., Gastaldelli, A., Tura, A., Krebs, M., Promintzer-Schifferl, M., Kautzky-Willer, A., Stadler, M., DeFronzo, R. A., Pacini, G., and Bischof, M. G. (2011). Mechanism and effects of glucose absorption during an oral glucose tolerance test among females and males. *J. Clin. Endocrinol. Metab.*, 96(2):515–24.

Arakawa, T., Uno, H., Fukuda, T., Higuchi, K., Kobayashi, K., and Kuroki, T. (1997). New aspects of gastric adaptive relaxation, reflex after food intake for more food: involvement of capsaicin-sensitive sensory nerves and nitric oxide. *J. Smooth Muscle Res.*, 33(3):81–8.

Baggio, L. L. and Drucker, D. J. (2007). Biology of Incretins: GLP-1 and GIP. *Gastroenterology*, 132(6):2131–2157.

Ballance, S., Sahlstrøm, S., Lea, P., Nagy, N. E., Andersen, P. V., Dessev, T., Hull, S., Vardakou, M., and Faulks, R. (2013). Evaluation of gastric processing and duodenal digestion of starch in six cereal meals on the associated glycaemic response using an adult fasted dynamic gastric model. *Eur. J. Clin. Nutr.*, 52(2):799–812.

Barrett, K. E. (2005). *Gastrointestinal Physiology*. McGraw-Hill Education, New York.

Barrett, K. E., Boitano, S., Barman, S., and Brooks, H. L. (2005). Gastrointestinal physiology. In Barrett, K. E., editor, *Ganong's Rev. Med. Physiol.* McGraw-Hill, New York, 22nd edition.

Bastianelli, D., Sauvant, D., Rerat, A., Bastianelli, D., Sauvant, D., and Re, A. (1996). Mathematical Modeling of Digestion and Nutrient Absorption in Pigs. *J. Anim. Sci.*, 74:1873–1887.

Beckers, E. J., Leiper, J. B., and Davidson, J. (1992). Comparison of Aspiration and Scintigraphic Techniques for the Measurement of Gastric Emptying Rates of Liquids in Humans. *Gut*, 33(1):115–117.

Beenakker, C. W. J. (1984). The effective viscosity of a concentrated suspension of spheres (and its relation to diffusion). *Phys. A Stat. Mech. its Appl.*, 128(1-2):48–81.

Berghöfer, A., Pischon, T., Reinhold, T., Apovian, C. M., Sharma, A. M., and Willich, S. N. (2008). Obesity prevalence from a European perspective: a systematic review. *BMC Public Health*, 8:200.

Bornhorst, G. M., Ferrua, M. J., and Singh, R. P. (2015). A {Proposed} {Food} {Breakdown} {Classification} {System} to {Predict} {Food} {Behavior} during {Gastric} {Digestion}. *J. Food Sci.*, 80(5):n/a—-n/a.

Brand-Miller, J. C., Stockmann, K., Atkinson, F., Petocz, P., and Denyer, G. (2009). Glycemic index, postprandial glycemia, and the shape of the curve in healthy subjects: Analysis of a database of more than 1000 foods. *Am. J. Clin. Nutr.*, 89(1):97–105.

Breda, E., Cavaghan, M. K., Toffolo, G. M., Polonsky, K. S., and Cobelli, C. (2001). Oral glucose tolerance test minimal model indexes of beta-cell function and insulin sensitivity. *Diabetes*, 50(1):150–8.

Brener, W., Hendrix, T. R., and McHugh, P. R. (1983). Regulation of the gastric emptying of glucose. *Gastroenterology*, 85(1):76–82.

Brouns, F., Bjorck, I., Frayn, K. N., Gibbs, A. L., Lang, V., Slama, G., and Wolever, T. M. S. (2005). Glycaemic index methodology. *Nutr. Res. Rev.*, 18(01):145.

Brouns, F., Senden, J., Beckers, E., and Saris, W. H. M. (1994). Osmolarity does not affect the gastric emptying rate of oral rehydration solutions in man. *J. Physiol.*, 479(p):123P–123P.

Bürmen, B., Locatelli, I., Bürmen, A., Bogataj, M., and Mrhar, A. (2014). Mathematical modeling of individual gastric emptying of pellets in the fed state. *J. Drug Deliv. Sci. Technol.*, 24(4):418–424.

Calbet, J. A. and MacLean, D. A. (1997). Role of caloric content on gastric emptying in humans. *J. Physiol.*, 498(2):553–559.

Carbonell, R. (1975). Mass Transfer Coeficients in Coiled Tubes In. *Biotechnol. Bioeng.*, 17(9):1383–1385.

Carlslaw, H. and Jaeger, J. (1959). *Conduction of Heat in Solids*. Oxford University Press, London.

Carmagnola, S., Cantù, P., and Penagini, R. (2005). Mechanoreceptors of the proximal stomach and perception of gastric distension. *Am. J. Gastroenterol.*, 100(8):1704–1710.

Chaudhri, O., Small, C., and Bloom, S. (2006). Gastrointestinal hormones regulating appetite. *Philos. Trans. R. Soc. Lond. B. Biol. Sci.*, 361(1471):1187–1209.

Cheeseman, C. I. (2002). Intestinal hexose absorption: transcellular or paracellular fluxes. *J. Physiol.*, 544(2):336–336.

Clegg, M. E., Ranawana, V., Shafat, a., and Henry, C. J. (2013). Soups increase satiety through delayed gastric emptying yet increased glycaemic response. *Eur. J. Clin. Nutr.*, 67(1):8–11.

Collins, P. J., Houghton, L. A., Read, N. W., Horowitz, M., Chatterton, B. E., Heddle, R., and Dent, J. (1991). Role of the proximal and distal stomach in mixed solid and liquid meal emptying. *Gut*, 32(6):615–619.

Cummings, D. E. and Overduin, J. (2007). Gastrointestinal regulation of food intake. *J. Clin. Invest.*, 117(1):13–23.

Dalla Man, C., Camilleri, M., and Cobelli, C. (2006). A system model of oral glucose absorption: Validation on gold standard data. *IEEE Trans. Biomed. Eng.*, 53(12):2472–2478.

Dalla Man, C., Caumo, A., Basu, R., Rizza, R., Toffolo, G., and Cobelli, C. (2004). Minimal model estimation of glucose absorption and insulin sensitivity from oral test: validation with a tracer method. *Am. J. Physiol. Endocrinol. Metab.*, 287(4):E637–43.

Dalla Man, C., Yarasheski, K. E., Caumo, A., Robertson, H., Toffolo, G., Polonsky, K. S., and Cobelli, C. (2005). Insulin sensitivity by oral glucose minimal models: validation against clamp. *Am. J. Physiol. - Endocrinol. Metab. Endocrinol. Metab.*, 289(6):E954–E959.

De Gaetano, A. and Arino, O. (2000). Mathematical modelling of the intravenous glucose tolerance test. *J. Math. Biol.*, 40(2):136–168.

de Loubens, C., Lentle, R. G., Love, R. J., Hulls, C., and Janssen, P. W. M. (2013). Fluid mechanical consequences of pendular activity, segmentation and pyloric outflow in the proximal duodenum of the rat and the guinea pig. *J. R. Soc. Interface*, 10(83):20130027.

De Wijk, R. A., Prinz, J. F., Engelen, L., and Weenen, H. (2004). The role of \alpha-amylase in the perception of oral texture and flavour in custards. *Physiol. Behav.*, 83(1 SPEC. ISS.):81–91.

Depoortere, I. (2014). Taste receptors of the gut: emerging roles in health and disease. *Gut*, 63(1):179–190.

Di Mario, F. and Goni, E. (2014). Gastric acid secretion: changes during a century. *Best Pract. Res. Clin. Gastroenterol.*, 28(6):953–65.

Di Muria, M., Lamberti, G., and Titomanlio, G. (2010). Physiologically Based Pharmacokinetics: A Simple, All Purpose Model. *Ind. Eng. Chem. Res.*, 49(6):2969–2978.

Dikeman, C. L., Barry, K. A., Murphy, M. R., and Fahey Jr, G. C. (2007). Diet and measurement techniques affect small intestinal digesta viscosity among dogs. *Nutr. Res.*, 27:56–65.

Dillard, S., Krishnan, S., and Udaykumar, H. S. (2007). Mechanics of flow and mixing at antroduodenal junction. *J. Gastroenterol.*, 13(9):1365–1371.

Ebert, K. and Witt, H. (2016). Fructose malabsorption. *Mol. Cell. Pediatr.*, 3(1):10.

Elashoff, J., Reedy, T., and Meyer, J. (1982). Analysis of gastric emptying data. *Gastroenterology*, 83(6):1306–12.

Ellis, P. R., Roberts, F. G., Low, A. G., and Morgan, L. M. (1995). The effect of high-molecular-weight guar gum on net apparent glucose absorption and net apparent insulin and gastric inhibitory polypeptide production in the growing pig: relationship to rheological changes in jejunal digesta. *Br. J. Nutr.*, 74(4):539–56.

Englyst, K. N. and Englyst, H. N. (2005). Carbohydrate bioavailability. *Br. J. Nutr.*, 94(1):1–11.

Fan, L.-S. and Srivastava, R. (1981). A stochastic model for particle disintegration—I. *Chem. Eng. Sci.*, 36(6):1091–1096.

FAO/WHO (1998). Carbohydrates in human nutrition. Technical report, WHO, Rome.

Feinle, C., Kunz, P., Boesiger, P., Fried, M., and Schwizer, W. (1999). Scintigraphic validation of a magnetic resonance imaging method to study gastric emptying of a solid meal in humans. *Gut*, 44(1):106–11.

Ferrua, M. and Singh, R. (2010). Modeling the Fluid Dynamics in a Human Stomach to Gain Insight of Food Digestion. *J. Food Sci.*, 75(7):R151–R162.

Ferrua, M. J., Kong, F., and Singh, R. P. (2011). Computational modeling of gastric digestion and the role of food material properties. *Trends Food Sci. Technol.*, 22(9):480–491.

Ferrua, M. J. and Singh, R. P. (2011). Understanding the fluid dynamics of gastric digestion using computational modeling. *Procedia Food Sci.*, 1:1465–1472.

Fonseca, M. (2011). *An Engineering Understanding of the Small Intestine*. PhD thesis, The University of Brimingham.

Gidley, M. J. (2013). Hydrocolloids in the digestive tract and related health implications. *Curr. Opin. Colloid Interface Sci.*, 18(4):371–378.

Gouseti, O., Fonseca, M., Fryer, P., Mills, C., Wickham, M., and Bakalis, S. (2014). Hydrocolloids in human digestion: Dynamic in-vitro assessment of the effect of food formulation on mass transfer. *Food Hydrocoll.*, 42(3):378–385.

Gritti, I., Banfi, G., and Roi, G. S. (2000). Pepsinogens: physiology, pharmacology pathophysiology and exercise. *Pharmacol. Res.*, 41(3):265–281.

Grötzinger, U., Bergegardh, S., and Olbe, L. (1977). Effect of fundic distension on gastric acid secretion. *Gut*, 18:105–110.

Hasan, M. and Ferguson, A. (1981). Measurements of intestinal villi in non-specific and ulcer-associated duodenitis correlation between area of microdissected villus and villus epithelial cell count. *J clin Pathol*, 34:1181–1186.

Haslam, D. W. and James, W. P. T. (2005). Obesity. *Lancet*, 366:1197–1209.

Hass, N., Schwarzenbacher, K., and Breer, H. (2010). T1R3 is expressed in brush cells and ghrelin-producing cells of murine stomach. *Cell Tissue Res.*, 339(3):493–504.

Heddle, R., Dent, J., Read, N., Houghton, L., Toouli, J., Horowitz, M., Maddern, G., and Downton, J. (1988a). Antropyloroduodenal motor responses to intraduodenal lipid infusion in healthy volunteers. *Am J Physiol.*, 254(5 pt.1):G671–9.

Heddle, R., Fone, D., Dent, J., and Horowitz, M. (1988b). Stimulation of pyloric motility by intraduodenal dextrose in normal subjects. *Gut*, 29(10):1349–1357.

Hellström, P. M., Grybäck, P., and Jacobsson, H. (2006). The physiology of gastric emptying. *Best Pract. Res. Clin. Anaesthesiol.*, 20(3):397–407.

Higham, A., Noble, P., Thompson, D. G., and Dockray, G. J. (1997). Increased sensitivity of gastrin cells to gastric distension following antral denervation in the rat. *J. Physiol.*, 503(1):169–175.

Hoang, K. C. T. (1995). Physiologically based pharmacokinetic models: Mathematical fundamentals and simulation implementations. *Toxicol. Lett.*, 79(1-3):99–106.

HSCIC (2014). Statistics on obesity, physical activity and diet: England. *Heal. Soc. care Inf. Cent.*

Hunt, J. N. and Stubbs, D. F. (1975). The volume and energy content of meals as determinants of gastric emptying. *J. Physiol.*, 245:209–225.

Hveem, K., Jones, K. L., Chatterton, B. E., and Horowitz, M. (1996). Scintigraphic measurement of gastric emptying and ultrasonographic assessment of antral area: relation to appetite. *Gut*, 38(6):816–821.

Ikram-Ul-Haq, M., Moshin, J., Uzam, H., and Fazal, A. (2010). Kinetics and Thermodynamic Studies of Alpha Amylase From Bacillus Licheniformis Mutant. *Pak. J. Bot*, 42(5):3507–3516.

Jain, R. K., Gerlowski, L. E., Jonas, M. W., Wang, J., and Pierson Jr., R. N. (1981). Kinetics of uptake, distribution, and excretion of zinc in rats. *Ann. Biomed. Eng.*, 9(4):347–361.

Jalabert-Malbos, M. L., Mishellany-Dutour, A., Woda, A., and Peyron, M. A. (2007). Particle size distribution in the food bolus after mastication of natural foods. *Food Qual. Prefer.*, 18(5):803–812.

Janssen, P. W. M., Lentle, R. G., Asvarujanon, P., Chambers, P., Stafford, K. J., and Hemar, Y. (2007). Characterization of flow and mixing regimes within the ileum of the brushtail possum using residence time distribution analysis with simultaneous spatio-temporal mapping. *J. Physiol.*, 582(3):1239–1248.

Jenkins, D. J., Wolever, T. M., Taylor, R. H., Barker, H., Fielden, H., Baldwin, J. M., Bowling, A. C., Newman, H. C., Jenkins, A. L., and Goff, D. V. (1981). Glycemic index of foods: a physiological basis for carbohydrate exchange. *Am. J. Clin. Nutr.*, 34(3):362–366.

Jew, S., AbuMweis, S. S., and Jones, P. J. H. (2009). Evolution of the human diet: linking our ancestral diet to modern functional foods as a means of chronic disease prevention. *J. Med. Food*, 12(5):925–934.

Johnson, I. T. and Gee, J. M. (1981). Effect of gel-forming gums on the intestinal unstirred layer and sugar transport in vitro. *Gut*, 22(5):398–403.

Joseph, I. M. P., Zavros, Y., Merchant, J. L., and Kirschner, D. (2003). A model for integrative study of human gastric acid secretion. *J. Appl. Physiol.*, 94(4):1602–18.

Jumars, P. A. (2000). Animal Guts as Nonideal Chemical Reactors: Partial Mixing and Axial Variation in Absorption Kinetics. *Am. Nat.*, 155(4):544–555.

Keet, A. D. (1962). Diameter of the pyloric aperture in relation to the contraction of the canalis egestorius. *Acta radiol.*, 57(1):31–44.

Keller, J. and Layer, P. (2005). Human pancreatic exocrine response to nutrients in health and disease. *Gut*, 54(suppl VI):1–28.

Kendall, C. W., Esfahani, A., and Jenkins, D. J. (2010). The link between dietary fibre and human health. *Food Hydrocoll.*, 24(1):42–48.

Kim, H. J. and White, P. J. (2013). Impact of the molecular weight, viscosity, and solubility of β-glucan on in vitro oat starch digestibility. *J. Agric. Food Chem.*, 61(13):3270–7.

Kim, M. (2005). High-methoxyl pectin has greater enhancing effect on glucose uptake in intestinal perfused rats. *Nutrition*, 21(3):372–377.

Komasaka, M., Horie, S., Watanabe, K., and Murayama, T. (2002). Antisecretory effect of somatostatin on gastric acid via inhibition of histamine release in isolated mouse stomach. *Eur. J. Pharmacol.*, 452(2):235–243.

Komolprasert, V. and Ofoli, R. Y. (1991). Starch hydrolysis kinetics of Bacillus licheniformis α-amylase. *J. Chem. Technol. Biotechnol.*, 51(2):209–223.

Kong, F. and Singh, R. P. (2008). Disintegration of Solid Foods in Human Stomach. *J. Food Sci.*, 73(5):R67–R80.

Kong, F. and Singh, R. P. (2009). Modes of Disintegration of Solid Foods in Simulated Gastric Environment. *Food Biophys.*, 4(3):180–190.

Kopelman, P. (2007). Health risks associated with overweight and obesity. *Obes. Rev.*, 8 Suppl 1(11):13–17.

Kozu, H., Kobayashi, I., Nakajima, M., Uemura, K., Sato, S., and Ichikawa, S. (2010). Analysis of Flow Phenomena in Gastric Contents Induced by Human Gastric Peristalsis Using CFD. *Food Biophys.*, 5(4):330–336.

Kusano, M., Zai, H., Shimoyama, Y., Hosaka, H., Kuribayashi, S., Kawamura, O., and Mori, M. (2011). Rapid gastric emptying, rather than delayed gastric emptying, might provoke functional dyspepsia. *J. Gastroenterol. Hepatol.*, 26(3):75–8.

Leclère, C. J., Champ, M., Boillot, J., Guille, G., Lecannu, G., Molis, C., Bornet, F., Krempf, M., Delort-Laval, J., and Galmiche, J. P. (1994). Role of viscous guar gums in lowering the glycemic response after a solid meal. *Am. J. Clin. Nutr.*, 59(4):914–921.

Lehmann, E. and Deutsch, T. (1992). A physiological model of glucose-insulin interaction in type 1 diabetes mellitus. *J. Biomed. Eng.*, 14(3):235–242.

Lentle, R. G. and Janssen, P. W. M. (2008). Physical characteristics of digesta and their influence on flow and mixing in the mammalian intestine: a review. *J. Comp. Physiol. B.*, 178(6):673–90.

Lentle, R. G. and Janssen, P. W. M. (2011). *The Physical Processes of Digestion*. Springer New York, New York, NY.

Levine, J. S., Nakane, P. K., and Allen, R. H. (1981). Human Intrinsic-Factor Secretion - Immuno-Cytochemical Demonstration of Membrane-Associated Vesicular Transport in Parietal-Cells. *J. Cell Biol.*, 90(3):644–655.

Levitt, D. G. (2013). Quantitation of small intestinal permeability during normal human drug absorption. *BMC Pharmacol. Toxicol.*, 14(1):34.

Li, J., Kuang, Y., and Li, B. (2001). Analysis of IVGTT glucose-insulin interaction models with time delay. *Discret. Contin. Dyn. Syst. Ser. B*, 1(1):103–124.

Li, J.-M. and Nie, S.-P. (2015). The functional and nutritional aspects of hydrocolloids in foods. *Food Hydrocoll.*, 53:46–61.

Lim, Y. F., de Loubens, C., Love, R. J., Lentle, R. G., and Janssen, P. W. M. (2015). Flow and mixing by small intestine villi. *Food Funct.*, 6(6):1787–95.

Logan, D., Joern, A., and Wolesensky, W. (2002). Location, Time, and Temperature Dependence of Digestion in Simple Animal Tracts. *J. Theor. Biol.*, 216(1):5–18.

Love, R. J., Lentle, R. G., Asvarujanon, P., Hemar, Y., and Stafford, K. J. (2013). An expanded finite element model of the intestinal mixing of digesta. *Food Dig.*, 4:26–35.

Makroglou, A., Li, J., and Kuang, Y. (2006). Mathematical models and software tools for the glucose-insulin regulatory system and diabetes: an overview. *Appl. Numer. Math.*, 56(3-4):559–573.

Marciani, L., Gowland, P. A., Fillery-Travis, A., Manoj, P., Wright, J., Smith, A., Young, P., Moore, R., and Spiller, R. C. (2001a). Assessment of antral grinding of a model solid meal with echo-planar imaging. *Am. J. Physiol. Gastrointest. Liver Physiol.*, 280(5):G844–G849.

Marciani, L., Gowland, P. A., Spiller, R. C., Manoj, P., Moore, R. J., Young, P., Al-Sahab, S., Bush, D., Wright, J., and Fillery-Travis, A. J. (2000). Gastric response to increased meal viscosity assessed by echo-planar magnetic resonance imaging in humans. *J. Nutr.*, 130(1):122–127.

Marciani, L., Gowland, P. A., Spiller, R. C., Manoj, P., Moore, R. J., Young, P., and Fillery-Travis, A. J. (2001b). Effect of meal viscosity and nutrients on satiety, intragastric dilution, and emptying assessed by MRI. *Am. J. Physiol. Gastrointest. Liver Physiol.*, 280(6):G1227–G1233.

Marciani, L., Hall, N., Pritchard, S. E., Cox, E. F., Totman, J. J., Lad, M., Hoad, C. L., Foster, T. J., Gowland, P. A., and Spiller, R. C. (2012). Preventing gastric sieving by blending a solid/water meal enhances satiation in healthy humans. *J. Nutr.*, 142(7):1253–1258.

Marino, S., Ganguli, S., Joseph, I. M. P., and Kirschner, D. E. (2003). The importance of an inter-compartmental delay in a model for human gastric acid secretion. *Bull. Math. Biol.*, 65(6):963–90.

Mason, W., Winer, N., Kochak, G., Cohen, I., and Bell, R. (1979). Kinetics and absolute bioavailability of atenolol. *Clin. Pharmacol. Ther.*, 25(408-415).

McDonald, D. E., Pethick, D. W., Mullan, B. P., and Hampson, D. J. (2001). Increasing viscosity of the intestinal contents alters small intestinal structure and intestinal growth , and stimulates proliferation of enterotoxigenic Escherichia coli in newly-weaned pigs. *Br. J. Nutr.*, 86:487–498.

McHugh, P. R. (1983). The control of gastric emptying. *J. Auton. Nerv. Syst.*, 9(1):221–31.

McHugh, P. R. and Moran, T. H. (1979). Calories and gastric emptying: a regulatory capacity with implications for feeding. *Am. J. Physiol.*, 236(10):R254–R260.

McPherson, K., Marsh, T., and Brown, M. (2007). Modelling future trends in obesity and the impact on health. *Foresight tackling obesities Futur. choices*.

Meeroff, J. C., Go, V. L., and Phillips, S. F. (1975). Control of gastric emptying by osmolality of duodenal contents in man. *Gastroenterology*, 68(5 Pt 1):1144–51.

Meyer, J., Elashoff, J., Porter-Fink, V., Dressman, J., and Amidon, G. (1988). Human postprandial gastric emptying of 1-3-millimeter spheres. *Gastroenterology*, 94(6):1315–1325.

Mishra, A. K. and Dubey, V. (2016). Obesity: An overview of possible role(s) of gut hormones, lipid sensing and gut microbiota. *Metabolism*, 65:48–65.

Moog, F. (1981). The lining of the Small Intestine. *Sci. Am.*, 245(5):154–176.

Moran, T. H., Wirth, J. B., Schwartz, G. J., and McHugh, P. R. (1999). Interactions between gastric volume and duodenal nutrients in the control of liquid gastric emptying. *Am J Physiol Regul. Integr. Comp Physiol*, 276(4):R997–1002.

Mourot, J., Thouvenot, P., Couet, C., Antoine, J., Krobicka, A., and Debry, G. (1988). Relationship between the rate of gastric emptying and glucose and insulin responses to starchy foods in young healthy adults. *Am. J. Clin. Nutr.*, 48:1035–1040.

Moxon, T. E. and Bakalis, S. (2016). Simulation based food process design. In Martin, M., Eden, M., and Chemmangattuvalappil, N., editors, *Tools Chem. Prod. Des.* Elsevier, 1st edition.

Moxon, T. E., Gouseti, O., and Bakalis, S. (2016). In silico modelling of mass transfer & absorption in the human gut. *J. Food Eng.*, 176:110–120.

Moxon, T. E., Latty, C., Gouseti, O., and Bakalis, S. (2015). In-Vitro and In-Silico Models of Digestion: Limitations and Challenges. In Cozzini, P., editor, *From Med. Chem. to Food Sci. A Transf. Silico Methods Appl.*, pages 35–60. Nova.

Moxon, T. E., Nimmegeers, P., Telen, D., Fryer, P. J., Van Impe, J., and Bakalis, S. (2017). Effect of chyme viscosity and nutrient feedback mechanism on gastric emptying. *Chem. Eng. Sci.*, 171:318–330.

Nadeem, S., Ashiq, S., and Ali, M. (2012). Williamson Fluid Model for the Peristaltic Flow of Chyme in Small Intestine. *Math. Probl. Eng.*, 2012:1–18.

Ni, P., Ho, N., Fox, J., Leuenberger, H., and Higuchi, W. (1980). Theoretical Model Studies of Intestinal Drug Absorption V. Non-Steady-State Fluid Flow and Absorption. *Int. J. Pharm.*, 5:33–47.

O'Hara, A. M. and Shanahan, F. (2006). The gut flora as a forgotten organ. *EMBO Rep.*, 7(7):688–693.

Paintal, A. (1954). A study of gastric stretch receptors. Their role in the peripheral mechanism of satiation of hunger and thirst. *J. Physiol.*, 126:255–270.

Pedersen, M. G. and Cobelli, C. (2013). *Insulin Modelling*. Elsevier Inc., 2nd edition.

Peng, H. and Cheung, B. (2009). A review on pharmacokinetic modeling and the effects of environmental stressors on pharmacokinetics for operational medicine:. Technical Report September, Defence R&D Canada.

Penry, D. L. and Jumars, P. A. (1986). Chemical reactor analysis and optimal digestion. *Bioscience*, 36(5):310–315.

Penry, D. L. and Jumars, P. A. (1987). Modeling Animal Guts as Chemical Reactors. *Am. Nat.*, 129(1):69.

Phillips, W. T., Schwartz, J. G., Blumhardt, R., and McMahan, C. A. (1991). Linear Gastric Emptying of Hyperosmolar Glucose Solutions. *J. Nucl. Med.*, 32:377–381.

Piper, D. and Fenton, B. (1965). pH stability and activity curves of pepsin with special reference to their clinical importance. *Gut*, 6:506–508.

Pocock, G. and Richards, C. D. (2006). *Human Physiology: The basis of medicine*. Oxford core texts, 3rd edition.

Popkin, B. M. (2006). Global nutrition dynamics: The world is shifting rapidly toward a diet linked with noncommunicable diseases. *Am. J. Clin. Nutr.*, 84(2):289–298.

Powley, T. L. and Phillips, R. J. (2004). Gastric satiation is volumetric, intestinal satiation is nutritive. *Physiol. Behav.*, 82(1):69–74.

Pröve, J. and Ehrlein, H. J. (1982). Motor function of gastric antrum and pylorus for evacuation of low and high viscosity meals in dogs. *Gut*, 23(2):150–156.

Punkkinen, J., Konkka, I., Punkkinen, O., Korppi-Tommola, T., Färkkilä, M., and Koskenpato, J. (2006). Measuring gastric emptying: Comparison of 13C-octanoic acid breath test and scintigraphy. *Dig. Dis. Sci.*, 51(2):262–267.

Rayner, C. K., Hebbard, G. S., and Horowitz, M. (2012). Physiology of the Antral Pump and Gastric Emptying. In Johnson, L. R., editor, *Physiol. Gastrointest. Tract*, chapter 35, pages 959–976. Elsevier Inc., 5th edition.

Rayner, C. K., Park, H. S., Wishart, J. M., Kong, M., Doran, S. M., and Horowitz, M. (2000). Effects of intraduodenal glucose and fructose on antropyloric motility and appetite in healthy humans. *Am. J. Physiol. Regul. Integr. Comp. Physiol.*, 278(2):R360–6.

Read, N. W., Al-Janabi, M. N., Holgate, A. M., Barber, D. C., and Edwards, C. A. (1986). Simultaneous measurement of gastric emptying, small bowel residence and colonic filling of a solid meal by the use of the gamma camera. *Gut*, 27(3):300–308.

Reed, K. K. and Wickham, R. (2009). Review of the Gastrointestinal Tract: From Macro to Micro. *Semin. Oncol. Nurs.*, 25(1):3–14.

Riahi, D. N. and Roy, R. (2011). Mathematical Modeling of Peristaltic Flow of Chyme in Small Intestine. *pplications Appl. Math.*, 6(2):428–444.

Sallee, Y. L., Wilson, F. A., and Dietschy, J. M. (1972). Determination of Unidirectional Uptake Rates for Lipids Across the Intestinal Brush Border. *J. Lipid Res.*, 13(2):184–192.

Salmeron, J., Ascherio, A., Rimm, E. B., Colditz, G. A., Spielgelman, D., Jenkins, D. J., Stampfer, M. J., Wing, A. L., and Willett, W. C. (1997a). Dietary fiber, glycemic load, and risk of NIDDM in men. *Diabetes Care*, 20(4):545–550.

Salmeron, J., Manson, J., Stampfer, M., Colditz, G., Wing, A., and Willett, W. (1997b). Dietary fiber, glycemic load, and risk of non-insulin-dependent diabetes mellitus in women. *J. Am. Med. Assoc.*, 277(6):472–477.

Santangelo, A., Peracchi, M., Conte, D., Fraquelli, M., and Porrini, M. (1998). Physical state of meal affects gastric emptying, cholecystokinin release and satiety. *Br J Nutr*, 80(6):521–527.

Sasaki, T. and Kohyama, K. (2012). Effect of non-starch polysaccharides on the in vitro digestibility and rheological properties of rice starch gel. *Food Chem.*, 127(2):541–6.

Satomura, S., Okajima, S., Hamanaka, T., Shintani, A., Miyashita, Y., and Sakata, Y. (1984). Kinetics of human pancreatic and salivary α-amylases with carboxymethylamyloses as substrates. *Clin. Chim. Acta*, 138(1):21–29.

Sauter, M., Curcic, J., Menne, D., Goetze, O., Fried, M., Schwizer, W., and Steingoetter, A. (2012). Measuring the interaction of meal and gastric secretion: a combined quantitative magnetic resonance imaging and pharmacokinetic modeling approach. *Neurogastroenterol Motil*, 24(7):632–e273.

Schubert, M. L. and Makhlouf, G. M. (1993). Gastrin secretion induced by distention is mediated by gastric cholinergic and vasoactive intestinal peptide neurons in rats. *Gasteroenterology*, 104:834–9.

Schultz, S. and Solomon, A. (1961). Determination of the Effective Hydrodynamic Radii of Small Molecules by Viscometry. *J. Gen. Physiol.*, 44(6):1189–1199.

Schulze, K. (2006). Imaging and modelling of digestion in the stomach and the duodenum. *Neurogastroenterol. Motil.*, 18(3):172–183.

Schulze, M. B., Liu, S., Rimm, E. B., Manson, J. E., Willett, W. C., and Hu, F. B. (2004). Glycemic index, glycemic load, and dietary fiber intake and incidence of type 2 diabetes in younger and middle-aged women. *Am.J.Clin.Nutr.*, 80(2):348–356.

Schwizer, W., Maecke, H., and Fried, M. (1992). Measurement of gastric emptying by magnetic resonance imaging in humans. *Gastroenterology*, 103(2):369–376.

Schwizer, W., Steingötter, A., Fox, M., Zur, T., Thumshirn, M., Bösiger, P., and Fried, M. (2002). Non-invasive measurement of gastric accommodation in humans. *Gut*, 51(Suppl 1):i59–62.

Shahidullah, M., Kennedy, T. L., and Parks, T. G. (1975). The vagus, the duodenal brake, and gastric emptying. *Gut*, 16(5):331–6.

Shimoyama, Y., Kusano, M., Kawamura, O., Zai, H., Kuribayashi, S., Higuchi, T., Nagoshi, a., Maeda, M., and Mori, M. (2007). High-viscosity liquid meal accelerates gastric emptying. *Neurogastroenterol. Motil.*, 19(11):879–86.

Siegel, J. A., Urbain, J. L., Adler, L. P., Charkes, N. D., Maurer, A. H., Krevsky, B., Knight, L. C., Fisher, R. S., and Malmud, L. S. (1988). Biphasic nature of gastric emptying. *Gut*, 29(1):85–89.

Sim, L., Quezada-Calvillo, R., Sterchi, E. E., Nichols, B. L., and Rose, D. R. (2008). Human Intestinal Maltase-Glucoamylase: Crystal Structure of the N-Terminal Catalytic Subunit and Basis of Inhibition and Substrate Specificity. *J. Mol. Biol.*, 375(3):782–792.

Singh, J., Dartois, A., and Kaur, L. (2010). Starch digestibility in food matrix: a review. *Trends Food Sci. Technol.*, 21(4):168–180.

Sky-Peck, H. and Thuvasethakul, P. (1977). Human pancreatic alpha-amylase. II. Effects of pH, substrate and ions on the activity of the enzyme. *Ann Clin Lab Sci.*, 7(4):310–317.

Slaughter, S. L., Ellis, P. R., Jackson, E. C., and Butterworth, P. J. (2002). The effect of guar galactomannan and water availability during hydrothermal processing on the hydrolysis of starch catalysed by pancreatic alpha-amylase. *Biochim. Biophys. Acta - Gen. Subj.*, 1571(1):55–63.

Smith, G. D. (1978). *Numerical solution of partial differential equations: finite difference methods*. Oxford: Clarendon Press, 2nd edition.

Sobotta, J. (1906). *Atlas and text-book of human anatomy, Vol. 1*. Saunders, Philadelphia.

Soenen, S., Giezenaar, C., Hutchison, A. T., Horowitz, M., Chapman, I., and Luscombe-Marsh, N. D. (2014). Effects of intraduodenal protein on appetite, energy intake, and antropyloroduodenal motility in healthy older compared with young men in a randomized trial. *Am. J. Clin. Nutr.*, 100(4):1108–1115.

Steverson, E. M., Korus, R. A., Admassu, W., and Heimsch, R. C. (1984). Kinetics of the amylase system of Saccharomycopsis fibuliger. *Enzyme*, 6:549–554.

Stoll, B., Batycky, R., Leipold, H., Milstein, S., and Edwards, D. (2000). A theory of molecular absorption from the small intestine. *Chem. Eng. Sci.*, 55(3):473–489.

Strikwerda, J. C. (2004). *Finite difference schemes and partial differential equations*. Society for industrial and applied mathematics, 2nd edition.

Strocchi, A. and Levitt, M. D. (1993). Role of villous surface area in absorption. Science versus religion. *Dig. Dis. Sci.*, 38(3):385–7.

Stümpel, F., Burcelin, R., Jungermann, K., and Thorens, B. (2001). Normal kinetics of intestinal glucose absorption in the absence of GLUT2: evidence for a transport pathway requiring glucose phosphorylation and transfer into the endoplasmic reticulum. *Proc. Natl. Acad. Sci. U. S. A.*, 98(20):11330–5.

Taghipoor, M., Barles, G., Georgelin, C., Licois, J.-R., and Lescoat, P. (2014). Digestion Modelling in the Small Intestine: Impact of Dietary Fibre. *Math. Biosci.*, 258:101–112.

Taghipoor, M., Lescoat, P., Licois, J. R., Georgelin, C., and Barles, G. (2012). Mathematical modeling of transport and degradation of feedstuffs in the small intestine. *J. Theor. Biol.*, 294:114–121.

Takahashi, T. and Sakata, T. (2004). Viscous Properties of Pig Cecal Contents and the Contribution of Solid Particles to Viscosity. *Nutrition*, 20:377–382.

Takahashi, T., Yokawa, T., Ishihara, N., Okubo, T., Chu, D. C., Nishigaki, E., Kawada, Y., Kato, M., and Raj Juneja, L. (2009). Hydrolyzed guar gum decreases postprandial blood glucose and glucose absorption in the rat small intestine. *Nutr. Res.*, 29(6):419–425.

Tharakan, A., Norton, I., Fryer, P., and Bakalis, S. (2010). Mass Transfer and Nutrient Absorption in a Simulated Model of Small Intestine. *J. Food Sci.*, 75(6):E339–E346.

Treacy, P., Jamieson, G., and Dent, J. (1990). Pyloric motor function during emptying of a liquid meal from the stomach in the conscious pig. *J. Physiol.*, 422:523–538.

Tripathi, D. (2011a). A mathematical model for the peristaltic flow of chyme movement in small intestine. *Math. Biosci.*, 233(2):90–97.

Tripathi, D. (2011b). Peristaltic transport of a viscoelastic fluid in a channel. *Acta Astronaut.*, 68(7-8):1379–1385.

Tripathi, D. (2011c). Peristaltic transport of fractional Maxwell fluids in uniform tubes: Applications in endoscopy. *Comput. Math. with Appl.*, 62(3):1116–1126.

Tripathi, D., Pandey, S. K., and Das, S. (2011). Peristaltic transport of a generalized Burgers' fluid: Application to the movement of chyme in small intestine. *Acta Astronaut.*, 69(1-2):30–38.

Tuma, P. L. and Hubbard, A. N. N. L. (2003). Transcytosis : Crossing Cellular Barriers. *Physiol. Rev.*, 83(3):871–932.

Urbain, J. L. C., Siegel, J. A., Charkes, N. D., Maurer, A. H., Malmud, L. S., and Fisher, R. S. (1989). The two-component stomach: effects of meal particle size on fundal and antral emptying. *Eur. J. Nucl. Med.*, 15(5):254–259.

Urso, R., Blardi, P., and Giorgi, G. (2002). A short introduction to pharmacokinetics. *Eur. Rev. Med. Pharmacol. Sci.*, 6(2):33–44.

US National Library of Medicine (2012). [online] https://medlineplus.gov/ency/imagepages/19221.htm [Accessed 27/09/2016].

Van Wey, A., Cookson, A., Roy, N., McNabb, W., Soboleva, T., Wieliczko, R., and Shorten, P. (2014). A mathematical model of the effect of pH and food matrix composition on fluid transport into foods: An application in gastric digestion and cheese brining. *Food Res. Int.*, 57:34–43.

Viebke, C., Al-Assaf, S., and Phillips, G. O. (2014). Food hydrocolloids and health claims. *Bioact. Carbohydrates Diet. Fibre*, 4(2):101–114.

Vist, G. E. and Maughan, R. J. (1995). The effect of osmolality and carbohydrate content on the rate of gastric emptying of liquids in man. *J. Physiol.*, 486(2):523–531.

Wachters-Hagedoorn, R. E., Priebe, M. G., Heimweg, J. A. J., Heiner, A. M., Englyst, K. N., Holst, J. J., Stellaard, F., and Vonk, R. J. (2006). The rate of intestinal glucose absorption is correlated with plasma glucose-dependent insulinotropic polypeptide concentrations in healthy men. *J. Nutr.*, 136(6):1511–6.

Wagner, J. (1993). *Pharmacokinetics for the pharmacokinetical scientists*. technomic publishing company, Inc., Pennsylvania.

Wang, Y., Brasseur, J. G., Banco, G. G., Webb, A. G., Ailiani, A. C., and Neuberger, T. (2010). A multiscale lattice Boltzmann model of macro- to micro-scale transport, with applications to gut function. *Philos. Trans. R. Soc. A Math. Phys. Eng. Sci.*, 368(1921):2863–2880.

Weber, E. and Ehrlein, H. J. (1998). Relationships between gastric emptying and intestinal absorption of nutrients and energy in mini pigs. *Dig. Dis. Sci.*, 43(6):1141–53.

Weickert, M. O. and Pfeiffer, A. F. H. (2008). Metabolic effects of dietary fiber consumption and prevention of diabetes. *J. Nutr.*, 138(3):439–442.

WHO (2014). Global status report on noncommunicable diseases. Technical report, WHO, Geneva.

Wilding, I., Hardy, J., Maccari, M., Ravelli, V., and Davis, S. (1991). Scintigraphic and pharmacokinetic assessment of a mltiparticulate sustained release formulation of diltiazem. *Int. J. Pharm.*, 76:133–143.

Willett, W., Manson, J., and Liu, S. (2002). Glycemic index, glycemic load, and risk of type 2 diabetes. *Am J Clin Nutr*, 76:274–280.

Williams, E. K., Chang, R. B., Strochlic, D. E., Umans, B. D., Lowell, B. B., and Liberles, S. D. (2016). Sensory Neurons that Detect Stretch and Nutrients in the Digestive System. *Cell*, 166(1):209–221.

Williamson, G. (2013). Possible effects of dietary polyphenols on sugar absorption and digestion. *Mol. Nutr. Food Res.*, 57(1):48–57.

Wøjdemann, M., Traberg, P., Stadil, F., Sternby, B., Larsen, S., Hilsted, L., and Olsen, O. (1998). Effect of sham feeding and acute suppression of acid secretion on human gastric lipase secretion. *Am. J. Gastroenterol.*, 93(2):244–248.

Wolever, T. M., Jenkins, D. J., Jenkins, a. L., and Josse, R. G. (1991). The glycemic index: methodology and clinical implications. *Am. J. Clin. Nutr.*, 54(5):846–854.

Woods, C. M., Mawe, G. M., Toouli, J., and Saccone, G. T. P. (2005). The sphincter of Oddi: Understanding its control and function. *Neurogastroenterol. Motil.*, 17:31–40.

Yankov, D., Dobreva, E., Beschkov, V., and Emanuilova, E. (1986). Study of optimum conditions and kinetics of starch hydrolysis by means of thermostable α-amylase. *Enzyme Microb. Technol.*, 8(11):665–667.

Young, R. L. (2011). Sensing Via Intestinal Sweet Taste Pathways. *Front. Neurosci.*, 5(23):1–13.

Yu, K., Ke, M.-Y., Li, W.-H., Zhang, S.-Q., and Fang, X.-C. (2014). The impact of soluble dietary fibre on gastric emptying, postprandial blood glucose and insulin in patients with type 2 diabetes. *Asia Pac. J. Clin. Nutr.*, 23(1):210–8.

Yu, L. X. and Amidon, G. L. (1999). A compartmental absorption and transit model for estimating oral drug absorption. *Int. J. Pharm.*, 186(2):119–125.

Yu, L. X., Crison, J. R., and Amidon, G. L. (1996). Compartmental transit and dispersion model analysis of small intestinal transit flow in humans. *Int. J. Pharm.*, 140(1):111–118.

Zhang, G., Hasek, L. Y., Lee, B.-H., and Hamaker, B. R. (2015). Gut feedback mechanisms and food intake: a physiological approach to slow carbohydrate bioavailability. *Food Funct.*, 6:1072–1089.